Relative Performance Analyses of Articulated Vehicles with Multiple Conventional, Liftable and Self-Steering Axles

Sheng Luo

A Thesis

in

The Department

of

Mechanical and Industrial Engineering

Presented in Partial Fulfillment of the Requirements
for the Degree of Master of Applied Science (Mechanical Engineering) at
Concordia University
Montreal, Quebec, Canada

September 2004

Your file Votre référence
ISBN: 0-612-94730-0
Our file Notre référence
ISBN: 0-612-94730-0

Abstract

Relative Performance Analyses of Articulated Vehicles with Multiple Conventional, Liftable and Self-Steering Axles

Sheng Luo

The gross vehicle weight (GVW) and dimensions of articulated freight vehicles have been considerably relaxed during the past few decades, which has encouraged the use of multi-axle trailers. Multiple axle trailers with liftable and self-steering axles are commonly used to enhance their maneuverability on tight turns and minimize the tire scrub. Many concerns have been raised on the use of liftable axle, as they transmit considerably higher tire loads to the pavement, when retracted. The self-steering axles, on the other hand, could provide adequate maneuverability and reduce the tire scrub, while limiting the magnitudes of tire loads transmitted to the pavement. The reduced cornering forces due to self-steering axle tires, and higher axle loads due to retracted liftable axles, could further alter the handling and directional performance of the vehicle. This dissertation is concerned with relative directional performance and pavement-loading characteristics of multiple axle articulated vehicles with conventional, liftable and self-steering axles. A general-purpose three-dimensional model of an articulated vehicle with 3-, 4-, 5- and 6-axle semitrailers, including one or more liftable or self-steering axles, is developed on the basis of the well-established yaw/roll model, which is reformulated to incorporate the dynamics due to liftable and self-steering axles, and the tire interactions with random road surfaces. A series of performance measures are formulated to

investigate the role of liftable and self-steering axles, road roughness and suspension damping ratio on the directional characteristics and the road damage potential of the selected vehicle configurations. The analyses are performed to assess the relative directional dynamics characteristics and pavement damage potentials of candidate vehicle configurations with conventional, liftable and self-steering axles. The analyses are further performed to study the influences of road roughness and suspension damping on the performance measures. The results of the investigation show that both the liftable and self-steering axles affect different aspects of the directional performance measures of the candidate vehicle configurations. The vehicle with retracted lift axles would yield lower roll stability limit and considerably lower jackknife potential on low friction surfaces, such as icy roads. The vehicle with self-steering axles, on the other hand, poses huge friction demand at low as well as high speeds, suggesting higher jackknife potential. The vehicle operation with one or more raised axles, however, imposes higher axle loads and significantly higher stresses on the pavement. The variations in the road roughness and suspension damping also influence some of the directional performance measures in a significant manner. The results are further used to demonstrate the phenomenon of 'spatial repeatability' of dynamic tire forces on the selected pavement profiles, which is strongly influenced by the road roughness, suspension characteristics and axle operating condition.

Acknowledgement

The author is sincerely grateful to his supervisor Dr. Subhash Rakheja for his guidance and continuous support, encouragement and effort during the course of this investigation.

The author wishes to acknowledge Mr. Norman D. Hebert and Port of Montreal for their fellowship and award, respectively.

The author also wishes to further thank the colleagues, faculty and staff of CONCAVE Research Center, Department of Mechanical engineering, Concordia University, for their contribution to this effort.

Finally, the author would like to express a deep appreciation to his parents, and wife for their continuous concerns, encouragement and support.

CONTENTS

LIST OF FIGURES

LIST OF TABLES

NOMENCLATURE

A_l : Dual tire spacing of tires on axle l

$\vec{a}_c$: Acceleration at the articulation point

a_l : Lateral acceleration of self-steering axle l

$\vec{a}_{mul}$: Acceleration of unsprung mass l

$\vec{a}_{msf}$: Acceleration of sprung mass f

$\vec{a}_{mul/Rl}$: Acceleration of unsprung mass l with respect to the roll center

a_{rl} : Normalized resultant lateral force respect to the axle load in unit of g

$\vec{a}_{Rl/msf}$: Acceleration of the roll center of axle l with respect to the *c.g.* of the sprung mass f

a_y : Lateral acceleration of sprung mass

AT_{lm} : Aligning moment due to tire m on axle l

b : The distance between the retracted axle and the articulation point

C_s : Longitudinal stiffness of tires on self-steering axle

F_{ll}, F_{il} : Force due to the left side and right side of suspension spring on axle l

F_r : The resultant lateral force resisting the angular displacement of the tires on self-steering axle

F_{ro} : The centering force of self-steering axle

F_{Rl} : Lateral force through the roll center of axle l

F_{suspl} : Suspension force of axle l transmitted to the sprung mass

F_{yl} : Total lateral force developed by the tires on axle l

F_{zlm} : Instantaneous vertical loads of tire m on l axle

F_{ylm} : Lateral force developed at the road interface of tire m on axle l

g : Acceleration due to gravity

HR_l : Height of the roll center of axle l from the ground plane

H_{ul} : Height of the *c.g.* of axle l from the ground plane

I_{xxsf} : Roll mass moment of inertia of the sprung mass f

I_{xxul} : Roll mass moment of inertia of the unsprung mass l

I_{yysf} : Pitch mass moment of inertia of the sprung mass f

I_{zzsf} : Yaw mass moment of inertia of the sprung mass f

I_{zzul} : Yaw mass moment of inertia of the unsprung mass l

k_5 : Constraint stiffness of the fifth wheel

k_{ss} : Cornering stiffness of self-steering axle

K_{lm} : Vertical Stiffness of suspension spring on axle l

KRS_l : Auxiliary roll stiffness of the suspension spring on axle l

KT_{lm} : Vertical stiffness of tire m on axle l

m_{sf} : Mass of sprung mass f

m_{ss} : Mass of self-steering axle

m_{ul} : Mass of unsprung mass of axle l

M_{xf} : Constraint roll moment acting on the sprung mass f from the fifth wheel

M_{yf}: Constraint pitch moment acting on the sprung mass f from the fifth wheel

M_r: The resultant moment that resists the angular displacement of the tires about their pivot points on the self-steering axle

M_{dt}: Dual tire moment

N_1: The number of axles on vehicle

N_2: The number of retracted axle on vehicle

p_{sf}: Roll rate of sprung mass f

p_{ul}: Roll rate of unsprung mass l

q_{sf}: Pitch rate of the sprung mass f

r_{sf}: Yaw rate of the sprung mass f

r_{ul}: Yaw rate of the unsprung mass l

R_{lm}: Tire radius of tire m on axle l

ΔR_{lm}: Vertical deflection of tire m on axle l

S_{lm}: Tire-road contact area of tire m on axle l

s_l: Half the suspension lateral spread of axle l

t_{ss}: The corrected caster trail of self-steering axle

t_p: Pneumatic trail of the tires on self-steering axle

t_m: Mechanical caster trail of the tires on self-steering axle

t_s: The distance between the self-steering axle *c.g.* and the pivot point

T_l : Half-track width of inner tires on axle l

u_{sf} : Longitudinal velocity of the sprung mass f

u_{tirelm} : Forward velocity of tire m on axle l

v_{axlel} : Lateral velocity of axle l

v_{sf} : Lateral velocity of the sprung mass f

w_k : Kingpin offset of self-steering axle

w_{lm} : Tire width of tire m on axle l

w_{sf} : Vertical velocity of the sprung mass f

W : Total weight of the sprung and unsprung masses

W_{sl} : Sprung weight supported by axle l

W_{ul} : Weight of the unsprung mass l

x_{Rl} : Longitudinal distance between the *lth* roll center and the *c.g.* of the sprung mass

x_{ul} : Longitudinal distance from the *c.g.* of sprung mass to axle l

z_{Rl} : Vertical distance between the *lth* roll center and *c.g.* of the sprung mass

z_{ul} : Vertical distance between *c.g.* of unsprung mass and roll center on axle l

z_{uol} : Vertical distance between the *lth* roll center and the *lth* axle *c.g.* at $t = 0$

Δz_{sf} : Vertical deflection of the *c.g.* of sprung mass f along the inertial axis $\vec{k}_n$

α_{lm} : Sideslip angle of tire m on axle l

δ_o: Self-steering angle corresponding to the axle centering force

δ_l: Wheel steer angle of axle l

δ_{ssal}: Steer angle of self-steering axle l

Δ_{lm}: Vertical deflection of the tire m on axle l

Δ^*_{lm}: Vertical deformation of the tire m on axle l due to vehicle motion and road roughness

Δ_{0l}: Vertical deflection of the axle l at $t = 0$

Δ_{sf}: Vertical deflection of the *c.g.* of the sprung mass f along the inertial axis $\vec{k}_n$

Δ_{ul}: Vertical deflection of the *c.g.* of the unsprung mass l along the inertial axis $\vec{k}_n$

ϕ_{sf}: Roll angle of sprung mass f

ϕ_{ul}: Roll angle of unsprung weight l

ψ_{sf}: Yaw angle of sprung mass f

θ_{sf}: Pitch angle of sprung mass f

CHAPTER 1 : INTRODUCTION

1.1 GENERAL

For the reasons of economy, the population of commercial vehicles with multi-axle trailers has been steadily growing over the past few decades. Gross vehicle weight (GVW) and dimensional regulations for heavy vehicles were greatly relaxed during the 80's, which permitted the use of multi-axle trailer combinations to carry much larger loads. The use of articulated vehicles with three-, four-, five- or even six-axle semitrailers has thus grown considerably. The increasing use of such heavy vehicle configurations with significantly higher weights and dimensions has raised many concerns related to highway safety and the potential damage to the pavement infrastructure. Owing to their excessive weights and dimensions, and high location of the sprung mass center of gravity (c.g.), it has been further established that the handling and directional control characteristics of articulated vehicles are considerably lower than those of the other road vehicles. The increase in the weight, dimension, wheelbase, *c.g.* height, all contribute to the poor yaw and roll stability limits of these vehicles, and thus the highway safety performance [1].

Although the use of multiple-axle semitrailers enhances the load carrying capacity of the vehicle combinations significantly, the resulting long combination vehicles (LCV) yield poor maneuverability during tight turns. Such vehicles cause excessive off-tracking phenomenon during turning maneuvers, which yields rapid tire scrub and wear, and

interferes with the flow of traffic at intersections [2]. In order to minimize the unnecessary tire scrub and wear, the semitrailers with multiple widespread axles are frequently equipped with liftable axles. Such vehicles permit the driver to lift one or more trailer axles from the ground using the pneumatic control mechanism, when negotiating a turn, to enhance the maneuverability and reduce the tire scrub. The vehicle load supported by the remaining axles in contact with the road, however, increases, which may cause rapid pavement damage and affect the directional dynamic performance of the vehicle. The most common multi-axle configuration is the tandem or tridem axle group semitrailers with the forward "belly" lift axle(s) [2]. The road damage due to increased loads on the remaining axles on the ground increases exponentially with the increased axle loads on the basis of the fourth power law [3], which states that the road damage generated by a wheel is proportional to the fourth power of the static wheel load. This 'law' was developed from road test results [4] carried out by the American Association of State Highway Officials (AASHO) in the late 1950s. Owing to excessive public cost associated with the maintenance of the road infrastructure, the provincial transportation authorities in Canada have expressed many concerns on the operation of liftable axle vehicle combinations. Revisions of the current regulations to limit the use of such vehicles have been suggested [5].

Alternatively, self- and force-steering axle trailers have been proposed to enhance the maneuverability performance of LCVs, while retaining all the axles on the ground [6]. Self-steering axles on semitrailers are being increasingly encouraged by the

regulatory bodies to limit the potential pavement damage and to achieve acceptable maneuverability. The self-steering axles, however, tend to limit the effective cornering forces, specifically at high speeds, which may affect the directional performance of LCV in an adverse manner. A number of multi-axle semitrailer configurations with one or more self-steering axles are currently being employed in different LCVs. The number and location of self-steering axles in such combinations could strongly influence the directional dynamic performance.

In this dissertation, LCVs with three different axle types are investigated to explore their relative directional performance and road damage potential. The axle types include the conventional solid axle, liftable axle and self-steering axles. A general-purpose three-dimensional model of LCV is formulated comprising the models of the three types of axles. The constant velocity models are analyzed to study their relative directional and dynamic pavement loading performance characteristics.

1.2 REVIEW OF PREVIOUS INVESTIGATIONS

The handling, directional control and stability characteristics of heavy trucks and articulated vehicles have been extensively investigated during the past two decades. A comprehensive review of the reported studies on lateral dynamics of articulated vehicles has been presented by Vlk [7]. The influence of size and weight variables on the dynamic stability and directional control characteristics of heavy trucks and vehicle combinations have been investigated by Ervin et al. [1]. A few analytical and experimental studies of

vehicle combinations with conventional axles have clearly established that the directional performance characteristics of these vehicles are greatly influenced by their weights, dimensions and many other vehicle design parameters [1,5,7]. The previous studies on the tire-road interaction have further concluded that the excessive dynamic tire forces transmitted from the heavy vehicles cause premature pavement failure and the road damage potential of heavy vehicles have been related to many vehicle and road design factors [8]. A review of previous investigations, relevant to the directional dynamics and tire loads performance of articulated freight vehicles with conventional, liftable and self-steering axles, are presented in the following sections to develop the scope of the dissertation.

1.2.1 Directional Dynamics of Heavy Vehicles

The directional dynamics of heavy vehicles are investigated to assess their handling, directional control and directional stability characteristics under steady and transient steering maneuvers. During the process from the transient steering input to the steady state vehicle motion, the vehicle system is considered to be in a transient state. The overall handling characteristics of the vehicle in this period strongly depend on its transient response behavior. The steady state handling performance of a vehicle, on the other hand, is concerned with the directional behavior of a vehicle during a turn, when the contributions due to time-vary conditions are considered to be relatively small.

The handling, directional response and stability characteristics of various LCVs have been widely investigated through analytical and experimental means. The analytical

studies have been based upon simple two-degree-of-freedom (DOF) models to several DOF models incorporating nonlinear component models. These studies have clearly established that the handling and directional performance of articulated vehicles depend upon various design and operating factors, such as weight, dimension, tire and suspension properties, steering and braking system, articulation mechanism, speed and road conditions.

The earliest investigations on directional dynamics of truck-trailer combinations were performed by Huber and Dietz [9], and Dietz [10,11]. The reported experimental studies were mainly concerned with the lateral stability of the running vehicle configurations with two-axle tow bar trailers equipped with either turntable or Ackerman steering, although in the absence of a steering input. The experiments involved testing of scale models of laterally constrained trailers moving on an endless belt. The study concluded that a viscously damped turntable could most effectively reduce the trailer yaw oscillations, and that the coulomb damping was not as desirable. These earliest studies were followed by a complementary theoretical effort by Ziegler [12,13], who considered the tire forces similar to the coulomb damping in his study. The directional stability analysis of a truck-trailer combination performed by Laurien [14] concluded that the trailer yaw motion can be mostly limited by using coulomb damping at the hitch and at the trailer steering mechanism. Furthermore, the trailer with turntable (dolly) steering was observed to cause less lateral oscillations than the trailers with Ackerman steering. The yaw oscillations of a two-axle trailer with turntable steering was further theoretically

investigated by Paslay and Slibar [15] by considering yaw motions of the drawbar and the trailer. In their investigation, it was the first time that the tire cornering forces were considered to be influenced by the tire sideslip, and the equations of motion were solved to determine the natural frequencies of a two-axle drawbar trailer with negligible damping.

Zakin [16, 17, 18] investigated the influence of the vehicle dimensions on the lateral motion of the trailers. The experimental and analytical study of one- and two-axle tow bar trailers concluded that increasing the wheelbase and the tow bar length could reduce the lateral motion of the trailer. In order to theoretically investigate the lateral dynamics, Morozov et al. [19] developed an analog computer model of a two-axle turntable trailer incorporating coulomb friction. In this model the trailer was modeled as a double pendulum, and the influence of friction moment at the turntable and the location of the *c.g.* on the hitch lateral oscillations was assessed. A further investigation on the influence of tire cornering forces, wheelbase of the trailer and overall trailer length on the yaw oscillations was performed by Meyer [20] by employing a two-degree-of-freedom vehicle model. However, in all of the above-mentioned studies, dynamics of the trailer was investigated as an uncoupled unit while neglecting the dynamic interactions between the truck and the trailer.

The interaction between the truck and trailer motions was first investigated by Schimid [21] and Jindra [22]. By using the analog computer simulation of a coupled truck-trailer model, Jindra [22] concluded that the yaw oscillations of the trailer increase

with the increase of the yaw mass moment of inertia of the trailer. On the other hand, increasing viscous damping at the hitch or turntable, drawbar length and trailer wheelbase can decrease the yaw oscillations of the trailer. Gerlach [23] established a similar mathematical model with turntable offset, coulomb and/or viscous damping at the hitch and the turntable. This investigation concluded that the dynamic stability limits of truck-trailer combinations could be enhanced through high cornering stiffness tires, either coulomb or viscous damping at the hitch, longer drawbar and the turntable center located ahead of the dolly axle.

Nordstrom et al. [24] developed a vehicle dynamics simulation program at the National Swedish Road and Traffic Research Institute to study the lateral and roll dynamic stability of heavy vehicles, including the tank trucks. A limited number of full-scale field tests were performed to validate the simulation program and to develop test methods for assessing the directional performance of heavy vehicles. Furthermore, a comprehensive digital computer program was developed to simulate for directional dynamics of vehicle combinations adopting up to three articulations and nine axles, driving or braking forces, lateral load transfer, etc. [25]. The resulting 8-degree-of-freedom analytical model considered fixed roll centers, linear suspension springs, uncoupled lateral and longitudinal tire forces, and negligible pitch motion and longitudinal load transfer [26]. The simulation results attained under a lane-change type of maneuver revealed that a longer trailer wheelbase, lighter static loads on tires, shorter tow pin offset (distance between the truck rear axle and the tow pin) could reduce the

vehicle lateral offset, while a longer drawbar would cause greater amplitude of lateral oscillations.

The role of driver in the directional response of the coupled driver-vehicle system was investigated by Bakhmutskii and Gineburg [27] through road testing of various vehicle combinations and drivers. The handling characteristics of the vehicle and the driver-vehicle systems were derived from the test data acquired under step-steer and lane-change maneuvers. A linear 4-degree-of-freedom mathematical model was proposed to study the directional behavior of the vehicle. Mallikarjunarao and Fancher [28] developed a similar linear yaw-plane mathematical model to investigate the directional response and lateral stability of multi-axle and multi-articulated tank trucks assuming negligible roll dynamics. The natural modes of oscillation and the directional stability limits of the vehicle were determined through the eigen value analysis. The study revealed that the lateral acceleration of the pup trailer of the Michigan double tank is considerably higher than that of the tractor under a obstacle-avoidance maneuver at highway speed. Increasing the lateral stiffness of the hitch could effectively reduce this high rearward amplification of the lateral acceleration.

On the basis of a review of the reported studies on lateral dynamics of articulated vehicles, Vlk [7] stated that the lateral dynamics of articulated vehicles have not been adequately addressed, while relatively little information was available on the comparison of the reported models. Furthermore, the reported vehicle models mostly assumed linear cornering forces due to tires. Ervin et al. [1] investigated the influence of vehicle sizes

and weights on the stability and control characteristics of heavy trucks and tractor-trailer combinations and provided most significant knowledge for formulating the weights and dimensional regulations in the 80's. The results attained from computer simulations were validated through a limited number of field tests. These models clearly predicted the periodic yaw response of the trailer about its equilibrium, but did not give any information about a periodic trailer swing and jackknife because of the lack of a bounded and nonlinear tire model.

In recent years, the research efforts have been directed towards development of increasingly sophisticated computer simulation models to handle complex tire models. Owing to the strong dependence of the directional dynamics of a vehicle combination on the forces generated at the tire-road interface, a wide range of nonlinear tire models have evolved for the lateral stability analysis of heavy vehicles under braking and steering maneuvers [29]. Susemihl and kranter [30] developed a nonlinear vehicle model to investigate the performance in view of current design features, such as fifth wheel reactions and anti-lock braking system.

A comprehensive three-dimensional simulation program, referred to as the "Yaw/Roll model", was developed by the UMTRI (University of Michigan Transportation Research Institute) to simulate the directional dynamics of heavy vehicle combinations under steering input at constant forward speed [31]. The simulation program has been widely used to assess the relative directional performance characteristics of different vehicle combinations. The simulation program used nonlinear

tire forces, and force-deflection characteristics of the suspension using look-up tables. The program could simulate for an open-loop (steer input) or a close-loop (path coordinates input) steering maneuvers. Yaw/roll model has been extensively used to assess roll, yaw and lateral directional responses of heavy vehicle combinations comprising up to 4 units and 11 axles with 4 different types of articulation mechanisms. This model was further enhanced to study the vehicle response to simultaneous steering and braking inputs [31]. This model, referred to as the "Phase IV model", is capable of simulating the directional dynamics of trucks, tractor-semitrailers, doubles and triples. The mathematical model incorporates up to 71 degrees-of-freedom depending upon the vehicle configuration.

El-Gindy and Wong [32] performed a comparative study of various simulation programs of different complexities developed for directional response analysis of articulated vehicles. The study considered four simulation models: the linear yaw-plane model [28]; the total braking and steering (TBS) model [33]; the yaw/roll model; and the Phase IV model [31]. The study concluded that a more sophisticated simulation model, such as Phase IV model, does not necessarily create more accurate results than the simple models, such as the linear yaw-plane model and the TBS models. The transient steering response characteristics of a tractor-semitrailer in a lane-change maneuver, simulated by the four programs, were observed to be comparable.

The directional dynamic response characteristics of heavy vehicles have been mostly reported for perfectly smooth roads, assuming negligible effect of road surface

roughness. The effects of road roughness on the various handling and directional control measures have been investigated in only a few studies [34]. The tire's interactions with rough road tend to cause variations in the normal forces acting on the tires, which would influence the tire cornering and adhesion properties, and thus the handling performance.

1.2.2 MULTI – AXLE TRAILERS WITH LIFTABLE AXLES

Commercial vehicles, for the reasons of economy, have been seeking means for transporting larger loads, while conforming to the provincial laws governing the maximum weights and dimensions. The use of multi-axle trailers has been steadily growing for transportation of higher loads. Multi-axle trailer combinations, however, are known to cause significantly high magnitude of steady-state and transient off-tracking and thus limited maneuverability during turns [35]. Excessive off-tracking of the vehicle also causes substantial tire scrub and rapid tire wear [5]. Liftable trailer axles have been employed to enhance the load carrying capacity of the LCV's, which when lifted during turns provide acceptable maneuverability and reduced tire wear [2]. The LCV with raised axles would yield significantly different axle loads, mass/inertial distribution, and tire loads and thus the cornering properties. The variations in these parameters may also cause differences in the handling and directional performance characteristics of the LCVs. The use of liftable axles in a LCV is acceptable within the road laws, where the primary purpose is enhance the maneuverability, while only minimal efforts were made to study the impact of such axles on the resulting handling performance [2].

Furthermore, the higher loads on the axles on the ground, when either one or more axles are raised, impose excessive dynamic loads on the pavement leading to rapid fatigue and premature failure. A few recent studies have shown that certain vehicle configurations using liftable axles cause significant infrastructure wear because these lift axles are often raised to negotiate corners, which can severely overload the remaining axles [5]. Many concerns on the continuing use of liftable axles have thus been raised by various regulatory bodies.

The Ontario Ministry of Transportation undertook a test program to investigate the influence of liftable axles on the dynamic performance of vehicle combinations under different operating conditions [36]. The test program included ten different tractor-semitrailer configurations comprising 3-axle tractors and five- or more axle semi-trailers. The performance for each vehicle configuration within the program was evaluated with liftable axles down, and raised as is commonly necessary to allow this vehicle to turn. The results attained from the test program revealed that the combinations with liftable axles down yield slightly better high-speed dynamic performance, while none of these configurations could turn with the liftable axles down. Owing to the significant overloads of the remaining axles, the study stated that none of these configurations could be considered "infrastructure-friendly" [37].

1.2.3 MULTI – AXLE TRAILERS WITH SELF-STEERING AXLE

Owing to the performance limits of liftable axles, a number of concepts in self- and forced-steering axles have been proposed. A forced-steering axle provides the

steering of a trailer axle in proportion to either the front axle steering or the articulation angle using a control algorithm and an actuation mechanism [5]. Complex control algorithms, however, are required to account for the speed dependence of the desired steer angle. The implementation of such axles, however, has been severely limited due to associated high cost and hardware requirements. The self-steering axles, on the other hand, provide steering action in response to the lateral forces developed at the tire-road interface in a passive manner [5].

Self-steering axle may be a fixed axle mounted on a turntable (turntable type), or a steering axle with a tilted kingpin installed as a supplementary axle without being connected to the steering system [6]. All self-steering axles are equipped with a self-centering mechanism to offset the effects of unbalanced braking forces between wheels of the axle and a restoring mechanism that returns the steering axle to the zero steer position.

Leblanc et al. [6] have described the principles of self-steering axles and conducted an analytical study of two types of self-steering axles. The study investigated the influences of self-steering axle parameters on the steady-state handling behavior of different vehicle configurations, while neglecting coulomb friction and assuming linear cornering characteristics of the self-steering axle. Woodrooffe et al. [38] concluded that a self-steering axle must generate a minimum lateral force of 25% of the rated axle load and a minimum longitudinal force of 10% at the same axle load in order to satisfy the high speed handling requirements. Moreover, these minimum force requirements must be

achieved within 1 degree of self-steer angle, and the minimum force requirement should be maintained over angular displacement of 15 degree.

An experimental study conducted by the MTO (Ministry of Transportation of Ontario) [36] revealed that the directional characteristics of a vehicle configuration with semitrailer with a self-steering belly axle were comparable to those of the fixed axle semitrailer. It was speculated that the lateral acceleration level during the test might not have been high enough to activate the self-steering mechanism. It was also shown that the self-steering axle in the forward location results in off-tracking similar to that of the two-axle semitrailer configuration. Comparing with the vehicles with fixed axles, the self-steering axle could reduce the tire scrub. Billing et al. [39] indicated that there was little experience about self-steering axles on semitrailer at that time, which was perhaps the primary reason for the CCMTA (Canadian Council of Motor Trucking Administrator) and RTAC (Road and Transport Association of Canada) to not to recommend the use of self-steering axle in the Vehicle Weights and Dimension Study [5].

Aurell et al. [40] studied the influence of steered axles on the dynamic stability of different vehicle configurations. Since the self-steering axles provide considerably lower cornering force, vehicle configurations with such axles yield poor directional stability and control performance, which contradicts the findings of Billing et al. [39]. It was thus emphasized that the self-steering axles must generate sufficient cornering forces for the total vehicle weight. The influence of the location of the steered axles on the dynamics stability was further investigated using the linear and nonlinear models. The study

showed that a self-steering axle located at the trailer rear could lead to vehicle instability. Better directional performance was achieved when the self-steering axle was located as the leading trailer axle.

Sankar et al. [41] investigated the dynamic characteristics of a self-steering axle integrated to a three-dimensional yaw/roll model of an articulated tractor-semitrailer vehicle. Computer simulations were performed to determine the directional response characteristics of a tractor-semitrailer with self-steering axles for low- or high-speed maneuvers. The directional response characteristics of the vehicles with self-steering axles were discussed in view of the self-steering parameters, and compared with those of the vehicle with conventional fixed axles. The study concluded that the low-speed maneuverability and dynamic directional performance of the vehicle are strongly influenced by the self-steering axle location, and its static and dynamic properties. The greatest advantage of the self-steering axle was stated as the reduced tire wear, especially for a low stiffness self-steering axle.

1.2.4 Road Damage Potential of Vehicle Combinations

Heavy vehicle tires are known to transit high magnitude dynamic forces to the pavement, which are caused by their relative high axle loads and dynamic tire-road interactions. Such high tire loads cause rapid pavement deterioration and premature failure. Owing to the high costs associated with maintenance of highway infrastructure, the transportation authorities have invariably emphasized the need to regulate the vehicle weights and dimensions [42-44]. A number of experimental and analytical studies have

been undertaken to assess the damage caused by heavy vehicles, and the role of various contributory factors. These studies have resulted in considerable knowledge on the influences of various vehicle design and operating parameters on the dynamic loads transmitted to the pavement and the pavement damage potential [8,45,46]. These studies have further classified these contributory factors according to: axle configuration (weight and spacing), tire configuration (number per axle, type and pressure), static load sharing ability of the suspension, and dynamic tire forces.

Many studies have identified the high significance of the dynamic component of the tire forces with regard to the road damaging potential of the vehicle [8,47-49]. The magnitudes of such components could be of sizeable proportion of the mean tire forces, while the magnitudes strongly depend upon the vehicle weight, vehicle configuration, axle load, tire and suspension properties, road roughness and speed [49-51]. Moreover, the dynamic tire forces exhibit high "spatial repeatability" for different vehicles, which implies that certain points along the road will continually sustain peak dynamic tire forces, thereby increasing the damage incurred at those points [52-55].

Although dynamic tire forces of heavy vehicles are known to accelerate the pavement fatigue, generally accepted methods to quantify the road damage potential have not been established. Alternatively, a number of performance measures have been proposed to assess the relative damage potential of the heavy vehicles and the influence of various design and operation conditions. These include the spatial repeatability,

dynamic load coefficient (DLC), road stress factor (RSF), aggregate force criterion (AFC), etc. [56-62]

On the basis of the tire forces observed for three different vehicles with different suspensions but operating on the same road, Ervin [56] observed that the peak dynamic forces occurred at the same point along the road for all vehicles. Collop and Cebon [54] have showed that the road damage is strongly influenced by the degree of such spatial repeatability of the applied dynamic loads. Cole and Cebon [53] simulated the spatial repeatability of a fleet of leaf sprung articulated vehicle models and concluded that up to two-thirds of these vehicles have a repeated feature of tire loading. The high degree of spatial repeatability indicates the importance of controlling dynamic tire forces of heavy vehicles.

A measure based on the variations in the tire forces, referred to as 'Dynamic load coefficient' (DLC), has been widely used to assess the relative road-friendliness or damage potential of different vehicles. The DLC for a vehicle tire is defined as:

$$\mathrm{DLC} = \frac{\text{RMS dynamic tyre force}}{\text{static tire force}} \tag{1-1}$$

Many studies have shown that the DLC of articulated vehicle tires is strongly depended on the road surface roughness, vehicle configuration, geometry and mass distribution, axle loads, properties of the axle suspension and tires, vehicle speed and vehicle vibration modes [8, 49, 57-59]. Typical values of DLC in the 0.1 to 0.3 range have been widely reported under normal straight-line driving conditions.

While the DLC of tire loads serves as a convenient measure for assessing relative road-friendliness of different vehicles, it does not relate to the stresses imposed on the pavement. Moreover, a lightly loaded tire may yield a higher value of DLC due to the normalization used in the definition. Eisenmann [60] proposed an alternate measure, referred to as the road stress factor (RSF), which is based on the 'fourth power law' [3]. Assuming that the dynamic wheel force is normally distributed, Eisenmann [60] showed that the expected value of the fourth power of the instantaneous force Φ is given by:

$$\Phi = (1 + 6\bar{s}^2 + 3\bar{s}^4)P_{stat}^4 \qquad (1\text{-}2)$$

where P_{stat} is the static tire force, and $\bar{s}$ is the coefficient of variation of the dynamic tire force, such as DLC.

While the RSF approach for estimating the road damage potential has been widely applied [57, 61], it has been recognized that the RSF does not account for the spatial distribution of the dynamic tire forces. The 'Aggregate force criterion' (AFC) measure was proposed to account for the spatial repeatability of the tire force [62]. The proposed road damage criterion relates to the forces applied to particular points along the road surface for assessing the road damage. The method simply involves the summing of the measured dynamic tire forces or tire-road contact stresses due to each axle applied to each location along the road, raised to power n. Such a criterion has also been referred to as the dynamic aggregate force criterion (DAFC) and dynamic aggregate stress criterion (DASC) [62]. The aggregate force criterion gives the most realistic and accurate indication of the road damage potential of the dynamic tire forces.

1.3 SCOPE AND LAYOUT OF THE THESIS

1.3.1 SCOPE OF THE THESIS

From the literature review, it is evident that while significant progress has been made on establishing the directional stability limits of articulated vehicles, the influence of road roughness on the directional stability has not been adequately addressed. Although liftable axles have been implemented to improve the vehicle maneuverability, and reduce the tire scrub and wear, the overloading of the remaining axles on the ground raises two important concerns that have not been clearly addressed: the influence of liftable axles being retracted on vehicle dynamic tire loads and the impact on the pavement; the influence of liftable axles being retracted on the vehicle directional stability. The self-steering axles seem to be most appropriate for controlling the axle overloading caused by liftable axles. The handling and directional control characteristics of multi-axle vehicle combinations with one or more steering axles have been investigated in a few studies only.

The scope of this dissertation research is thus formulated to study the relative directional dynamic and dynamic pavement loading performance characteristics of different heavy vehicle combinations equipped with conventional, and one or more liftable and steerable axles. The specific objectives of the study are:

1) To formulate the analytical model of an articulated freight vehicle with 3- to 6-axle semitrailers, comprising nonlinear tire-road interactions and one or more liftable axles to study the directional dynamic performance of the vehicle under excitations arising from both the steering input and the road roughness.

2) To develop an analytical model of a self-steering axle and integrate the model to the total vehicle model, and investigate the directional dynamic response of the vehicle combinations with self-steering axles.

3) Investigate the influences of the road roughness and suspension damping ratio on the various directional performance measures of the vehicles with conventional, liftable and self-steering axles.

4) Investigate the relative road damaging potentials of the vehicle combinations with conventional / self-steering axles, and liftable axles.

1.3.2 LAYOUT OF THE THESIS

In chapter 2, an analytical model of a tractor-semitrailer configuration is presented and the equations of motion for the model are derived to study the response to road roughness and steering inputs. Various assumptions made in the formulations are also presented. Furthermore, the analytical model of a self-steering axle is formulated and relationships for deriving the self-steering angle is formulated and integrated into the vehicle model.

In chapter 3, the performance measures and evaluation methods related to the dynamic directional performance and relative road damage potentials of the vehicle combinations are discussed in detail. The road roughness is characterized on the basis of the roughness index (RI) values to investigate the vehicle performance under different road conditions. Different steering maneuvers required for assessment of various performance measures are also discussed.

The vehicle configurations together with the associated mass distribution and static axle loads are derived in chapter 4, with one or more liftable axles retracted. The

simulation parameters, such as suspension and tire properties, for the vehicle configurations with conventional, liftable, and self-steering axles are also presented. The simulation matrix together with the data analysis methods are discussed.

The performance measures related to directional control and road-friendliness, derived from the simulation results are presented in chapter 5 and 6. The influences of one or more liftable axles retracted are discussed by comparing the performance characteristics with those of the conventional axle vehicles. The influences of variations in the road roughness and suspension damping ratio on the performance measures are further discussed.

The major conclusions drawn from the simulation results are summarized in chapter 7 together with the major highlights of the study and recommendations for further studies.

CHAPTER 2 : DEVELOPMENT OF VEHICLE MODEL

2.1 GENERAL

A large number of in-plane and three-dimensional models of heavy vehicles have been developed to study the yaw, lateral and roll directional dynamic responses to steering inputs [34]. These models vary from a simple linear yaw-plane model to a sophisticated 71-degrees-of-freedom nonlinear model [34]. Apart from these, a number of vehicle dynamics simulation programs have been commercially developed to assess the directional response characteristics of heavy trucks and truck-trailer combinations subject to steering and braking inputs [32]. These programs, however, do not permit the required analysis of different vehicle combinations with liftable and self-steering axles, subject to steering inputs and random road roughness.

A comprehensive three-dimensional yaw/roll plane vehicle simulation program developed by UMTRI [31] has been adopted in this study as the baseline simulation program. The program incorporates nonlinear tire and suspension characteristics of different articulated vehicle combinations comprising up to 4 units and 11 axles, and different articulation mechanisms. The program, however, considers perfectly smooth roads and fixed conventional axles. The baseline program is thus appropriately modified to incorporate the tire interactions with randomly distributed road roughness, while the variations in the liftable axles are realized by varying the vehicle configuration and the resulting axle loads. Furthermore, an analytical model of a self-steering axle is

formulated and integrated with the simulation program. The yaw/roll simulation program, thus developed, is used to study the relative directional and pavement load response characteristics of vehicle configurations with conventional, liftable and steerable axles.

2.2 YAW / ROLL MODEL

The yaw/roll vehicle model, developed by UMTRI [31] has been widely used to assess the directional performance characteristics of vehicle combinations subject to steering input at constant forward speeds [31,34]. The program could be applied to simulate for a road train of up to 4 units and 11 axles in any arbitrary configuration. In this investigation, the simulation program is applied to assess the directional dynamics and road-friendliness of a tractor-semitrailer combination comprising a three-axle tractor, and a three-, four-, five- or six-axle semitrailer.

The yaw/roll vehicle model incorporates the nonlinear corning characteristics of tires as a function of the sideslip angle and normal load, and nonlinear suspension characteristics using look-up tables. The nonlinear suspension characteristics, such as backlash, could also be incorporated within the load-deflection tables. The additional roll moment caused by leaf springs twist in the roll plane can also be included by an auxiliary roll stiffness parameter in the program. The vehicle model can be simulated in both the closed-loop and open-loop steering modes. In the open-loop mode, the time history of the steering wheel angle of tractor front axle is applied as the steering input to the model. In the closed-loop mode, a path-follower model incorporating the driver's preview ability

and transport lag is used to compute the steering wheel angle to follow the desired trajectory.

The present investigation uses both open-loop and closed-loop steering inputs, and road roughness input to evaluate the directional performance and dynamic tire forces of the vehicle. The equations of motion for the vehicle model have been reported in many earlier studies [34]. The governing equations of motion for the tractor with three axles combined with a semitrailer with three-, four-, five-, and six-axle are modified in this study to include the tire interaction with the road roughness and self-steering axle mode. Various assumptions of the yaw/roll model and the final form of the equations of motion are presented in the following subsections.

2.2.1 ASSUMPTIONS

The yaw/roll model of the articulated vehicle is developed subject to a number of simplifying assumptions. The major assumptions include:

1) The vehicle is assumed to move at a constant forward speed on a horizontal surface with uniform frictional feature;

2) It is assumed that pitch angles of the sprung masses and the relative roll angles between the sprung and unsprung masses are very small, such that small angle simplifications, $\sin(*) \approx 0$ and $\cos(*) \approx 1$, are applicable;

3) The model assumes that each unit (tractor and semitrailer) consists of a rigid body sprung mass and a number of beam axles represented by unsprung masses, which are connected to the sprung mass by a complaint suspension system;

4) The relative roll motions between the sprung and unsprung masses are assumed to take place about the roll center of each axle, which is located at a fixed distance

beneath the sprung mass and free to move along the vertical axis of the unsprung mass;

5) Each suspension is independent of the other suspension, which means the load transfers and sharing among various axles are neglected and thus the total load on each axle is constant during the simulation;

6) The fifth wheel coupling allows each unit to roll, pitch and yaw with respect to another unit. The relative roll motion between the two units, however, is limited by the nonlinear moment-deflection properties of the articulation mechanism.

Unlike the reported yaw/roll model, this study concerns with the vehicle combination moving on a road with random surface irregularities. Furthermore, the liftable or self-steering axles are considered to replace a number of rigid axles on the semitrailer.

2.2.2 EQUATIONS OF MOTION

Figure 2-1 illustrates the schematic of a tractor-semitrailer combination together with the axis system used. Although the figure shows a 4 axles semitrailer, a general model is formulated for 3 to 6 axles semitrailer considered in the study. Owing to the constant forward velocity, each sprung mass is considered as a rigid body with 5-degrees-of- freedom (DOF), including lateral, vertical, yaw, roll and pitch motions. Each unsprung mass is considered to possess 2-degrees-of-freedom (DOF): vertical and roll motions.

Three axis systems are used in this model, which include an inertial axis system (i_n, j_n, k_n), axis system fixed to each of the sprung mass (i_s, j_s, k_s), and axis system fixed

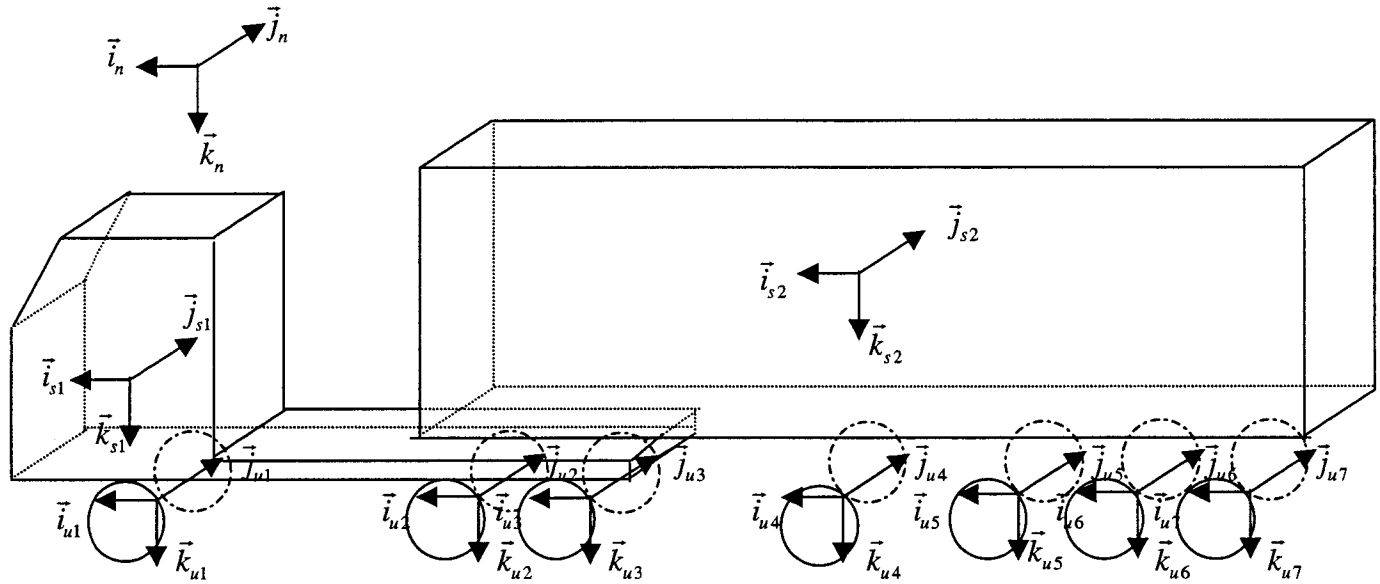

Figure 2-1: Tractor-semitrailer configuration and its axis systems (12F13).

to each of the unsprung mass (i_u, j_u, k_u). Three Euler angles, namely yaw (ψ_s), pitch (θ_s) and roll (ϕ_s), are used to indicate the orientation of each of the sprung mass axis system with respect to its inertial axis system. The pitch angular deflection, however, are assumed to be small, such that $\sin\theta_s \approx \theta_s$, and $\cos\theta_s \approx 1$. The transformation matrix relating the body fixed sprung mass axis system and the inertial axis system can be obtained as [63]:

$$\begin{Bmatrix} \bar{i}_s \\ \bar{j}_s \\ \bar{k}_s \end{Bmatrix}_f = \begin{bmatrix} \cos\psi_s & \sin\psi_s & -\theta_s \\ -\sin\psi_s\cos\phi_s + \theta_s\cos\psi_s\sin\phi_s & \cos\psi_s\cos\phi_s + \theta_s\sin\psi_s\sin\phi_s & \sin\phi_s \\ \sin\psi_s\sin\phi_s + \theta_s\cos\psi_s\cos\phi_s & -\cos\psi_s\sin\phi_s + \theta_s\sin\psi_s\cos\phi_s & \cos\phi_s \end{bmatrix}_f \begin{Bmatrix} \bar{i}_n \\ \bar{j}_n \\ \bar{k}_n \end{Bmatrix} \quad (2\text{-}1)$$

in the above equation, the subscript f is used to denote the unit (for tractor, $f = 1$; for semitrailer, $f = 2$).

Each axle is allowed to only roll and bounce with respect to the sprung mass to which the axle is attached. The orientation of the axle with respect to the inertial axis system is defined by the yaw angle (ψ_s). The transformation matrix relating the unsprung mass axis system and the sprung mass axis system is given by:

$$\begin{Bmatrix} \bar{i}_u \\ \bar{j}_u \\ \bar{k}_u \end{Bmatrix}_l = \begin{bmatrix} 1 & \theta_{sf}\sin\phi_{sf} & \theta_{sf}\cos\phi_{sf} \\ -\theta_{sf}\sin\phi_u & \cos(\phi_{sf} - \phi_u) & -\sin(\phi_{sf} - \phi_u) \\ -\theta_{sf}\cos\phi_u & \sin(\phi_{sf} - \phi_u) & \cos(\phi_{sf} - \phi_u) \end{bmatrix}_l \begin{Bmatrix} \bar{i}_s \\ \bar{j}_s \\ \bar{k}_s \end{Bmatrix}_f \quad (2\text{-}2)$$

where l represents the axle number. For tractor $(f = 1)$, $l = 1,2,3$; and for trailer $(f = 2)$, $l = 4,5,..9$.

The equations of motion of each sprung mass are written in terms of the body fixed translation (u_s, v_s, w_s) and angular (p_s, q_s, r_s) velocities, and their derivatives $(\dot{u}_s, \dot{v}_s, \dot{w}_s, \dot{p}_s, \dot{q}_s, \dot{r}_s)$.

Figure 2-2 illustrates the roll plane of the three-dimensional vehicle model representing a sprung mass supported on the suspension springs. Each spring can generate either compressive or tensile forces along an axis parallel to the $\vec{k}_{ul}$ axis of the unsprung mass. Each sprung mass rolls about a roll center, which is located at a fixed distance (z_{Rl}) beneath the sprung mass. The components of force developed in the roll plane that are perpendicular to the suspension springs axis are assumed to act at the roll center. The roll center is allowed to move only along the $\vec{k}_{ul}$ axis of the unsprung mass. The suspension force of axle l transmitted to the sprung mass can be expressed as:

$$F_{suspl} = F_{Rl}\vec{j}_{ul} - (F_{l1} + F_{l2})\vec{k}_{ul} \tag{2-3}$$

By using the coordinate transformation matrix relating unsprung and the sprung masses, expressed in equation (2-2), the suspension force in the sprung mass coordinate system can be computed as:

$$\begin{aligned} F_{suspl} = {} & [-F_{Rl}\theta_{sf}\sin\phi_{ul} + (F_{l1} + F_{l2})\theta_{sf}\cos\phi_{ul}]\vec{i}_{sf} \\ & + [F_{Rl}\cos(\phi_{sf} - \phi_{ul}) - (F_{l1} + F_{l2})\sin(\phi_{sf} - \phi_{ul})]\vec{j}_{sf} \\ & - [F_{Rl}\sin(\phi_{sf} - \phi_{ul}) + (F_{l1} + F_{l2})\cos(\phi_{sf} - \phi_{ul})]\vec{k}_{sf} \end{aligned} \tag{2-4}$$

The roll center force F_{Rl} acting through the roll center is an internal force, which can be computed from the lateral dynamic equilibrium equation of the unsprung mass:

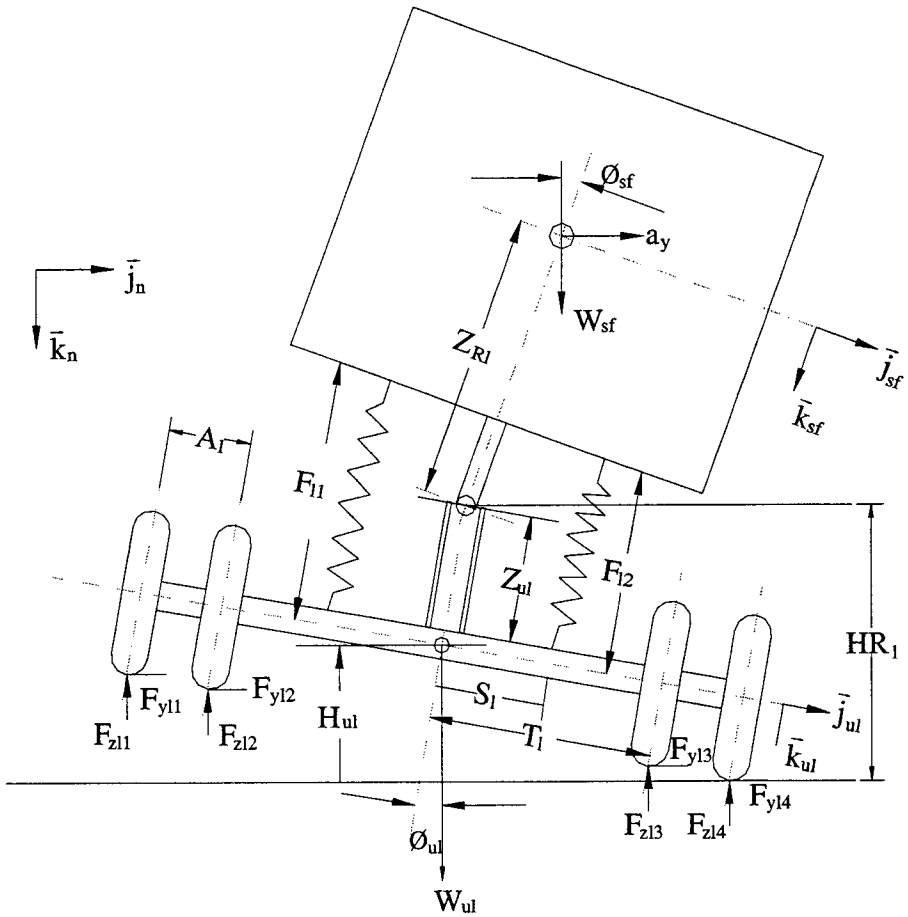

Figure 2-2: Forces and moments acting in the roll plane of the vehicle (rear view).

$$F_{Rl} = -m_{ul}[\vec{a}_{mul} \bullet \vec{j}_{ul}] + (F_{yl1} + F_{yl2} + F_{yl3} + F_{yl4})\cos\phi_{ul}\cos\delta_{ssal} - (F_{zl1} + F_{zl2} + F_{zl3} + F_{zl4})\sin\phi_{ul} + m_{ul}g\sin\phi_{ul} \quad (2\text{-}5)$$

in the above equation, m_{ul} is the unsprung mass and a_{mul} is its lateral acceleration along the $\vec{j}_{ul}$ axis, F_{ylm} $(m = 1,....,4)$ are the cornering forces due to tires and F_{zlm} $(m = 1,....,4)$ are tire normal forces. The above equation is generalized to incorporate the steer angle δ_{ssal} due to each axle. For conventional vehicle configuration comprising non-steerable drive and trailer axles $\delta_{ssal} = 0$ (for $l \neq 1$).

The lateral acceleration of the unsprung mass a_{mul} is derived in the following manner:

$$\vec{a}_{mul} = \vec{a}_{msf} + \vec{a}_{Rl/msf} + \vec{a}_{mul/Rl} \quad (2\text{-}6)$$

where a_{msf} is the lateral acceleration of the sprung mass, $a_{mul/Rl}$ is the unsprung mass acceleration relative to the roll center, and $a_{Rl/msf}$ is the roll center acceleration relative to the sprung mass, given by [34,63]:

$$\vec{a}_{msf} = (\dot{u}_s + q_s w_s - r_s v_s)_f \vec{i}_{sf} + (\dot{v}_s + u_{s_s} r_s - p_s w_s)_f \vec{j}_{sf} + (\dot{w}_s + p_s v_s - q_s u_s)_f \vec{k}_{sf} \quad (2\text{-}7)$$

$$\vec{a}_{Rl/msf} = \dot{\vec{v}}_{Rl/msf} = (\dot{q}_s z_{Rl} - x_{Rl} q_s^2 + p_s r_s z_{Rl} - x_{Rl} r_s^2)_f \vec{i}_{sf} + (-\dot{p}_s z_{Rl} + x_{Rl}\dot{r}_s + z_{Rl} q_s r_s + x_{Rl} q_s p_s)_f \vec{j}_{sf} + (-p_s^2 z_{Rl} + x_{Rl} r_s p_s - z_{Rl} q_s^2 - x_{Rl}\dot{q}_s)_f \vec{k}_{sf} \quad (2\text{-}8)$$

$$\vec{a}_{mul/Rl} = \dot{\vec{v}}_{mul/Rl} = p_{ul} r_{ul} z_{ul}\vec{i}_{ul} - (\dot{p}_{ul} z_{ul} + 2p_{ul}\dot{z}_{ul})\vec{j}_{ul} - (p_{ul}^2 z_{ul} - \ddot{z}_{ul})\vec{k}_{ul} \quad (2\text{-}9)$$

Equations (2-6) to (2-9) yield following expression for the sprung mass lateral acceleration:

$$\begin{aligned}\bar{a}_{mul} \bullet \bar{j}_{ul} &= -(\dot{u}_s + q_s w_s - r_s v_s + \dot{q}_s z_{Rl} - x_{Rl} q_s^2 + p_s r_s z_{Rl} - x_{Rl} r_s^2)_f \theta_{sf} \sin\phi_{ul} \\ &+ (\dot{v}_s + u_s r_s - p_s w_s - \dot{p}_s z_{Rl} + x_{Rl} \dot{r}_s + z_{Rl} q_s r_s + x_{Rl} q_s p_s)_f \cos(\phi_{sf} - \phi_{ul}) \\ &- (\dot{w}_s + p_s v_s - q_s u_s - p_s^2 z_{Rl} + x_{Rl} r_s p_s - z_{Rl} q_s^2 - x_{Rl} \dot{q}_s)_f \sin(\phi_{sf} - \phi_{ul}) \\ &- \dot{p}_{ul} z_{ul} - 2 p_{ul} \dot{z}_{ul}\end{aligned} \tag{2-10}$$

The roll center force F_{Rl} is derived from equations (2-5) and (2-10), as:

$$\begin{aligned}F_{Rl} &= -m_{ul}[-(\dot{u}_s + q_s w_s - r_s v_s + \dot{q}_s z_{Rl} - x_{Rl} q_s^2 + p_s r_s z_{Rl} - x_{Rl} r_s^2)_f \theta_{sf} \sin\phi_{ul} \\ &+ (\dot{v}_s + u_s r_s - p_s w_s - \dot{p}_s z_{Rl} + x_{Rl} \dot{r}_s + z_{Rl} q_s r_s + x_{Rl} q_s p_s)_f \cos(\phi_{sf} - \phi_{ul}) \\ &- (\dot{w}_s + p_s v_s - q_s u_s - p_s^2 z_{Rl} + x_{Rl} r_s p_s - z_{Rl} q_s^2 - x_{Rl} \dot{q}_s)_f \sin(\phi_{sf} - \phi_{ul}) \\ &- \dot{p}_{ul} z_{ul} - 2 p_{ul} \dot{z}_{ul}] + (F_{yl1} + F_{yl2} + F_{yl3} + F_{yl4}) \cos\phi_{ul} \cos\delta_{ssal} \\ &- (F_{zl1} + F_{zl2} + F_{zl3} + F_{zl4}) \sin\phi_{ul} + m_{ul} g \sin\phi_{ul}\end{aligned} \tag{2-11}$$

The equations of motion for the sprung masses are derived upon consideration of the suspension and tire forces, roll center forces and constraint forces.

Equation of Lateral Motion

$$\begin{aligned}m_{sf} \dot{v}_{sf} - m_{sf} (p_s w_s - r_s u_s)_f &= \sum \bar{j}_{sf} \text{ component of the constraint forces} \\ &+ \sum_{l=jl}^{j2} [F_{Rl} \cos(\phi_{sf} - \phi_{ul}) - (F_{l1} + F_{l2}) \sin(\phi_{sf} - \phi_{ul})] + m_{sf} g \sin\phi_{sf}\end{aligned} \tag{2-12}$$

where jl and j2 represents the number of axles attached to the sprung mass f. For f = 1 (tractor), jl = 1 and j2 = 3. For f = 2 (semitrailer), jl = 4 and j2 = 6 to 9, depending upon the number of trailer axles. F_{l1} and F_{l2} are the forces developed by suspension springs along the $\bar{k}_{ul}$ axis.

Equation of Vertical Motion

$$\begin{aligned}m_{sf} \dot{w}_{sf} - m_{sf} (q_s u_s - p_s v_s)_f &= \sum \bar{k}_{sf} \text{ component of the constraint forces} \\ &+ \sum_{l=jl}^{j2} [F_{Rl} \sin(\phi_{sf} - \phi_{ul}) + (F_{l1} + F_{l2}) \cos(\phi_{sf} - \phi_{ul})] + m_{sf} g \cos\phi_{sf}\end{aligned} \tag{2-13}$$

Equation of Roll Motion

$$I_{xxsf}\dot{p}_{sf} - (I_{yys} - I_{zzs})_f q_{sf} r_{sf} = \sum \text{roll moments from the constraints}$$
$$- \sum_{l=jl}^{j2} F_{Rl} \cos(\phi_{sf} - \phi_{ul}) z_{Rl} + \sum_{l=jl}^{j2} (F_{l1} + F_{l2}) s_l + \sum_{l=jl}^{j2} (F_{l1} + F_{l2}) \sin(\phi_{sf} - \phi_{ul}) z_{Rl} \qquad (2\text{-}14)$$
$$+ \sum_{l=jl}^{j2} KRS_l (\phi_{sf} - \phi_{ul})$$

where $I_{xxsf}, I_{yysf}, I_{zzsf}$ are roll, pitch and yaw mass moments of inertia of the sprung mass f, z_{Rl} is the vertical distance between the lth roll center and c.g. of the sprung mass f, s_l is the half suspension lateral spread of axle l and KRS_l is the auxiliary roll stiffness of the axle l suspension.

Equation of Pitch Motion

$$I_{yysf}\dot{q}_{sf} - (I_{zzs} - I_{xxs})_f p_{sf} r_{sf} = \sum \text{pitch moments from the constraints}$$
$$+ \sum_{l=jl}^{j2} [F_{Rl} \sin(\phi_{sf} - \phi_{ul}) + (F_{l1} + F_{l2}) \cos(\phi_{sf} - \phi_{ul})] x_{ul} \qquad (2\text{-}15)$$

where x_{ul} is the longitudinal distance from the sprung mass c.g. to axle l.

Equation of the Yaw Motion

$$[\sum_{l=jl}^{j2} I_{zzuf} + I_{zzsf}]\dot{r}_{sf} - (I_{xxs} - I_{yys})_f p_{sf} q_{sf} = \sum \text{yaw moments from the constraints} +$$
$$\sum_{l=jl}^{j2} ([F_{Rl} \cos(\phi_{sf} - \phi_{ul}) - (F_{l1} + F_{l2}) \sin(\phi_{sf} - \phi_{ul})] x_{ul}$$
$$+ \sum_{l=jl}^{j2} (AT_{l1} + AT_{l2} + AT_{l3} + AT_{l4}) \cos\phi_{sf} \cos\delta_{ssal}) \qquad (2\text{-}16)$$
$$+ \sum_{l=jl}^{j2} ([F_{zl1}(T_l + A_l) + F_{zl2} T_l - F_{zl3} T_l - F_{zl4}(T_l + A_l)] \sin\delta_{ssal})$$

where AT_{lm} $(m = 1,...,4)$ are the aligning moment due to tires on axle l, T_l is the half-track width of inner tires on axle l and A_l is the dual tire spacing on tires on axle l.

The equations of roll and bounce motions of each unsprung mass are derived in a similar manner and expressed below.

Equation of Roll Motion

$$\begin{aligned} I_{xxul}\dot{p}_{ul} &= -(F_{l1}-F_{l2})s_1 - F_{Rl}z_{ul} - [(F_{yl1}+F_{yl2}+F_{yl3}+F_{yl4})\cos\phi_{ul}\cos\delta_{ssal} \\ &+ (F_{zl1}+F_{zl2}+F_{zl3}+F_{zl4})\sin\phi_{ul}](HR_1\cos\phi_{ul}-z_{ul}) \\ &+ (F_{zl1}-F_{zl4})(T_1+A_1)\cos\phi_{ul} + (F_{zl2}-F_{zl3})T_1\cos\phi_{ul} + KRS_1(\phi_{sf}-\phi_{ul}) \end{aligned} \tag{2-17}$$

where I_{xxul} is the roll mass moment of inertia of unsprung mass 1, z_{ul} is vertical distance between the c.g. of the unsprung mass and the roll center for axle 1 and HR_1 is height of roll center 1 from the ground plane.

Equation of Vertical Motion

$$\begin{aligned} m_{ul}\vec{a}_{mul}\bullet\vec{k}_{ul} &= m_{ul}g\cos\phi_{ul} + F_{l1} + F_{l2} - (F_{zl1}+F_{zl2}+F_{zl3}+F_{zl4})\cos\phi_{ul} \\ &- (F_{yl1}+F_{yl2}+F_{yl3}+F_{yl4})\sin\phi_{ul}\cos\delta_{ssal} \end{aligned} \tag{2-18}$$

The acceleration of the unsprung mass along the $\vec{k}_{ul}$ axis can be evaluated in a manner similar to that described for $\vec{a}_{mui}\bullet\vec{j}_{ui}$ in equation (2-10), such that:

$$\begin{aligned} \vec{a}_{mul}\bullet\vec{k}_{ul} &= -(\dot{u}_s + q_s w_s - r_s v_s + \dot{q}_s z_{Rl} - x_{Rl}q_s^2 + p_s r_s z_{Rl} - x_{Rl}r_s^2)_f\,\theta_{sf}\cos\phi_{ul} \\ &+ (\dot{v}_s + u_s r_s - p_s w_s - \dot{p}_s z_{Rl} + x_{Rl}\dot{r}_s + z_{Rl}q_s r_s + x_{Rl}q_s p_s)_f\sin(\phi_{sf}-\phi_{ul}) \\ &+ (\dot{w}_s + p_s v_s - q_s u_s - p_s^2 z_{Rl} + x_{Rl}r_s p_s - z_{Rl}q_s^2 - x_{Rl}\dot{q}_s)_f\cos(\phi_{sf}-\phi_{ul}) \\ &+ (\ddot{z}_{ul} - p_{ul}^2 z_{ul}) \end{aligned} \tag{2-19}$$

Constraint Forces and Moments Equations

The differential equations of motion derived for the sprung unit comprise the constraint forces and moments imposed by the coupling between the tractor and the trailer. The tractor-semitrailer configurations considered in this study employ a conventional fifth wheel that permits the tractor and semitrailer to yaw freely relative to each other, but offers considerable resistance to roll and pitch motion. The constraint

forces can be determined from the kinematics expressions relating the accelerations due to the tractor and semitrailer at the coupling. The acceleration of the tractor sprung unit at the constraint location (a_{c1}) can be derived from the position vector as follows:

$$\begin{aligned}
&\vec{a}_{c1} = (\dot{u}_{s1} + q_{s1}w_{s1} - r_{s1}v_{s1} + \dot{q}_{s1}z_{c1} - x_{c1}q_{s1}^2 + p_{s1}r_{s1}z_{c1} - x_{c1}r_{s1}^2)\vec{i}_{s1} \\
&+ (\dot{v}_{s1} + u_{s1}r_{s1} - p_{s1}w_{s1} - \dot{p}_{s1}z_{c1} + x_{c1}\dot{r}_{s1} + z_{c1}q_{s1}r_{s1} + x_{c1}q_{s1}p_{s1})\vec{j}_{s1} \\
&+ (\dot{w}_{s1} + p_{s1}v_{s1} - q_{s1}u_{s1} - x_{c1}\dot{q}_{s1} - p_{s1}^2z_{c1} + x_{c1}r_{s1}p_{s1} - z_{c1}q_{s1}^2)\vec{k}_{s1} \\
&= a_1\vec{i}_{s1} + b_1\vec{j}_{s1} + c_1\vec{k}_{s1}
\end{aligned} \tag{2-20}$$

The acceleration of the semitrailer sprung unit at the constraint is also derived in a similar manner:

$$\begin{aligned}
&\vec{a}_{c2} = (\dot{u}_{s2} + q_{s2}w_{s2} - r_{s2}v_{s2} + \dot{q}_{s2}z_{c2} - x_{c2}q_{s2}^2 + p_{s2}r_{s2}z_{c2} - x_{c2}r_{s2}^2)\vec{i}_{s2} \\
&+ (\dot{v}_{s2} + u_{s2}r_{s2} - p_{s2}w_{s2} - \dot{p}_{s2}z_{c2} + x_{c2}\dot{r}_{s2} + z_{c2}q_{s2}r_{s2} + x_{c2}q_{s2}p_{s2})\vec{j}_{s2} \\
&+ (\dot{w}_{s2} + p_{s2}v_{s2} - q_{s2}u_{s2} - x_{c2}\dot{q}_{s2} - p_{s2}^2z_{c2} + x_{c2}r_{s2}p_{s2} - z_{c2}q_{s2}^2)\vec{k}_{s2} \\
&= a_2\vec{i}_{s2} + b_2\vec{j}_{s2} + c_2\vec{k}_{s2}
\end{aligned} \tag{2-21}$$

Considering that the accelerations of two units must be identical at the articulation point ($a_{c1} = a_{c2} = a_c$), the transformation to the semitrailer coordinate system yields following expressions for the lateral and vertical accelerations of the semitrailer sprung weight:

$$\begin{aligned}
b_2\vec{j}_{s2} = \{&a_1[-\cos\phi_{s2}\sin(\psi_{s2} - \psi_{s1}) - \theta_{s1}\sin\phi_{s2} + \sin\phi_{s2}\theta_{s2}\cos(\psi_{s2} - \psi_{s1})] \\
&+ b_1[\cos\phi_{s1}\cos\phi_{s2}\cos(\psi_{s2} - \psi_{s1}) + \sin\phi_{s1}\sin\phi_{s2} - \sin\phi_{s1}\theta_{s1}\cos\phi_{s2}\sin(\psi_{s2} - \psi_{s1}) \\
&+ \sin\phi_{s2}\theta_{s2}\cos\phi_{s1}\sin(\psi_{s2} - \psi_{s1})] + c_1[-\sin\phi_{s1}\cos\phi_{s2}\cos(\psi_{s2} - \psi_{s1}) \\
&+ \cos\phi_{s1}\sin\phi_{s2} - \cos\phi_{s1}\cos\phi_{s2}\theta_{s1}\sin(\psi_{s2} - \psi_{s1}) \\
&- \sin\phi_{s1}\sin\phi_{s2}\theta_{s2}\sin(\psi_{s2} - \psi_{s1})]\}\vec{j}_{s2}
\end{aligned} \tag{2-22}$$

and

$$
\begin{aligned}
c_2\vec{k}_{s2} = \{&a_1[\sin\phi_{s2}\sin(\psi_{s2}-\psi_{s1}) - \cos\phi_{s2}\theta_{s1} + \cos\phi_{s2}\theta_{s2}\cos(\psi_{s2}-\psi_{s1})] \\
&+ b_1[-\cos\phi_{s1}\sin\phi_{s2}\cos(\psi_{s2}-\psi_{s1}) + \cos\phi_{s2}\sin\phi_{s1} + \sin\phi_{s1}\sin\phi_{s2}\theta_{s1}\sin(\psi_{s2}-\psi_{s1}) \\
&+ \cos\phi_{s1}\cos\phi_{s2}\theta_{s2}\sin(\psi_{s2}-\psi_{s1})] + c_1[\sin\phi_{s1}\sin\phi_{s2}\cos(\psi_{s2}-\psi_{s1}) \\
&+ \cos\phi_{s1}\cos\phi_{s2} + \cos\phi_{s1}\sin\phi_{s2}\theta_{s1}\sin(\psi_{s2}-\psi_{s1}) \\
&- \sin\phi_{s1}\cos\phi_{s2}\theta_{s2}\sin(\psi_{s2}-\psi_{s1})]\}\vec{k}_{s2}
\end{aligned}
\tag{2-23}
$$

The constraint moments arising from the fifth wheel are evaluated from the relative angular displacement between the tractor and the semitrailer units. The roll moment acting on the tractor, M_{x1}, is computed from the product of the constraint stiffness k_5 and the relative angular displacement. On the other hand, the roll and pitch moments acting on the semitrailer (M_{x2} and M_{y2}) can be computed through the coordinate transformation, such that:

$$M_{x1} = K_5[\phi_{s2}\cos(\psi_{s2}-\psi_{s1}) - \theta_{s2}\sin(\psi_{s2}-\psi_{s1}) - \phi_{s1}] \tag{2-24}$$

$$M_{x2} = -M_{x1}[\cos(\psi_{s2}-\psi_{s1}) + \theta_{s1}\theta_{s2}] \tag{2-25}$$

$$M_{y2} = -M_{x1}[\theta_{s2}\cos(\psi_{s2}-\psi_{s1})\sin\phi_{s2} - \theta_{s1}\sin\theta_{s2} - \sin(\psi_{s2}-\psi_{s1})\cos\phi_{s2}] \tag{2-26}$$

2.3 FORCES AND MOMENTS AT THE TIRE-ROAD INTERFACE

The dynamic responses of the sprung and unsprung masses strongly depend on the forces and moments developed at the tire-road interface, namely lateral and vertical tire forces (F_{ylm} and F_{zlm}), and the tire aligning moment (AT_{lm}).

2.3.1 VERTICAL TIRE FORCE

The instantaneous vertical force developed at the interface of the tire m of axle l, F_{zlm}, is dependent on the tire vertical stiffness, KT_{lm}, and the tire deformation, Δ_{lm}. Assuming linear vertical stiffness of the tire, the vertical force can be expressed as:

$$F_{zlm} = KT_{lm}\Delta_{lm} \; ; \qquad m = 1,...,4 \text{ and } l = 1,...,9 \tag{2-27}$$

Assuming a smooth road surface, as considered in the reported yaw/roll model [31,63], the vertical tire deformation, Δ_{lm}, is derived from the vertical and roll motions of the sprung and unsprung masses. The vertical deformation of the left most tire ($m = 1$) of axle 1 is computed as:

$$\Delta_{11} = \Delta_{ol} + \Delta z_s - z_{Rl}(1-\cos\phi_s) + \Delta z_{ul} - \Delta z_{uol} - (T_l + A_l)\sin\phi_{ul} - x_{ul}\theta_s \tag{2-28}$$

where Δz_s and Δz_{ul} are the vertical deflections of the sprung and unsprung masses along the inertial axis $\bar{k}_n$. Δ_{ol} is the static tire deflection, and Δz_{uol} is the distance between the roll center and the c.g. of the unsprung mass.

The vertical deflections of the remaining tires can be derived from the following:

$$\Delta_{12} = \Delta_{11} + A_l \sin\phi_{ul} \tag{2-29}$$

$$\Delta_{13} = \Delta_{11} + (A_l + 2T_l)\sin\phi_{ul} \tag{2-30}$$

$$\Delta_{14} = \Delta_{11} + 2(A_l + T_l)\sin\phi_{ul} \tag{2-31}$$

The analysis of road friendliness or pavement damage potential of the vehicle necessitates consideration of the tire interaction with randomly rough road surface. Assuming that the dual tires set on one side of a axle is subjected to identical road roughness, and LRD and RRD describe the elevations of the road surface at the contact points of the left and the right tires, the tire deformation incorporating the surface elevation can be derived from:

$$\Delta^*_{11} = \Delta_{11} - \text{LRD} \tag{2-32}$$

$$\Delta^*_{12} = \Delta_{12} - \text{LRD} \tag{2-33}$$

$$\Delta^*_{13} = \Delta_{13} - \text{RRD} \tag{2-34}$$

$$\Delta^*_{14} = \Delta_{14} - \text{RRD} \tag{2-35}$$

where Δ^*_{lm} refers to the deformation of tire m on axle l due to vehicle motion and the road roughness. The instantaneous dynamic tire loads caused by road excitations and steering inputs can thus be evaluated using equations (2-27) to (2-35).

2.3.2 Lateral Tire Force and Aligning Moment

The equations of motion for the vehicle combinations employing self-steering axles at the semitrailer are derived in a similar manner as described in [31]. The steer angles due to self-steering axles, however, are assumed to sufficiently large in the study. Figure 2-3 illustrates the yaw-plane model of the vehicle incorporating a self-steering semitrailer axle. The cornering forces and aligning moments due to tires are influenced mostly by the vertical tire load and the tire sideslip angle in a nonlinear manner. In the yaw/roll model, the tire lateral forces and moments are computed using a look-up table with linear interpolation on the basis of the instantaneous vertical tire force and the sideslip angle.

The sideslip angle at the tire-road contact point is derived from the longitudinal and lateral velocities of the tire and steer angle of the wheel (Figure 2-4), which can be expressed as:

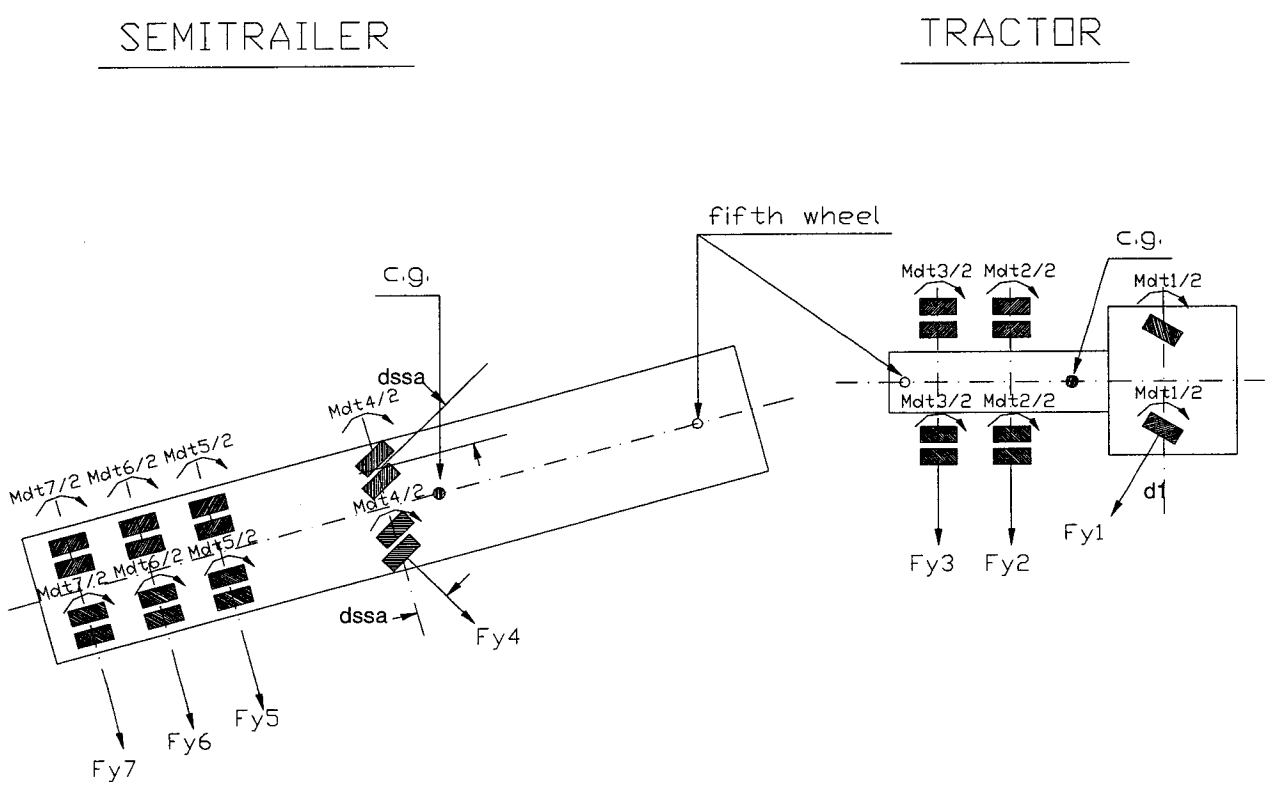

Figure 2-3: Lateral tire forces in yaw-plane of an articulated vehicle with self-steering semitrailer axle.

$$\alpha_{lm} = \tan^{-1}\left(\frac{v_{axlel}}{u_{tirelm}}\right) - \delta_l; \qquad l = 1,....,9 \text{ and } m = 1,...,4 \tag{2-36}$$

where α_{lm} is the sideslip angle of the tire, and v_{axlel} is the lateral velocity of axle l at the tire-road contact point which is expressed as:

$$v_{axlel} = (v_s - z_{Rl}p_s)_f \cos\phi_{sf} + \frac{x_{ul}r_{sf}}{\cos\phi_{sf}} - p_{ul}HR_l \cos\phi_{ul} \tag{2-37}$$

u_{tirelm} is the forward speed of the tire m on axle l, and is given by:

$$u_{tirel1} = u_{sf} + (T_l + A_l)r_{sf} \tag{2-38}$$

$$u_{tirel2} = u_{sf} + T_l r_{sf} \tag{2-39}$$

$$u_{tirel3} = u_{sf} - T_l r_{sf} \tag{2-40}$$

$$u_{tirel4} = u_{sf} - (T_l + A_l)r_{sf} \tag{2-41}$$

In equation (2-36), δ_l is the wheel steer angle. The steer angle for the non-steering axle is taken as $\delta_l = 0$, while that for the self-steering axle is considered as $\delta_l = \delta_{ssal}$.

2.4 SELF STEERING AXLE

The steer angle generated by a self-steering axle, δ_{ssa}, strongly influences the vehicle maneuverability and directional performance. Self-steering axle was first developed in Italy to serve as a second axle of the tandem axle group on straight trucks to improve off-tracking and reduce tire scuffing in tight turns [6]. In the tandem configuration, the fixed lead axle supported at least 60% of the tandem axle group load. It was further assumed that this fixed axle could provide the cornering force required for the

vehicle, which implies that the self-steering axle was not designed to produce primary cornering forces for the vehicle during high speed turning maneuver.

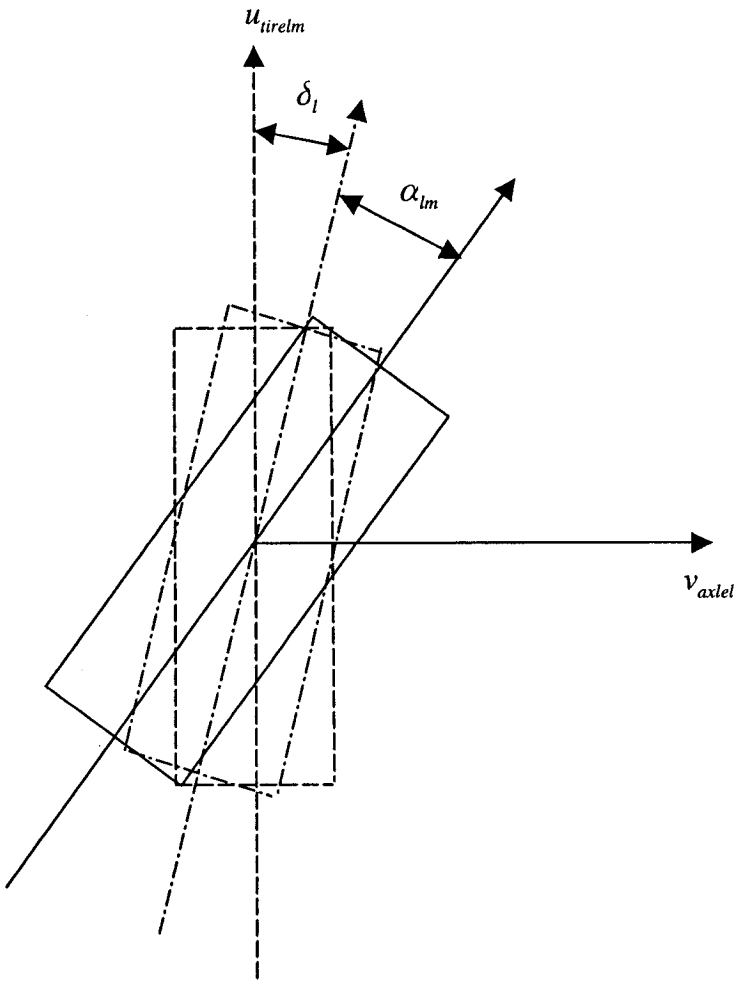

Figure 2-4: Self-steer and slip angles of tire m on axle l.

In order to compensate for the effect of unbalanced braking between wheels of the tandem axle group and to restore the steering axle to the zero steer position quickly and smoothly, a self-centering mechanism is widely used on most self-steering axles. In the

absence of this centering device, the internal friction within the self-steering axle would freeze the axle in a steered position until the magnitudes of the sideslip angles of the tires approach sufficiently high to overcome these friction forces [6]. When sufficient side force has been generated to overcome the friction, a rapid change in the steer angle of the self-steering axle occurs, which could result in a lateral force lash or jerk that is transmitted to the vehicle [6]. The self-steering axles are presently used in different heavy vehicle configurations, and specialty vehicles such as concrete mixers in the tag position. The self-steering axle can be divided into two generic types, namely, the automotive type and the turntable type.

The automotive self-steering axle utilizes kingpin and tie road assembly as shown in Figure 2-5. The turntable self-steering axle consists of a large diameter roller bearing or turntable that allows for relative rotation parallel to the ground plane between the main frame and the suspension. The axle is set aft of the center of rotation of the turntable to provide caster kinematics essential for the self-steering operation (Figure 2-5). Both types of self-steering axles use a center seeking or zero steer biased forcing system. The centering system may be the most varied component among the different axle designs. These axles are also equipped with a locking mechanism to lock the axle when the axle is in the zero steering position that must be ensured, when the vehicle runs on adverse road conditions or when the vehicle travels in reverse direction.

Figures 2-6 and 2-7 illustrate the free body diagrams of the turntable and the automotive self-steering axles. While the constructions of the two axles differ

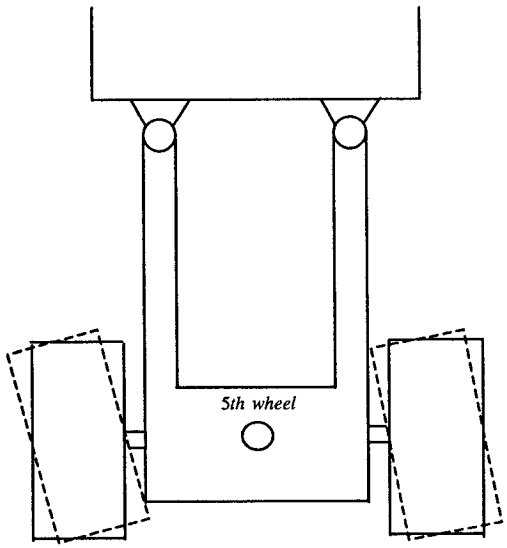

Automotive steer

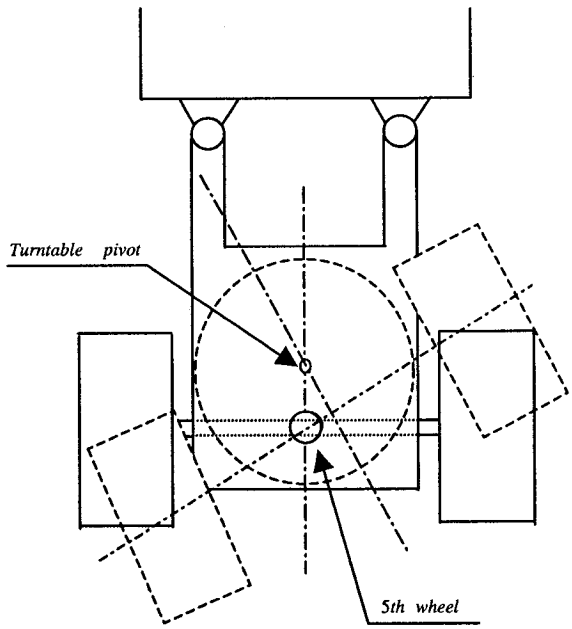

Turntable steer

Figure 2-5: Schematic representation of automotive and turntable type self-steering axle.

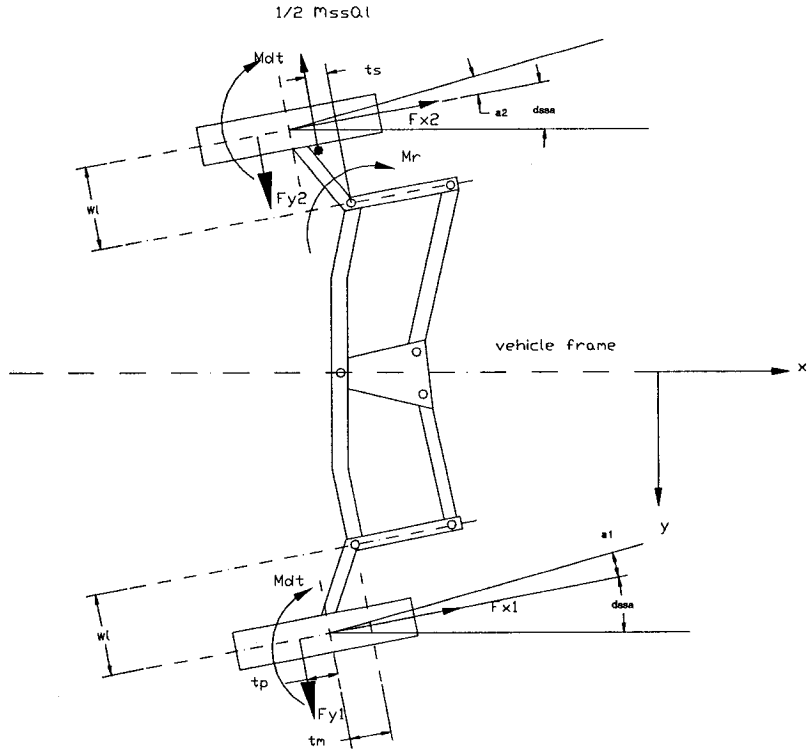

Figure 2-6: Free body diagram of the automotive self-steering axle.

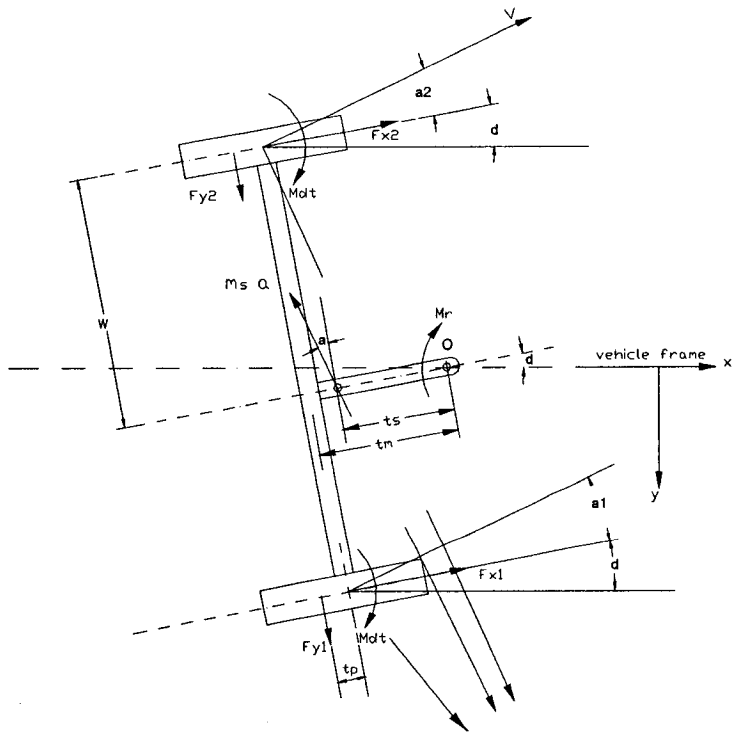

Figure 2-7: Free body diagram of the turntable self-steering axle.

considerably, both systems are governed by the equivalent steady-state moment balance. Let M_r represent the moment that resists the angular displacement of the tires about their pivot points. For the turntable self-steering axle, the pivot point is located at the center of the roller bearing (point *o* in Figure 2-6). For the automotive self-steering axle, the wheel kingpin represents the pivot point. Summation of moment about the pivot point yields:

$$M_r = (F_{yl1} + F_{yl2} + F_{yl3} + F_{yl4})t_{ss} + (F_{xl1} + F_{xl2} - F_{xl3} - F_{xl4})w_k - 2M_{dt} - m_{ss}t_s a_l \cos\alpha_{lm} \quad (2\text{-}42)$$

where F_{ylm} $(m = 1,...,4)$ are the tire lateral forces, F_{xlm} $(m = 1,...,4)$ are the tire longitudinal forces, M_{dt} is the dual tire moment, w_k is the kingpin offset, and t_{ss} is the corrected caster trail that represents the distance between the lateral tire force and the pivot point, and is equal to the sum of the pneumatic trail t_p and the mechanical caster trail t_m. Note that the dual tire arrangement is not shown in the Figures 2-6 and 2-7 to ensure clarity. The self-steering axle mass m_{ss} is determined by summing the masses due to all the components, which undergo the movement relative to the vehicle frame when the axle is subjected to an angular displacement. In equation (2-42), a_l is the lateral acceleration of the axle mass, t_s defines the distance between the location of the c.g. of the axle and the pivot point, and α_{lm} is the average sideslip angle of tire m on axle l taken as positive in the counter-clockwise direction.

Dividing each term in equation (2-42) by t_{ss}, the resultant lateral force due to self-steering axle could be obtained as:

$$F_r = F_{yl1} + F_{yl2} + F_{yl3} + F_{yl4} + (F_{x1} + F_{xl2} - F_{xl3} - F_{xl4})w_k / t_{ss} + C_s A_l^{\,2} / R - m_{ss} a_l \quad (2\text{-}43)$$

where $F_r = M_r / t_{ss}$ is the resultant lateral force resisting the angular displacement and acting at a distance t_{ss} from the pivot point, which is termed as the self-steering axle cornering force. The dual tire moments are expressed in terms of the equivalent longitudinal stiffness C_s, the dual tire spacing A_1 and the tire radius R [64]. The dimension t_s is assumed to be approximately equal to t_{ss} and the average tire sideslip angle α_{lm} is assumed to be very small, such that $t_s \cos\alpha_{lm} / t_{ss} \approx 1$.

Under a constant forward speed the longitudinal forces developed by the trailer tires are neglected. Moreover, the dual tire moment and self-steering axle inertial forces are relatively small when compared to the tire cornering forces. The resultant axle cornering forces may thus be expressed as summation of the lateral forces developed by individual tires:

$$F_r = \sum F_{ylm} \; ; \quad m = 1,...,4 \text{ and } l = 1,...,9 \tag{2-44}$$

The equation (2-42) reveals that the dual tire moments tend to deteriorate the self-steering axle's ability to resist the angular displacement caused by the tire lateral forces, while the axle inertial force enhances this ability of the self-steering axle. For a typical self-steering axle, the cornering characteristics could be expressed by axle cornering stiffness, k_{ss}, that is defined as the rate of change of axle cornering force with respect to change in the self-steering angle δ_{ssa}:

$$k_{ss} = \partial F_r / \partial \delta_{ssa} \tag{2-45}$$

Figures 2-8 and 2-9 illustrate the typical axle cornering characteristics of a self-steering axle [41]. Figure 2-8 illustrates the resultant force-deflection properties that are

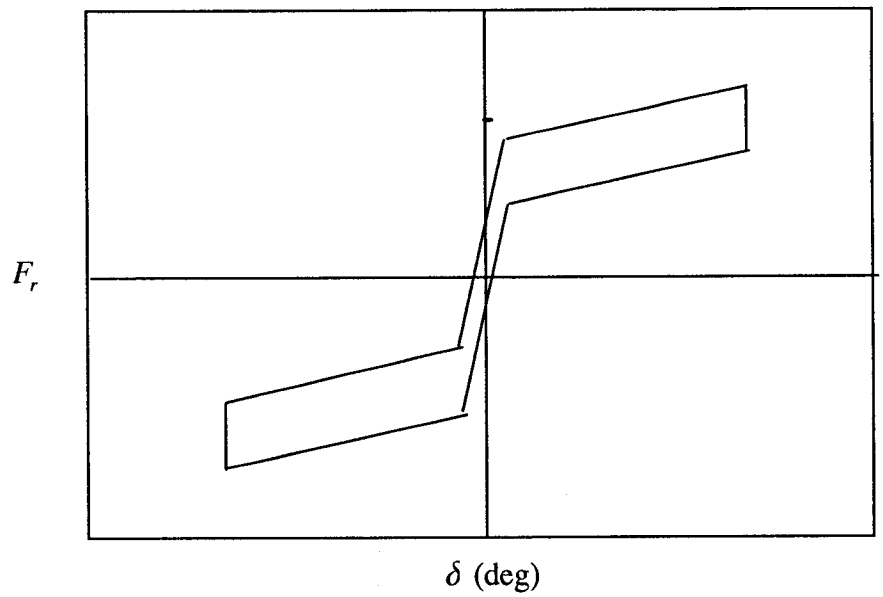

Figure 2-8: Self-steering axle cornering characteristics.

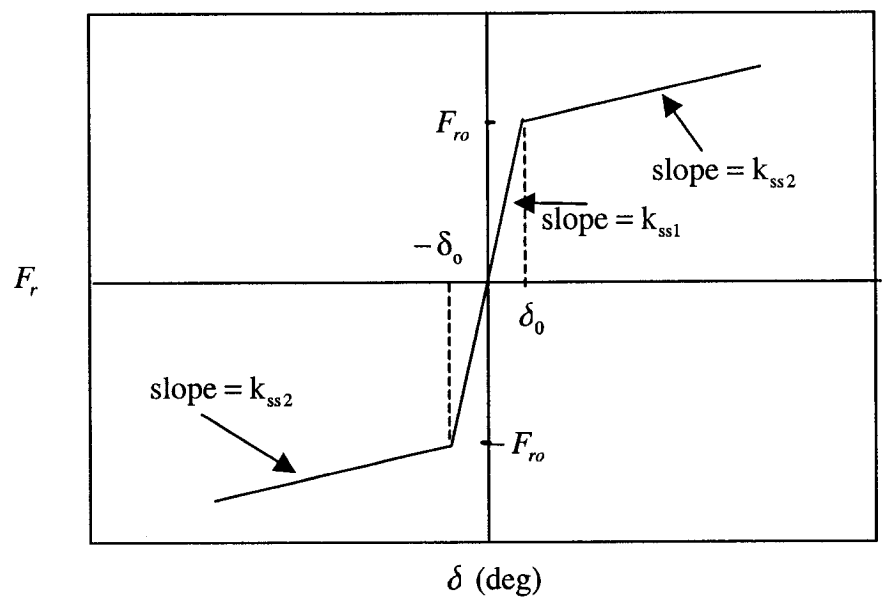

Figure 2-9: Ideal representation of a self-steering axle cornering characteristics.

hysteretic due to the presence of nonlinear spring rates and coulomb friction in the steering system. The mean force-deflection properties are obtained by neglecting the coulomb friction, as shown in Figure 2-9. Furthermore, the axle cornering force can be expressed in a piecewise linear manner, such that:

$$F_r = k_{ss2}\delta_{ssa} + F_{ro}(1 - k_{ss2}/k_{ss1}); \qquad \text{for } F_r > F_{ro} \tag{2-46}$$

$$F_r = k_{ss1}\delta_{ssa}; \qquad \text{for } -F_{ro} \le F_r \le F_{ro}, \tag{2-47}$$

$$F_r = k_{ss2}\delta_{ssa} - F_{ro}(1 + k_{ss2}/k_{ss1}); \qquad \text{for } F_r < -F_{ro}, \tag{2-48}$$

where $F_{ro} = k_{ss1}\delta_o$ is referred to as the self-steering axle centering force, δ_o represents the self-steering angle corresponding to the axle centering force, k_{ss1} is the equivalent cornering stiffness corresponding to small steering angle ($-\delta_0 < \delta_{ssa} < \delta_0$), k_{ss2} is the cornering stiffness corresponding to a larger steer angle ($\delta_{ssa} > \delta_o$). It is obvious that the cornering stiffness k_{ss2} of the self-steering axle is substantially reduced when the resultant cornering force exceeds the axle centering force. The performance characteristics of a self-steering axle is evaluated by its response to external moments, which are represented by the sum of the terms on the right hand side of the equation (2-42). The resultant lateral force due to a self-steering axle is frequently normalized with respect to the axle load and expressed in units of g, such that:

$$a_{rl} = F_r g / W_l \tag{2-49}$$

where a_{rl} is the normalized cornering force due to axle 1 and W_l is the rated axle load. The axle's centering force can also be expressed in a similar manner:

$$a_{rol} = F_{ro} g / W_1 \tag{2-50}$$

where a_{rol} is the normalized centering force. The steering angle developed by a self-steering axle, δ_{ssa}, can be derived from Equations (2-46) to (2-48) and expressed as:

$$\delta_{ssa} = F_r / k_{ss2} - F_{ro}(1 + k_{ss2} / k_{ss1}) / k_{ss2}, \quad \text{for } F_r < -F_{ro} \tag{2-51}$$

$$\delta_{ssa} = F_r / k_{ss1}, \quad \text{for } -F_{ro} \le F_r \le F_{ro} \tag{2-52}$$

$$\delta_{ssa} = F_r / k_{ss2} - F_{ro}(1 - k_{ss2} / k_{ss1}) / k_{ss2}, \quad \text{for } F_r > F_{ro} \tag{2-53}$$

2.5 LIFTABLE AXLES

Liftable axles permit for adjustment of the axle loads and may be retracted to eliminate the axle tires contact with the ground. These operations can be performed by the vehicle operator. The liftable axles thus provide the convenience of having one or more extra axles when required to carry larger loads in accordance with the load regulations, and eliminate unnecessary tire scrub and wear during turns when retracted. A liftable axle in a tractor-semitrailer configuration is often installed as a belly axle, as illustrated in Figure 2-10. More than one liftable axle may also be installed in multi-axle trailer configurations. The directional dynamics of vehicle combinations with one or more liftable axles can be evaluated using the yaw/roll model by introducing the following variations:

- The number of axles is reduced when the liftable axles are retracted. For a N_1 axles combination with N_2 retracted axles, the total number of axles in the simulation program is adjusted to $(N_1 - N_2)$.

- The retracted axles would yield changes in the sprung weight and coordinates of the mass center, as evident in Figure 2-10. The sprung mass of the semitrailer is increased by the masses of the liftable axles:

$$m'_{s2} = m_{s2} + N_2 m_u \tag{2-54}$$

where m_u is the unsprung mass due to the liftable axle.

The longitudinal coordinate of semitrailer sprung mass c.g. with respect to the articulation point would also shift from x to x', as shown in the Figure 2-10, where the shifted coordinate is given by:

$$x' = \frac{m_{s2}x + m_u b}{m_{s2} + m_u} \tag{2-55}$$

where b is the location of the lifted axle from the articulation point. The vertical coordinate of the sprung mass would also shift to a lower position, and could be computed in a similar manner.

- The roll, pitch and yaw mass moments of inertia of the sprung mass ($I_{xxs2}, I_{yys2}, I_{zzs2}$) would also be re-evaluated due to variations in the sprung mass and the c.g. coordinates.

- The axle loads supported by the remaining axles are increased due to one or more retracted axles. Furthermore, the load supported by the fifth wheel coupling would also increase, which transfers higher loads to the tractor axles. The simulation program is updated using the revised axle loads, which are derived from the static mass and force balance, assuming perfect load equalization of the tandem or tridem axle groups.

2.6 METHOD OF SOLUTION

The differential equations of motion for the vehicle combinations, expressed in equations (2-12) to (2-18), are solved in the time domain under specific steering and road roughness inputs. The steering input is described either by the time-history of the front wheel steer angle (δ_1) in an open-loop manner or by the path coordinates in a

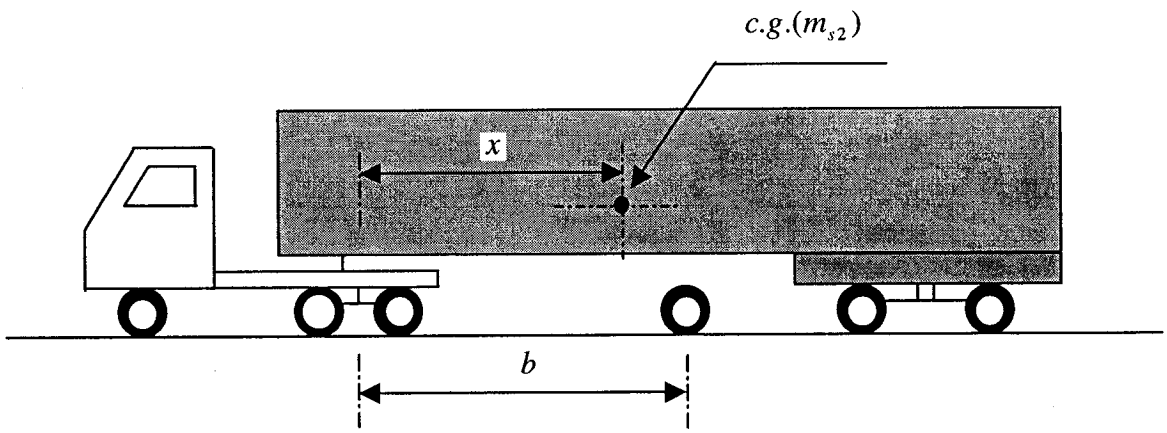

Liftable axle down

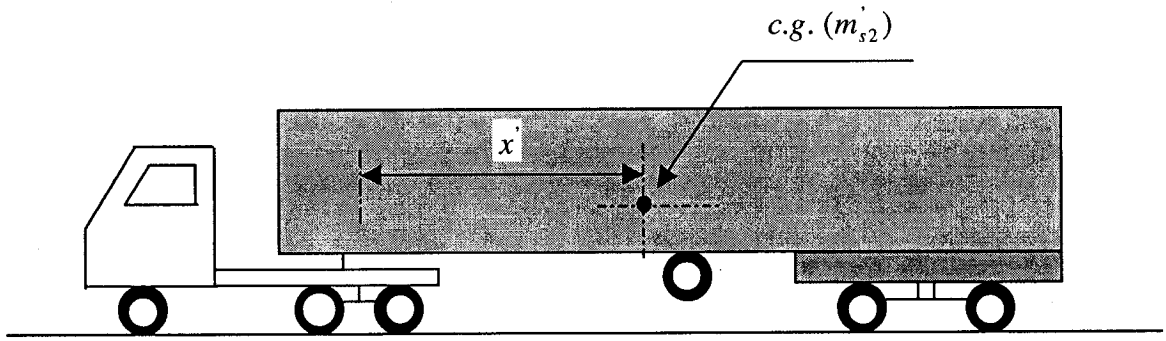

Liftable axle retracted

Figure 2-10: A schematic of a tractor-semitrailer combination with liftable axle on the ground and retracted.

closed-loop manner using a driver model. The road roughness input is represented by the elevations along the road, which can be more easily understood by converting to time-history of the elevation. The solution procedure is initiated by solving the differential equations of motion for a given steer input and road elevation over a small time increment, using numerical integration technique based on the predictor-corrector method. The vehicle configurations with liftable and steering axles are analyzed by introducing the variations discussed in section 2.5 and the self-steering model described in section 2.4, respectively. The cornering forces and aligning moments due to tires are computed at each interval using the look-up tables and responses in terms of normal loads and axle velocities. The suspension forces are also derived in a similar manner. The results are finally analyzed to derived the performance measures that are described in the following chapter.

CHAPTER 3 : PERFORMANCE MEASURES AND EXTERNAL INPUTS

3.1 INTRODUCTION

The directional response characteristics of heavy freight vehicles are assessed using a wide range of performance measures. These measures are frequently used to assess the relative highway safety and operational performance of different vehicle combinations and components designs. The selection of a set of performance measures depends upon the objective of the study. The measures to assess the overturning immunity may include the static rollover threshold acceleration, road safety factor, lateral load transfer ratio, axle roll angle, etc., while those for assessing the braking performance may include braking efficiency, stopping distance, time delays, stopping time, etc. The yaw performance of a vehicle combination is often assessed in terms of rearward amplification tendencies. Many other performance measures are also used to assess the off-tracking and jackknife tendencies, such as low-speed and high-speed off-tracking and friction demand [64].

The road damage potentials of heavy vehicles, on the other hand, employ measures based upon vertical tire forces. These include the dynamic load coefficient, road stress factor, aggregate force coefficient, etc., as described in chapter 1 [56-62]. These measures are evaluated either through field measurement or through simulations of

proven models. The choice of measures, however, depends upon the objective of the study.

The primary objectives of this dissertation concern with the constant velocity directional performance and road-friendliness of commercial vehicles with liftable and self-steering axles. Two sets of performance measures are thus formulated to assess the directional dynamics and road-friendliness of the vehicle combinations. These measures are discussed and formulated on the basis of various reported studies.

3.2 DIRECTIONAL DYNAMICS AND CONTROL MEASURES

Owing to the large weights and dimensions, and relative lower directional stability limits of heavy vehicles, the highway safety performance remains the most important design and operating issue for such vehicles. EI-Gindy [65] proposed a set of safety-related performance measures to assess the safety dynamic performance of heavy vehicles, which evolved from the weights and dimensions study performed by the University of Michigan Transportation Research Institute (UMTRI) [56]. Within Canada, these measures have been knows as the RTAC (Roads and Transportation Association of Canada) performance measures.

A number of performance measures are selected to assess the relative directional response of the candidate vehicles with liftable and self-steering axles, while subject to excitations due to road roughness. These measures are described in the following subsections.

3.2.1 STEADY – TURNING ROLLOVER THRESHOLD (SRT)

The rollover immunity of a heavy vehicle during a steady turn is evaluated in terms of static rollover threshold acceleration (SRT), defined as the maximum lateral acceleration that the vehicle can sustain before approaching a relative rollover condition [34,66]. For the vehicle configurations that are investigated in this study, the relative rollover condition is reached when tires on one track of all axles except the tractor front axle lose road contact. It has been suggested that the SRT value of a loaded vehicle must be above 0.35 g [67, 68].

SRT can be evaluated by subjecting the candidate tractor-semitrailer to a high-speed steady turn maneuver. The maneuver is conducted at a constant speed of 100 km / h , while the steering angle is increased at a very slow rate (2 degrees per second at the steering wheel). The steering angle is gradually increased until the relative rollover condition of the vehicle is reached. At this time the value of the semitrailer sprung mass lateral acceleration is taken as the SRT.

3.2.2 REARWARD AMPLIFICATION RATIO (RA)

When a vehicle combination is subjected to a rapid steering input at highway speeds, it generally exhibits considerably larger lateral and roll motions of the rearmost unit when compared to that of the lead unit. This characteristic of a vehicle can be assessed by the rearward amplification ratio, which is defined as the ratio of the peak lateral acceleration response of the rearmost trailer to that of the lead unit (tractor) [34,67]. This measure clearly indicates the amplification of lateral acceleration from the

tractor to the trailer unit during a maneuver. A large degree of rearward amplification implies higher likelihood of rollover of the trailer. It has been suggested that the rearward amplification ratio of a vehicle combination under a path change maneuver must not exceed a value of 2.2 [65]. This measure is obtained during a standardized path-change maneuver (described in section 3.4.2) conducted at a speed of $100\,km/h$, which yields lateral acceleration amplitude of $0.15\,g$ at the center of the front axle of the tractor within time period constraint of 3.0 seconds.

3.2.3 Dynamic Load Transfer Ratio (LTR)

While the SRT has been proven as an effective measure of roll stability in steady turns, it does not relate to the rollover potential at high speeds under dynamic steering maneuvers. Rollover immunity of a vehicle under transient directional maneuver can be directly related to load shift from the inboard tires to the outboard tires. The magnitude of this lateral load shift also relates to the relative rollover condition and can serve as an effective tool to assess dynamic rollover stability of the vehicle. The lateral load shift is measured in terms of Load Transfer Ratio (LTR) that is defined as the ratio of the sum of absolute value of the difference between the right wheel loads and the left wheel loads, to the sum of all the wheel loads [34], given by:

$$LTR = \frac{\sum_{l=1}^{N_1} \left| F_{zlleft} - F_{zlright} \right|}{\sum_{l=1}^{N1} (F_{zlleft} + F_{zlright})} \tag{3-1}$$

where F_{zlleft} is the vertical forces due to left tires, $F_{zlright}$ is the vertical forces due to right tires of axle l. N_l is the number of axle on the vehicle combination. From this equation, it is apparent that value of LTR approaches a unity value, when all the tires on a single track lose road contact. The LTR is evaluated under the high-speed path-change maneuver employed for assessing the Rearward Amplification conducted at a speed of 100 km / h . The recommended upper limit of the load transfer ratio is 0.6 [65,67].

3.2.4 FRICTION DEMAND

A vehicle combination under a steering maneuver requires certain road surface friction at the tractor drive axle(s) to prevent the tractor jackknifing specifically on low friction surfaces, such as icy roads. The required level of friction is defined by a measure, referred to as the Friction Demand, which is considered as the minimum friction request for a vehicle combination in order to negotiate a turn without suffering loss of control. This measure involves two different operating conditions: (i) the low-speed friction demand, which is assessed under a tight turn maneuver at a low speed; and (ii) the high-speed friction demand, which is computed under a high-speed path-change maneuver. Both friction demands are quantified by the peak frictional coefficient FD , given by:

$$FD = \left| \frac{\sum F_y}{\sum F_z \cos \Gamma} \right| \tag{3-2}$$

where $\sum F_y$ is the sum of drive-axle tire corning forces, $\sum F_z$ is the sum of drive-axle tire vertical loads, and Γ is the articulation angle between the tractor and the trailer. The higher value of the peak friction coefficient FD indicates a higher tendency to jackknife.

The vehicle would tend to lose control on low friction surface, such as on icy road. The maximum levels of high-speed and low-speed friction demand have been suggested as 0.3 and 0.1, respectively [65,67].

The vehicle model is analyzed under a 90° turn at a forward speed of 8.8 km/h, and the resulting forces at the drive-axle tires are applied in equation (3-2) to compute the low speed friction demand (LSFD). The vehicle path is monitored to ensure that the center of the front steer axle tracks an arc of 14m radius. The high speed friction demand of the vehicle combination is evaluated in a similar manner, while the analyses are performed under a path-change maneuver at a forward speed of 100 km/h. The high-speed friction demand of the drive-axle tires is usually much higher than the low-speed friction demand [65].

3.3 ROAD DAMAGE POTENTIAL CRITERIA

Dynamic tire forces applied to the road surfaces by heavy vehicles are believed to be an important factor leading to premature pavement failure. The rate of pavement damage is strongly dependent on the magnitude of the dynamic tire forces, which are influenced by the vehicle forward speed, road roughness, axle loads, and axle and vehicle configuration [49-51]. The pavement damage potential, also referred to as the road-friendliness of a heavy vehicles, is assessed by many different methods. The earlier methods that evolved for pavement and bridge designs were based on the 'static' function, which is evaluated on the basis of the static axle loads, the number of axles and

static load sharing between the axles [3]. The Equivalent Single Axle Load (ESAL) is widely considered to indicate the road damage potential of candidate vehicles. The dynamic load coefficient offers the most convenient mean to assess the relative road-friendliness of different vehicles. These two measures are described below and applied to evaluate the road friendliness of the vehicle with conventional and liftable axles.

3.3.1 EQUIVALENT SINGLE AXLE LOAD (ESAL)

The concept of Equivalent Single Axle Load (ESAL) is based on the relationship between the static axle load and its impact on the road, which is described by the 'fourth power law' [3]. This law was formulated from extensive field measurements performed by AASHO (the American Association of State Highway Officials) during 1958 to 1960. The 'fourth power law' suggests that the relationship between the axle load and its road damage potential is not linear, but increases by 4^{th} power. The ESAL measure defines the equivalent number of axles for a given axle and its load, as:

$$\mathrm{ESAL}_{\mathrm{axle}} = \left(\frac{\mathrm{F_{zl}}}{\mathrm{P_0}} \right)^4 \qquad (3\text{-}3)$$

where P_0 is a standard single axle load equal to $80\,kN$ (18,000lb), and $\mathrm{F_{zl}}$ is the actual axle load. The law is applied to compute the number of equivalent axles corresponding to an axle load, other than $80\ kN$. For example, an axle load of $111.2\ kN$ (25,000 lb) would represent 3.72 standard axles, and would pose 3.72 times greater potential for road damage.

For a specific vehicle configuration, the sum of ESAL for each axle or axle group is referred to as the "load equivalent factor" (LEF) for the vehicle type, which has been related to road damaging potential of the vehicle. The LEF for a vehicle combination is given by:

$$LEF = \sum_{l=1}^{N_1} \left(\frac{F_{szl}}{80000} \right)^4 \tag{3-4}$$

where N_1 is the total number of axles.

3.3.2 Dynamic Load Coefficient (DLC)

The total tire force that each axle of a vehicle exerts to the road surface consists of two components: (i) the static tire force; and (ii) the dynamic tire force caused by dynamic interactions of the vehicle with the road surface roughness. The dynamic tire force caused by a vehicle tire depends on speed, road roughness, vehicle configuration, axle load and particularly the characteristics of the suspensions and the tires [3]. The dynamic component of the tire force is considered as an additional force imposed on the road structure, which tends to accelerate the road structure failure. In order to compare the road damage potential and dynamic tire force caused by different vehicle configurations, a normalized measure of the dynamic force, referred to as the Dynamic Load Coefficient (DLC), was first introduced by Sweatman [49] in 1983, to assess the dynamic variations in the tire force. The DLC was defined as the ratio of the standard deviation of the tire force to the average tire force, such that:

$$DLC_l = \frac{\sigma_l}{\overline{F}_l} \tag{3-5}$$

where σ_l is the standard deviation of the force due to tires on axle 1, and $\overline{F}_l$ is the mean tire force on axle 1, which is equal to the static tire load. Typical values of DLC in the 0.05 to 0.3 range have been reported. A low value is generally considered desirable [34,69,70].

3.3.3 ROAD STRESS FACTOR (RSF)

Dynamic component of the tire load has been further applied to assess the road damage potential in terms of the road stress factor (RSF) [60]. The proposed measure is based upon three major assumptions: (i) the road damage is dependent on the instant dynamic tyre force at any point on the road surface raised to the fourth power on the basis of the 'fourth power law' [3]; (ii) the dynamic tire force follows a normal distribution, such that the dynamic tire force at any point on the road surface can be determined from [3]:

$$F(t) = \frac{1}{\sigma\sqrt{2\pi}} e^{-(t-\mu)^2/(2\sigma^2)} \tag{3-6}$$

where $F(t)$ yields the probable dynamic tire force value in the time range $(t, t+dt)$, μ is mean value and σ is standard deviation; and (iii) the vehicle can exert its peak wheel forces at any location along the road, while the spatial repeatability is ignored. The concept of road stress factor, Φ, was proposed by Eisenmann [60] in 1975, which can be computed from:

$$\Phi = E[(F(t)^4] = (1 + 6\bar{s}^2 + 3\bar{s}^4)P_{stat}^4 \quad (3\text{-}7)$$

where $F(t)$ is the dynamic tire force at a given time t, $\bar{s}$ is coefficient of variation of the dynamic tire force, P_{stat} is static tire force which is the same value as F_{szl} in equation (3-4), and operator E[] defines the expectation. The dynamic load coefficient (DLC) can be effectively applied as the coefficient of variation in equation 3-7 [34]. The road stress factor Φ_l of the tires on the axle l can thus be expressed in:

$$\Phi_l = (1 + 6DLC_l^2 + 3DLC_l^4)F_{szl}^4 \quad (3\text{-}8)$$

where F_{szl} is the static force of tires on axle l, and DLC_l can be obtained from equation (3-5).

3.3.4 Dynamic Aggregate Force Criterion (DAFC)

The field measurements performed by Cole and Cebon [53] revealed that the peak tire force applied by a vehicle tire tends to concentrate at specific locations along the road [70]. This contradicts the assumption (iii) in the formulation of the RSF, i.e. the road damage can be assessed from the average value of the tire force. The experiments showed that the 95th percentile aggregate force level gives the damage at the worst 5% of locations along the road. This phenomenon is known as the 'spatial repeatability', which has also been identified in other reported studies [52-55]. The concentration of the tire force at specific locations could cause accelerated road damage at the same locations. The study concluded that the measures of DLC and RSF couldn't assess the road damage potential caused by the dynamic tire force, specifically in the presence of spatial repeatability. Alternatively, the aggregate force at specific points along the road surface

could be applied for assessing the road damage potential. The proposed dynamic aggregate force criterion (DAFC) considers the sum of all tire forces on each track, raised to a power n, applied to particular points along the road. For a vehicle with N_1 axles, the aggregate *nth* power force criterion DAFC on each track is calculated from

$$DAFC = \sum_{l=1}^{N_1} F_{zl}{}^{n}(t + t_{1l}) \tag{3-9}$$

where $F_{zl}(t)$ is the tire forces of l axle on left or right track at time t, t_{1l} is the time delay between the first (steering) axle and axle l. The power n is chosen on the basis of the road damage type. In this study, a value of $n = 4$ is used, which has been considered to be suitable for assessing fatigue damage for flexible pavements [71].

3.3.5 Dynamic Aggregate Stress Criterion (DASC)

The DAFC measure, described in equation (3-9), implies that all tires have the same contact area with the road surface. The tire contact patch, however, is known to vary with the localized road roughness and tire load. While the DAFC measure can be effectively used to assess relative damaging potential of different vehicles, it has been suggested that consideration of a nominal tire contact area could yield a better measure of the road stress [70]. A measure referred to as the dynamic aggregate stress criterion (DASC) has thus been proposed to assess the pavement stress on a particular point due to the aggregate *nth* power nominal contact stress, given by [70]:

$$DASC = \sum_{l=1}^{N_1} \left(\frac{F_{zl}\ (t + t_{1l})}{S_l} \right)^{n} \tag{3-10}$$

where S_l is the nominal contact area of tires on axle l [69], which is derived from:

$$S_l = w_l[\sqrt{R_l^2 - (R_l - \Delta R_l)^2}] \tag{3-11}$$

where w_l is the width of the tires on axle l, R_l is the radius of the tire and ΔR_l is the tire deflection on axle l.

The measures based upon the dynamic tire forces, such as DLC, RSF, DAFC and DASC are attained from the dynamic responses of vehicle combination operating on a straight-line path at a forward speed of 100 km/h, while the length of the road segment is taken as a minimum of 100 m. For the DAFC and DASC measures, the forces are evaluated at particular points on the road section with longitudinal coordinates in the 100 – 200 m range, with increment of 10 m.

3.4 EXTERNAL INPUTS

The performance measures defined to estimate both the handling and directional characteristics and road damage potential of multi-axle heavy vehicles with liftable and self-steering axles are strongly influenced by the excitations caused by the road roughness and steering input. In order to assess the performance measures of the vehicle subject to different road roughness and steering maneuvers, it is necessary to identify respective maneuvers that are performed at high or low speeds, and the roughness characteristics of the typical roads. The handling characteristics are evaluated using standardized steering maneuvers described in section 3.4.2. These include the path change for assessing RA, LTR and HSFD, ramp-steer to evaluate the SRT, and a constant

radius turn to evaluate the LSFD. Three different types of roads are considered and classified as 'smooth', 'medium' and 'rough' roads on the basis of the roughness index (RI). The roughness characteristics of the roads in the vicinity of the two tracks are considered using the available measure data [34].

3.4.1 CHARACTERIZATION OF ROAD ROUGHNESS

The roughness profiles of different roads in Canada have been measured and reported [72]. These profiles describe the elevation of the road surface in the vicinity of both the left and right wheel tracks, including the local grades and abrupt variations, like potholes or cracks. The elevations of different road surface have been measured over a length of approximately 500 m at intervals of 0.3 m. The reported road profiles are classified under smooth, medium and rough roads based on a roughness index (RI), which was defined as the sum of absolute values of the elevations over 1 km length of the highway, expressed in m/km. The roughness index (RI) values are calculated from:

$$\text{Left track: } RI_l = \sum_{i=1}^{n} |LRD(X_i)| / L \tag{3-12}$$

$$\text{Right track: } RI_r = \sum_{i=1}^{n} |RRD(X_i)| / L \tag{3-13}$$

LRD and RRD are the elevations of the left and right road profiles, respectively, measured from the mean value at every 0.3 m interval; n is the total number of measured data points available over the length L, and X_i is the longitudinal coordinate of the ith location on the road profile. Gordan [73] proposed a road rating scale based on the RI values, as described in table 3-1.

In this study, three different road profiles with significantly different RI values are chosen for the simulation of the three-dimensional vehicle model, discussed in chapter 2. The reported elevation data for previous studies are processed to eliminate the local grades using a high-pass filter. The resulting peak elevations of these roads were observed to be 0.35, 0.65 and 1.5 cm, respectively. The RI values of the two tracks were further computed using equations (3-12) and (3-13), which are summarized in table 3-2. The selected roads were classified as 'smooth', 'medium-rough' and 'rough' on the basis of the RI values, as shown in table 3-2.

Table 3-1: Roughness rating of roads based upon RI values

Roughness Index (m/km)	Rating
0-0.79	Exceptionally smooth
0.8-1.19	Very good
1.2-1.5	Good
1.6-1.9	Fair
2.0-2.3	Acceptable
2.4-2.7	Poor
2.8-3.1	Very Poor
3.2 and above	Extremely Rough

Table 3-2: Roughness index of simulation roads

Road	RI (m/km)	
	Left-track	Right Track
Smooth	1.59	2.18
Medium-rough	3.18	4.37
Rough	5.95	4.98

3.4.2 DIRECTIONAL MANEUVERS

The relative steady-turning rollover threshold (SRT) characteristics of the vehicles with conventional, liftable and self-steering axles are evaluated under a ramp-steer maneuver, where the steering angle is increased at a 2 degrees/second at the steering wheel, while the forward speed is held at 100 km/h. The directional dynamic measures based on LTR, RA and HSFD are evaluated under a path-change maneuver. Figure 3-1 illustrates the coordinates of the standardized path-change maneuver recommended in [65]. The directional performance characteristics are investigated by using a closed-loop path follower model to compute the front wheel angle corresponding to the prescribed path. The low speed friction demand (LSFD) of the vehicle combinations is evaluated using the tight turn maneuver, whose path coordinates are presented in Figure 3-2. In the simulation, the vehicle is required to follow a tight turn such that the center of the front steer axle tracks an arc of 14 m radius at a speed of 8.8 km/h.

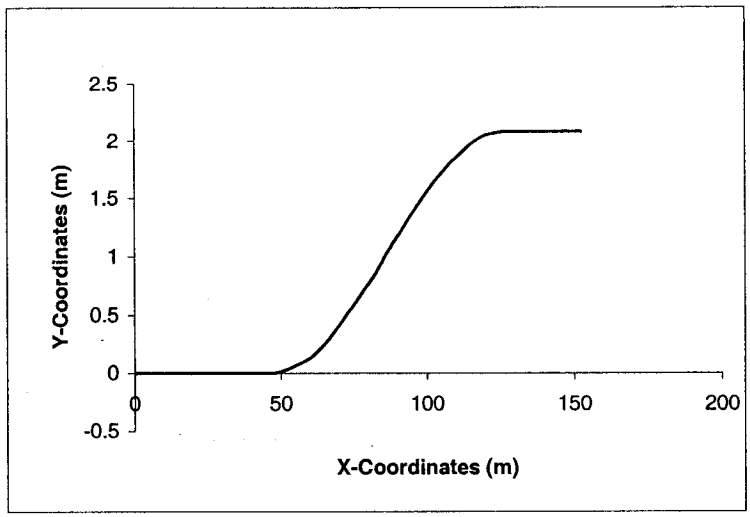

Figure 3-1: Trajectory of the high-speed path-change maneuver.

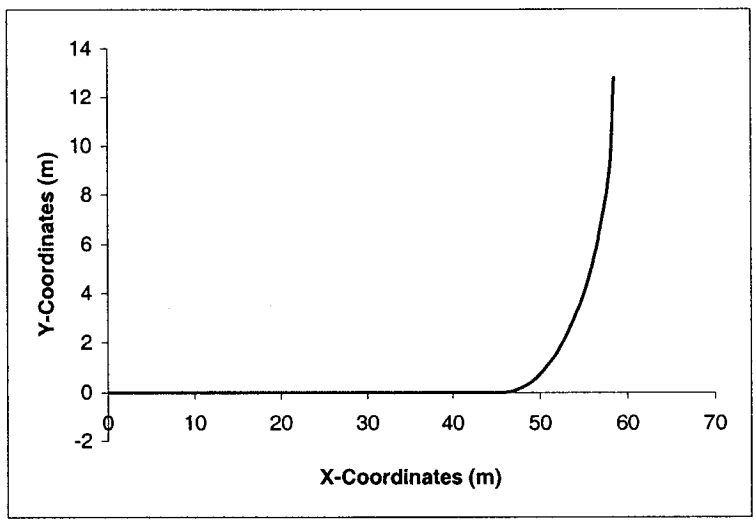

Figure 3-2: Trajectory of the low-speed tight turn maneuver.

CHAPTER 4 : CANDIDATE VEHICLE CONFIGURATION

4.1 CANDIDATE VEHICLE CONFIGURATION

Commercial freight vehicles of varying configurations operate on our highways. The dynamic response characteristics strongly rely on the vehicle configuration. A baseline candidate vehicle is selected in this study as a tractor-semitrailer combination. This selection was made on the basis of its high population on the roads [68]. The directional performance and road damage potential are analyzed for the selected tractor-semitrailer combination, where the number of axles on the semitrailer is varied from 3 to 6 axles. A number of different configurations are further realized by introducing one or more liftable and steerable axles. The sizes and weights of all the vehicle combinations are generated from the Vehicle Weight and Dimension Limits in the province of Ontario [74].

All of the combinations comprise a common three-axle tractor with a tandem drive axle group, as illustrated in Figure 4-1, with a 1.52 m drive axle spread. The wheelbase of the tractor is taken as 4.82 m and its tare weight as 89 kN . The c.g. height of the tractor is 1.12 m . The coordinates of the c.g., axles and the fifth wheel coupling are illustrated in the Figure. The unsprung masses of the front and each drive axle are taken as 544 kg and 1134 kg , respectively, while the corresponding axle loads are limited to 49 kN and 88 kN .

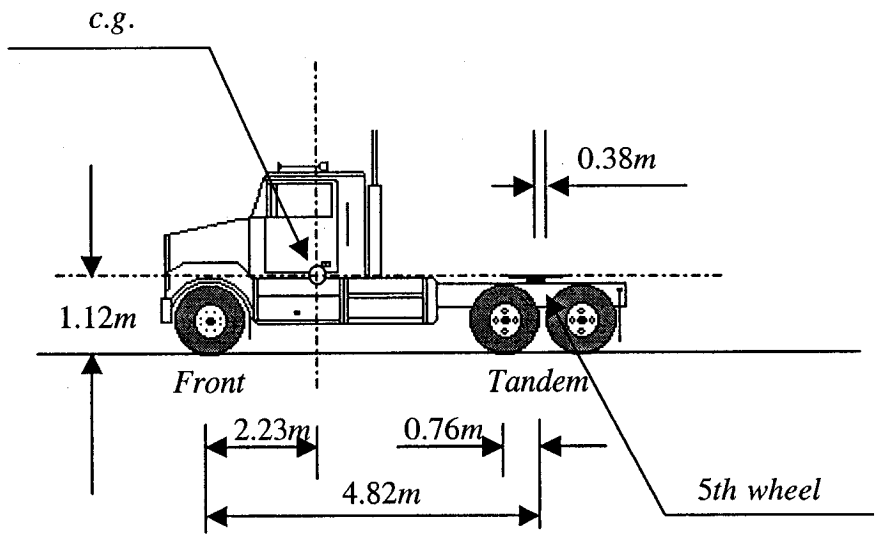

Figure 4-1: Tractor Configuration.

The analyses are performed for a generic 14.65 m (48 ft) semitrailer, while the axle locations were determined in the range of the base length for Ontario configurations. The sprung weight of each semitrailer in the defined configurations is computed on the basis of the weight limitations of the vehicle configuration [74]. The unsprung weight of each axle, irrespective of its type, is assumed to be 680 kg. Each vehicle configuration used in the simulation is specified by a code that comprises the number of axles in each axle group of both units. For example, the vehicle configuration code 12F13 describes the tractor with a single front axle and a tandem drive axle group coupled through the fifth wheel (F) with a semi-trailer with a single axle and a tridem axle group. Four different types of candidate vehicle configurations are considered in the study. Each configuration comprises the same tractor with a single front axle and a tandem drive axle group. The trailer's configuration in each candidate vehicle is described below:

Configuration 12F12 – semitrailer with a single axle and a tandem axle group;

Configuration 12F13 – semitrailer with a single axle and a tridem axle group;

Configuration 12F113 – semitrailer with two single axles and a tridem axle group;

Configuration 12F1113 – semitrailer with three single axles and a tridem axle group

Each configuration may further consist of one or more liftable or self-steering axles instead of the conventional axles. The load distributions of the combination with liftable axle are summarized in the following section.

4.2 WEIGHTS AND DIMENSIONS

Figure 4-2 illustrates the dimensions of the configuration 12F12, and Table 4-1 summarized the gross vehicle weight and axle loads of this configuration with a liftable axle. The simulation parameters of the combination are further presented in section 4.3. The single axle of the semitrailer could be considered as a conventional, liftable or self-steering axle. The load distributions for both the conventional and self-steering axle, however, remain identical, while a retracted liftable axle yields considerably different axle loads and coordinates of sprung weight c.g. , which are computed using the methodology described in section 2.5.

Figure 4-3 and Table 4-2 describe the dimensions and load distribution for the configuration 12F13, which may comprise of a single liftable or self-steering axle. Figure4-4 and Table 4-3, in a similar manner, illustrate the dimensions and load distribution for configuration 12F113. The two single axle employed in this configuration

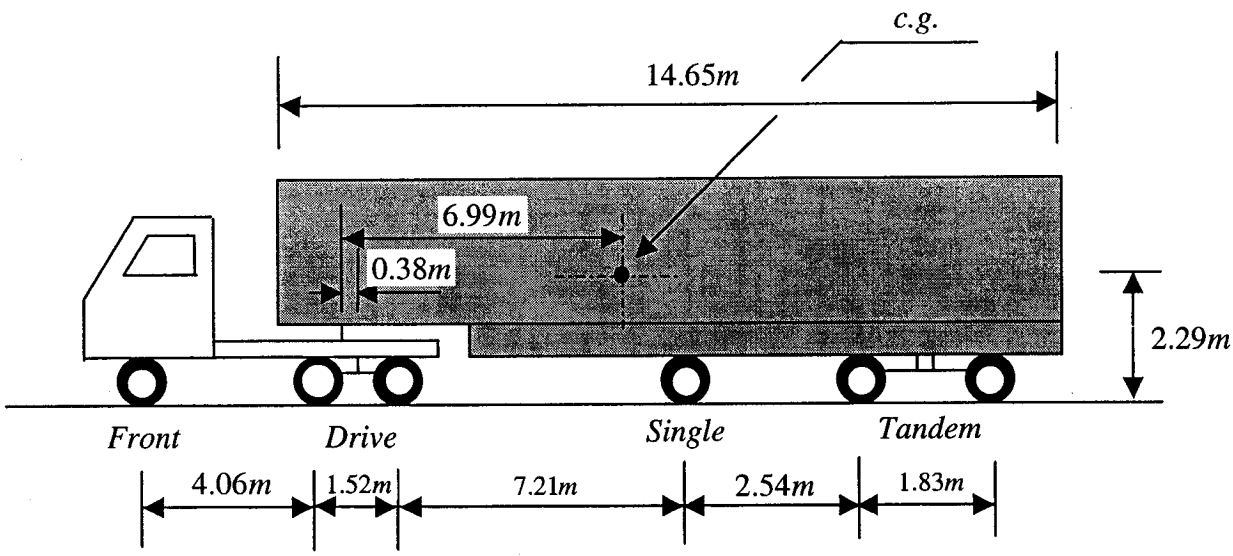

Figure 4-2: Configuration 12F12.

Table 4-1: GVW and axle loads of Configuration 12F12

Axle (4) type	Gross vehicle weight	Axle loads (kN)			
		Tractor		Semitrailer	
		Front	Drive	Single	Tandem
Conventional/self-steering or liftable axle down	506.17	49.00	176.40	93.59	187.18
Liftable axle up	506.17	51.20	201.81	/	253.16

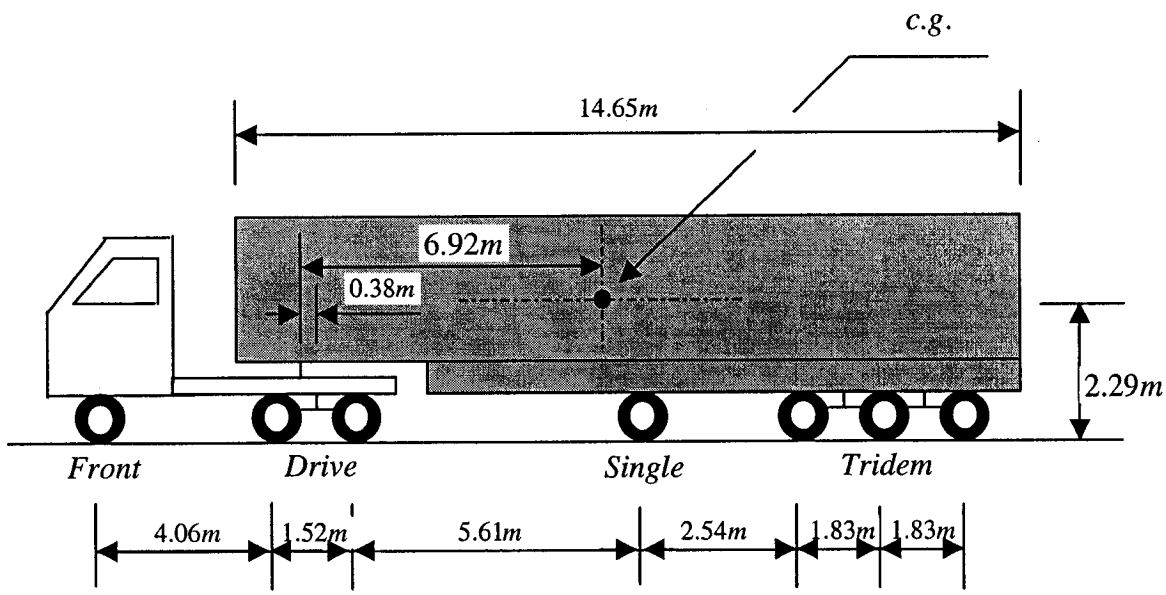

Figure 4-3: Configuration 12F13.

Table 4-2: GVW and axle loads of Configuration 12F13

Axle (4) type	Gross vehicle weight	Axle loads (kN)			
		Tractor		Semitrailer	
		Front	Drive	Single	Tridem
Conventional/self-steering or liftable axle down	555.66	49.00	176.40	82.57	247.70
Liftable axle up	555.66	51.58	206.25	/	297.83

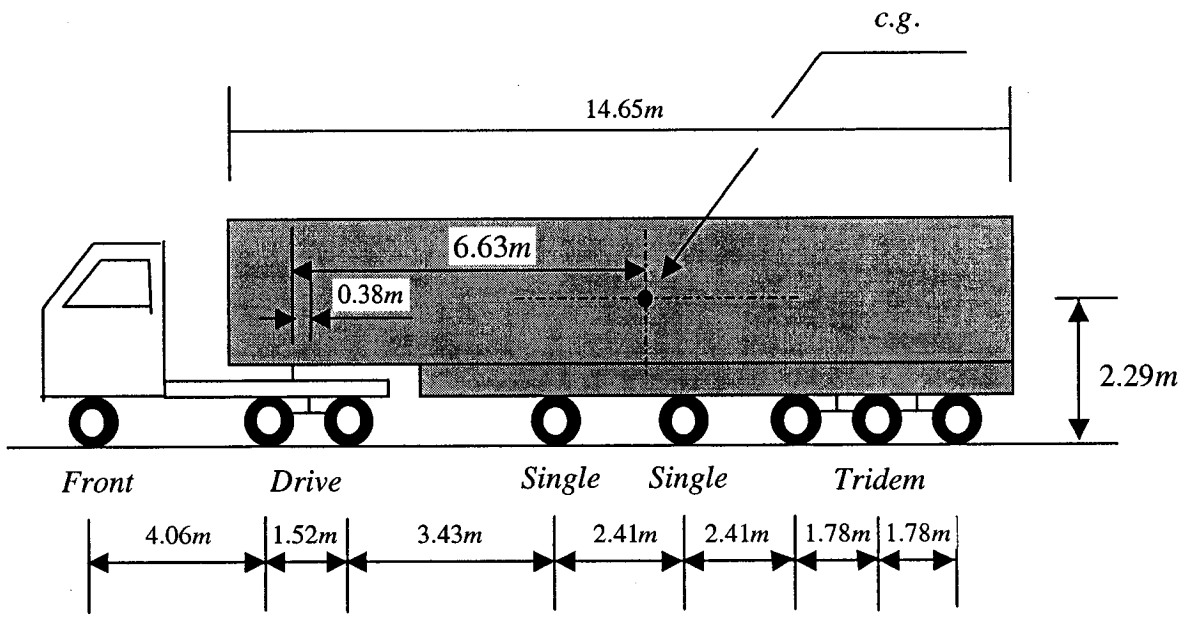

Figure 4-4: Configuration 12F113.

Table 4-3: GVW and axle loads of Configuration 12F113

Axles (4 and 5) type	Gross vehicle weight	Axle loads (kN)				
		Tractor		Semitrailer		
		Front	Drive	Single	Single	Tridem
Conventional/self -steering or liftable axle down	559.58	49.00	176.40	49.00	49.98	235.20
Lift axle 4 up	559.58	50.60	194.87	/	73.85	240.26
Lift axle 5 up	559.58	49.40	180.87	72.98	/	256.33
Lift axle 4/5 up	559.58	52.78	220.40	/	/	286.39

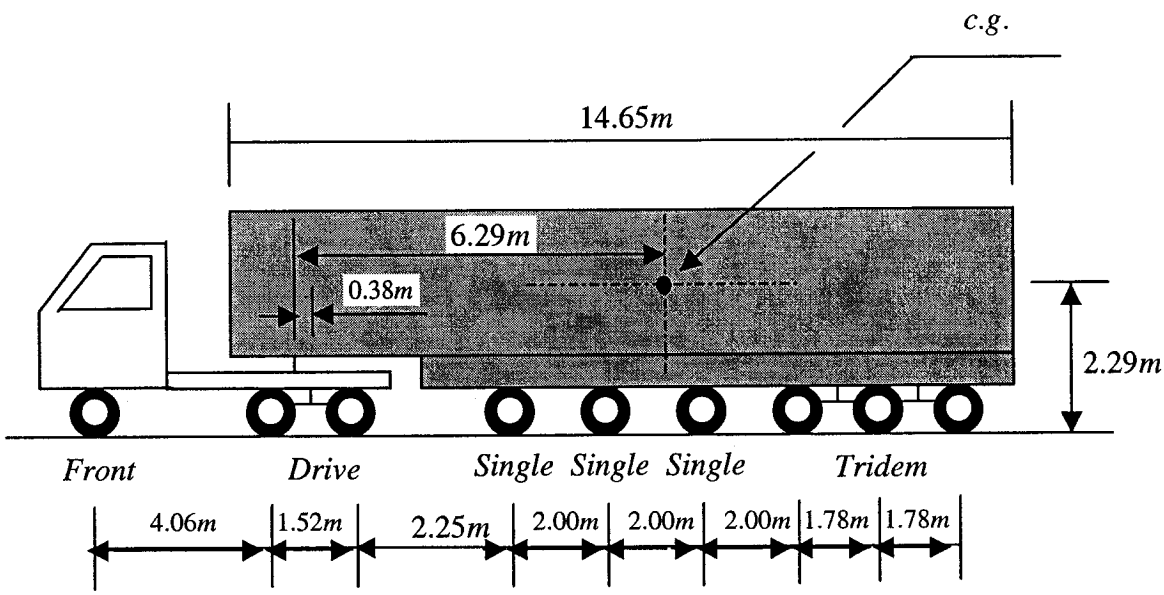

Figure 4-5: Configuration 12F1113.

Table 4-4: GVW and axle loads of Configuration 12F1113

Axles (4#,5#,6#) type	Gross vehicle weight	Axle loads (kN)					
		Tractor		Semitrailer			
		Front	Drive	Single	Single	Single	Tridem
Conventional/self-steering or liftable axle down	564.48	49.00	176.40	32.34	32.34	39.20	235.20
Lift axle 4 up	564.48	49.98	187.62	/	49.00	41.42	236.46
Lift axle 5 up	564.48	49.44	181.39	42.91	/	49.42	241.32
Lift axle 6 up	564.48	49.11	177.50	35.94	50.57	/	251.37
Lift axle 4/5 up	564.48	51.31	203.16	/	/	62.02	247.98
Lift axle 5/6 up	564.48	49.53	183.47	83.22	/	/	268.86
Lift axle 4/5/6 up	564.48	52.82	220.82	/	/	/	290.83

may be either liftable or self-steering type. The corresponding axle loads with either one or two axles lifted up are summarized in Table 4-3. The dimensions and load distribution of configuration 12F1113 are presented in Figure 4-5 and Table 4-4. The axle loads corresponding to one, two or three axles lifted are computed and summarized in Table 4-4.

4.3 SIMULATION PARAMETERS

The directional response characteristics and tire dynamic loads are known to be strongly affected by various operating factors, such as loading, speed, and road condition. A simulation matrix is formulated to consider variations in these factors in addition to the steering inputs for assessing the directional performance of different configurations. All the configurations comprise a common tractor with leaf-spring front-axle suspension and a tandem drive axle group with a walking-beam leaf-spring suspension [1]. The nonlinear force-deflection properties of the tractor axle suspensions are illustrated in Figures 4-6, and 4-7. The semitrailer axles are considered to be equipped with air suspension. Figures 4-8 and 4-9 illustrate the force-deflection properties of two different air suspensions with load capacity of 71 kN and 107 kN , respectively.

In order to investigate the influence of the suspension damping ratio on the directional performance and road damage potential, three different levels of damping ratio (0.05, 0.10, 0.15) are used. The damping ratio is computed assuming uncoupled sprung mass supported on a particular suspension and a linear spring rate corresponding

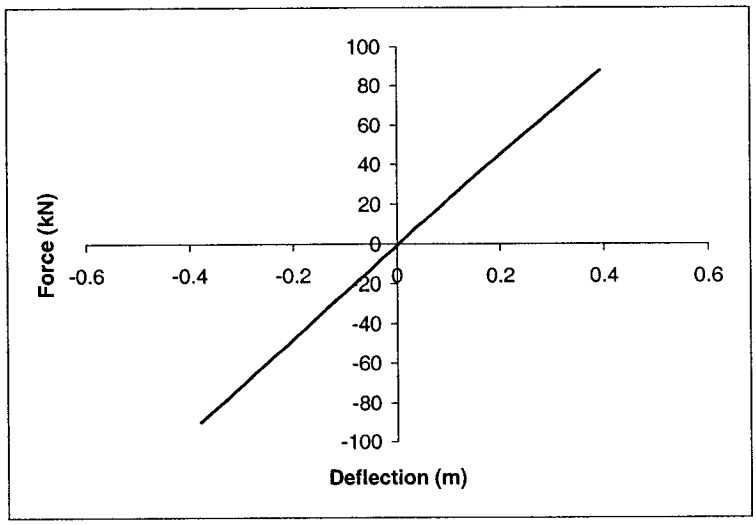

Figure 4-6. Force- deflection characteristics of front axle suspension spring.

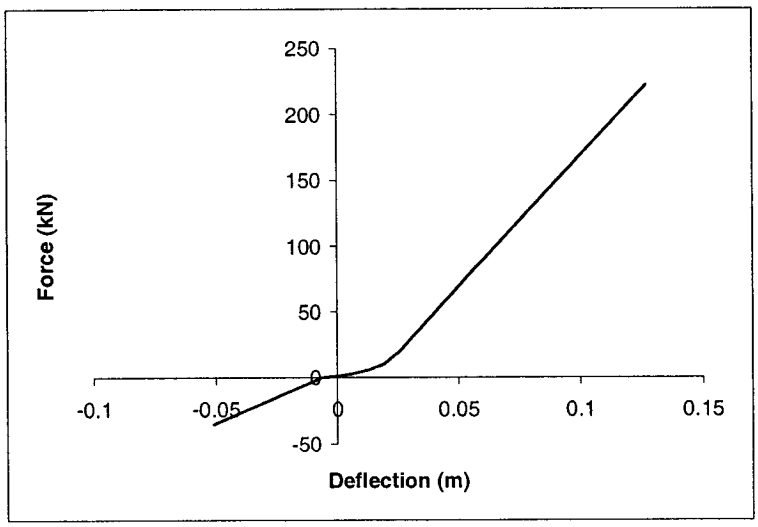

Figure 4-7. Force- deflection characteristics of drive axle suspension spring.

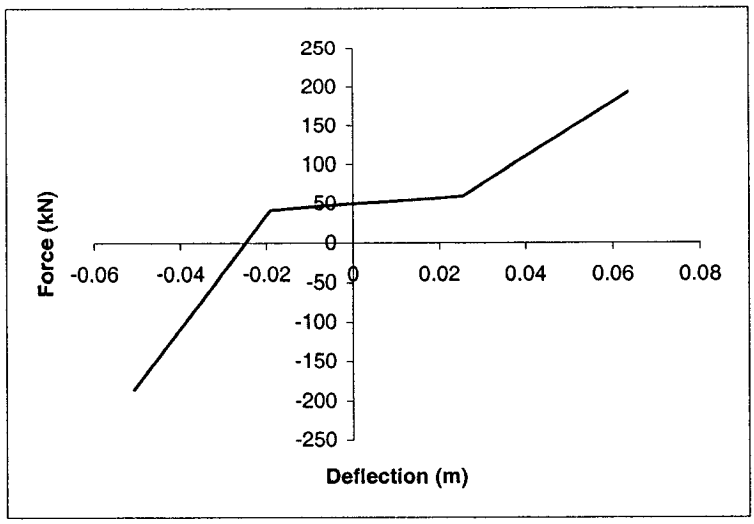

Figure 4-8. Force- deflection characteristics of Neway AR 95-17 air suspension spring (rated load: 107 *kN*).

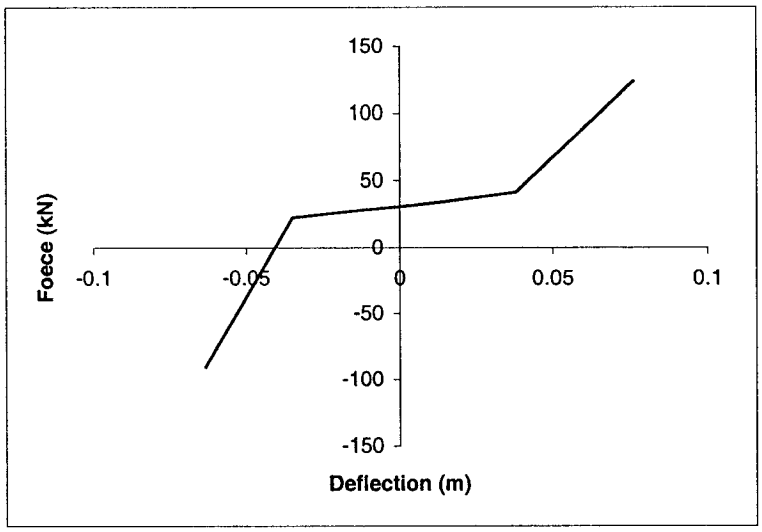

Figure 4-9: Force- deflection characteristics of Neway AR 95-17 air suspension spring (rated load: 71 *kN*).

to the static equilibrium, such that:

$$\zeta_l = \frac{C_l}{2\sqrt{(\frac{W_{ul} - m_{ul}g}{g})k_{sl}}} \tag{4-1}$$

where ζ_l is the suspension damping ratio of axle l, C_l is the damping coefficient, k_{sl} is the equivalent spring rate, W_{ul} is the axle load and m_{ul} is the unsprung mass of axle l.

The simulation matrix also considered two types of radial tires, one for the tractor front axle and the second type for rest of the axles of the vehicle. The cornering and aligning properties of the two types of tires are illustrated in Figures 4-10 and Figure 4-11, as functions of the normal load and sideslip angle. The tire data is described in the program through a three-dimensional look-up table. Linear interpolation is applied to compute the cornering force and aligning moments corresponding to the instantaneous normal load and sideslip angle.

The self-steering axles used in the study are considered to be the automotive type, which was shown in Figure 2-6. Assuming piecewise linear spring rate and negligible coulomb friction, the cornering stiffness of the self-steering axle is described as shown by Figure 4-14, and in equations (2-46), (2-47) and (2-48), where F_r is the self-steering cornering force and δ_{ssa} is the axle self-steer angle.

Tables 4-5 to 4-7 summarize the simulation parameters for different vehicle configurations considered in the study, namely 12F12, 12F13, 12F113, 12F1113. The simulations are performed for each configuration with conventional, liftable and self-

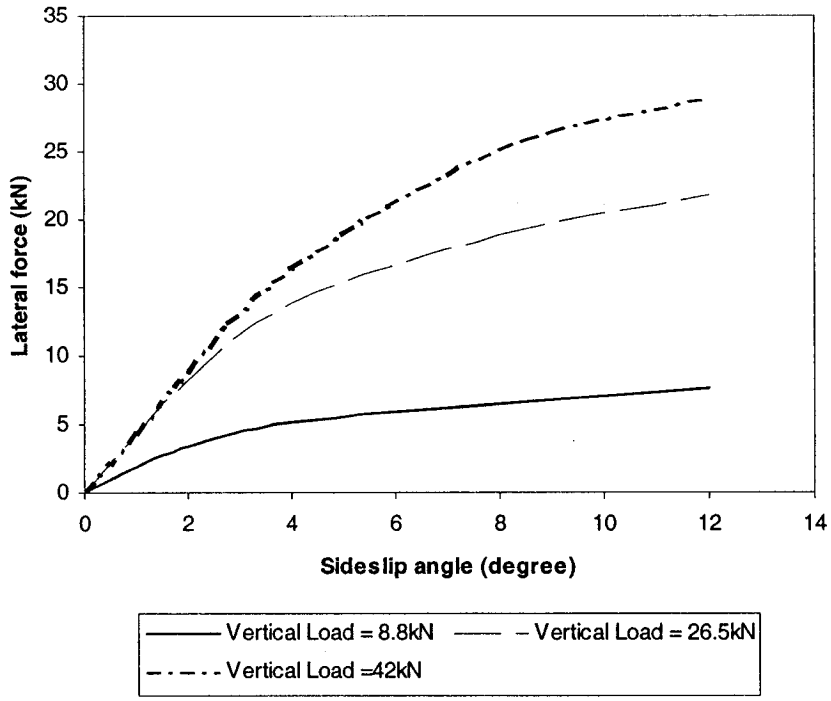

Figure 4-10: Cornering characteristics of tires on the front axle.

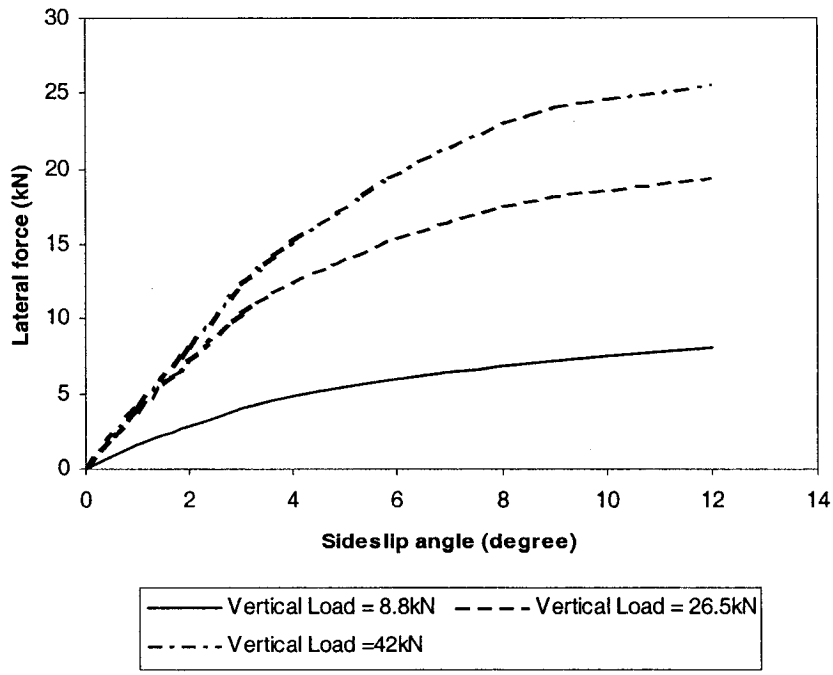

Figure 4-11: Cornering characteristics of tires on the tractor drive and trailer axles.

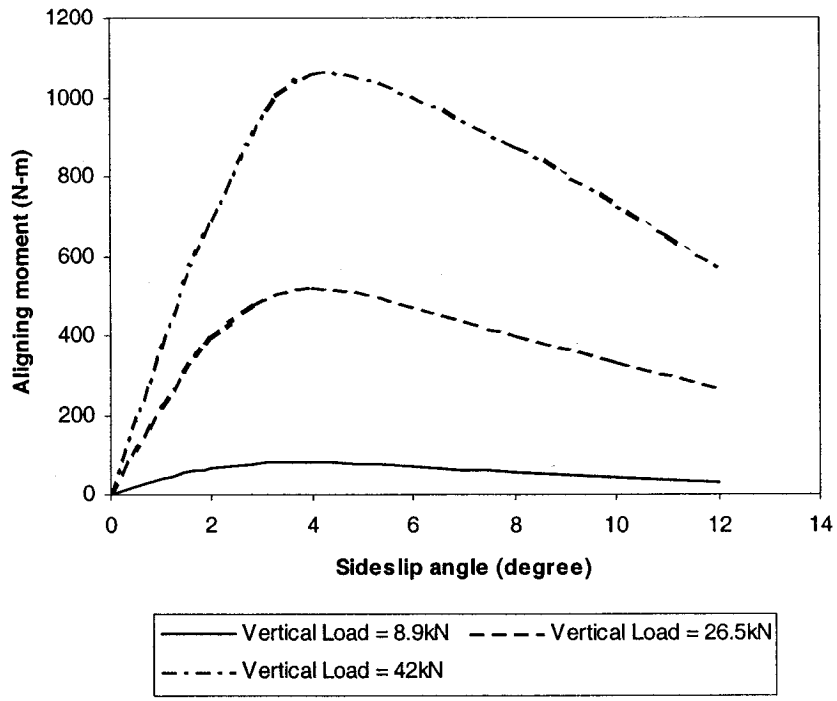

Figure 4-12: Aligning moment characteristics of tires on the front axle.

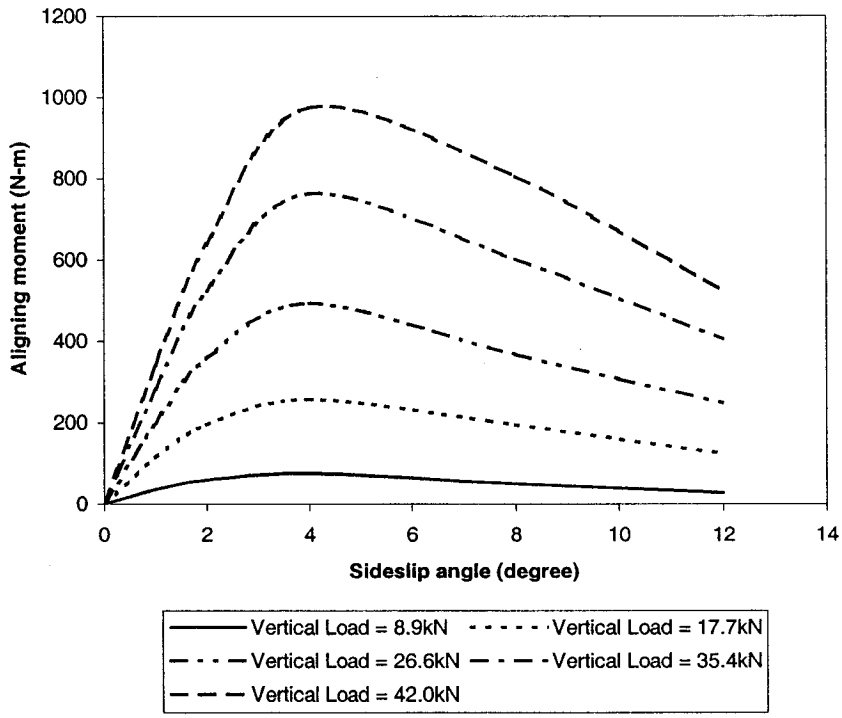

Figure 4-13: Aligning moment characteristics of tires on the tractor drive and trailer axles.

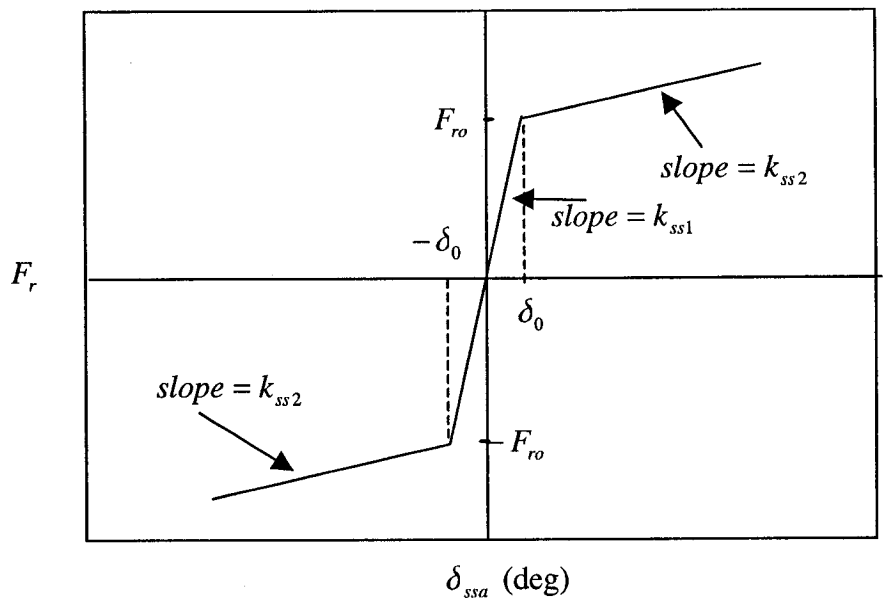

Figure 4-14: Cornering characteristics of self-steering axle.

steering axle in order to evaluate their relative performance characteristics. Three different simulations are considered for 12F12 and 12F13 configurations involving conventional trailer axles or liftable axle (axle 4) down, a self-steering axle (axle 4), and the liftable axle up. The configuration 12F113 involves 6 different cases: (i) conventional and liftable axle down; (ii) a single self-steering axle (axle 4); (iii) two self-steering axles (axles 4 and 5); (iv) single liftable axle (axle 4) up; (v) single liftable axle (5) up; (vi) two liftable axles (4 and 5) up. The configuration involves 11 different simulation cases, given below:

- Conventional trailer axles (all liftable axles down)
- Single self-steering axle (axle 4)
- Two self-steering axles (axles 4 and 5)

- Three self-steering axles (axles 4, 5 and 6)
- Single liftable axle up (axle 4)
- Two liftable axles up (axles 4 and 5)
- Three liftable axles up (axles 4, 5 and 6)
- Two liftable axles up (axles 5 and 6) and single self-steering axle (axle 4)
- Single liftable axle up (axle 5) and single self-steering axle (axle 4)
- Single liftable axle up (axle 6) and single self-steering axle (axle 4)
- Single liftable axle up (axle 6) and two self-steering axles (axles 4 and 5)

Table 4-5: Simulation parameters of tractor

	Tractor	
No of axles	3	
Sprung mass (kg)	6,246	
Sprung mass c.g. height (m)	1.12	
	Front axle	Drive axle
Axle mass (kg)	544	1134
Axle load (kN)	49.0	88.0
Axle *c.g.* height (m)	0.508	0.540
Roll center height (m)	0.464	0.838
Suspension type	IH12KFrnt	Hendrickson RTE 440
Suspension half spacing (m)	0.406	0.483
Half wheel track (m)	1.016	0.813
Dual tire spacing (m)	0	0.330
Tire width (m)	0.279	0.279
Tire radius (m)	0.572	0.572
Tire vertical stiffness (kN/m)	947.3	947.3
Roll steer coefficient	0	0.15
Auxiliary roll stiffness (N−m/deg)	431	Leading axle: 3387 Trailing axle: 9597
5th wheel height (m)	1.1	
Roll stiffness of 5th wheel (kN−m/deg)	621	

Table 4-6: Simulation parameters of self-steering axle

	Self-steering axle
Normalized centering force $a_{ro}(g)$	0.25
Normalized cornering stiffness k_{ss1} (g/deg)	0.25
Normalized cornering stiffness k_{ss2} (g/deg)	0.10
Corrected caster trail $t_{ss}(m)$	0.364

The results attained from each simulation are analyzed to derive the performance measures, such as SRT, RA, LTR, HSFD, LSFD, ESAL, DLC, RSF, DAFC and DASC. Table 4-8 summarizes the entire simulation matrix.

Table 4-7: Simulation parameters of different semitrailers

	Semitrailer of configuration 12F12		Semitrailer of configuration 12F13		Semitrailer of configuration 12F113			Semitrailer of configuration 12F1113			
	Single	Tandem	Single	Tridem	Single	Single	Tridem	Single	Single	Single	Tridem
Axle mass (kg)	680	680	680	680	680	680	680	680	680	680	680
Axle load (kN)	93.59	93.59	82.57	82.57	49.00	49.98	78.40	32.34	32.34	39.20	78.40
Axle *c.g.* height (m)	0.540	0.540	0.540	0.540	0.540	0.540	0.540	0.540	0.540	0.540	0.540
Roll center height (m)	0.737	0.737	0.737	0.737	0.737	0.737	0.737	0.737	0.737	0.737	0.737
Suspension type	Neway 95-17 (107 kN)	Neway 95-17 (107 kN)	Neway 95-17 (107 kN)	Neway 95-17 (107 kN)	Neway 95-17 (107 kN)	Neway 95-17 (107 kN)	Neway 95-17 (107 kN)	Neway 95-17 (71 kN)	Neway 95-17 (71 kN)	Neway 95-17 (71 kN)	Neway 95-17 (107 kN)
Suspension half spacing (m)	0.559	0.559	0.559	0.559	0.559	0.559	0.559	0.559	0.559	0.559	0.559
Half wheel track (m)	0.813	0.813	0.813	0.813	0.813	0.813	0.813	0.813	0.813	0.813	0.813
Dual tire spacing (m)	0.330	0.330	0.330	0.330	0.330	0.330	0.330	0.330	0.330	0.330	0.330
Tire width (m)	0.279	0.279	0.279	0.279	0.279	0.279	0.279	0.279	0.279	0.279	0.279
Tire radius (m)	0.572	0.572	0.572	0.572	0.572	0.572	0.572	0.572	0.572	0.572	0.572
Tire vertical stiffness (kN/m)	947.3	947.3	947.3	947.3	947.3	947.3	947.3	947.3	947.3	947.3	947.3
Roll steer coefficient	0.20	0.20	0.20	0.20	0.20	0.20	0.20	0.20	0.20	0.20	0.20
Auxiliary roll stiffness (N−m/deg)	6774	6774	6774	6774	6774	6774	6774	9371	9371	9371	6774

Table 4-8: Simulation Matrix

Simulation Code	SRT	RA	LTR	HSFD	LSFD	ESAL	DLC	RSF	DAFC	DASC
Con12F12-4down	Y	Y	Y	Y	Y	Y	Y	Y	Y	Y
Con12F12-4sest	Y	Y	Y	Y	Y					
Con12F12-4up	Y	Y	Y	Y	Y	Y	Y	Y	Y	Y
Con12F13-4down	Y	Y	Y	Y	Y	Y	Y	Y	Y	Y
Con12F13-4sest	Y	Y	Y	Y	Y					
Con12F13-4up	Y	Y	Y	Y	Y	Y	Y	Y	Y	Y
Con12F113-45down	Y	Y	Y	Y	Y	Y	Y	Y	Y	Y
Con12F113-4sest	Y	Y	Y	Y	Y					
Con12F113-45sest	Y	Y	Y	Y	Y					
Con12F113-4up	Y	Y	Y	Y	Y	Y	Y	Y	Y	Y
Con12F113-45up	Y	Y	Y	Y	Y	Y	Y	Y	Y	Y
Con12F113-5up4sest	Y	Y	Y	Y	Y	Y	Y	Y	Y	Y
Con12F1113-456down	Y	Y	Y	Y	Y	Y	Y	Y	Y	Y
Con12F1113-4sest	Y	Y	Y	Y	Y					
Con12F1113-45sest	Y	Y	Y	Y	Y					
Con12F1113-456sest	Y	Y	Y	Y	Y					
Con12F1113-4up	Y	Y	Y	Y	Y	Y	Y	Y	Y	Y
Con12F1113-45up	Y	Y	Y	Y	Y	Y	Y	Y	Y	Y
Con12F1113-456up	Y	Y	Y	Y	Y	Y	Y	Y	Y	Y
Con12F1113-56up4sest	Y	Y	Y	Y	Y	Y	Y	Y	Y	Y
Con12F1113-5up4sest	Y	Y	Y	Y	Y	Y	Y	Y	Y	Y
Con12F1113-6up4sest	Y	Y	Y	Y	Y	Y	Y	Y	Y	Y
Con12F1113-6up45sest	Y	Y	Y	Y	Y					

sest: self-steering

CHAPTER 5 : ANALYSIS OF DIRECTIONAL PERFORMANCE MEASURES

5.1 GENERAL

From the literature review presented in chapter 1, it is evident that the steady-state and transient directional responses of various vehicle combinations with conventional beam axles have been extensively investigated. The dynamics of such vehicles with liftable and self-steering axles have been addressed in a few studies [2,6,41]. Moreover, these studies consider the vehicle operating on a perfectly smooth road, assuming negligible contributions due to tire interactions with the randomly rough road surfaces. The dynamic interactions of tires with randomly rough road surfaces could lead to significant variations in the normal loads, which would not only impose higher pavement loads, but also alter the cornering properties of the tires. A number of reported studies have clearly established a strong relationship between the road roughness and the magnitudes of dynamic pavement loads [34]. The variations in the normal loads would be further amplified, when one or more liftable axles are retracted. Owing to the nonlinear dependence of the cornering forces and aligning moments due to tires on the normal load, the directional performance characteristics of the vehicle combination may be influenced by the road roughness, specifically when liftable or self-steering axles are used.

The present investigation focuses on the relative performance characteristics of vehicle combinations with conventional, liftable and self-steering axles under a constant forward speed motion on randomly rough roads, as described in chapter 3. The directional performance characteristics are evaluated in terms of the measures also described in chapter 3, namely the Static Rollover Threshold (SRT), Load Transfer Ratio

(LTR), Rearward Amplification Factor (RA), High-Speed Friction Demand (HSFD) and Low-Speed Friction Demand (LSFD). In all cases, the results are also compared with those obtained for a perfectly smooth road, while the relative road friendliness characteristics are also evaluated for the conventional and liftable axle configurations in terms of the measures described in section 3.2 (presented in the following chapter). The influence of suspension damping is also investigated for both the directional performance and road friendliness measures. The relative performance measures of the combination with conventional, liftable and self-steering axles are described in the following sections.

5.2 STATIC ROLLOVER THRESHOLD (SRT)

Static Rollover Threshold (SRT) is the limiting value of lateral acceleration that the vehicle could withstand in a steady turn, while approaching the static rollover condition. The simulations are performed under a ramp steering input with a rate of 2 degrees per second at the steering wheel, while the vehicle is running at 100 km/h constant forward speed. The lateral acceleration of the semitrailer corresponding to the static rollover condition of the combination is considered as the SRT. The static rollover condition is characterized by the loss of road contact of tires on a single track of the combination, except for the tractor front axle tires. The loss of tire road contact is considered to occur, when the vertical force of the tire diminishes to zero. The SRT values above 0.35 g and 0.40 g have been recommended by two different studies for the tractor-semitrailer combination [28, 65]. The results attained for different configurations with different axles are discussed in the following subsections. The data acquired under random rough roads revealed high frequency oscillations of the responses arising from tire-road interactions, which made the task of identifying the precise values of the

measures rather difficult. The simulation results were thus processed through a low-pass filter with cut-off frequency of 30 Hz to suppress some of the high frequency variations. Figure 5-1 illustrates the comparisons of filtered and unfiltered tire load transfer ratio (LTR) response of configuration 12F12 with fixed trailer belly axle, as a function of the suspension damping ratio (DR), while the vehicle is operating on a medium-rough road. From the figures, it is obvious that the low-pass filter tends to suppress high frequency oscillations, while it attenuates the peak responses.

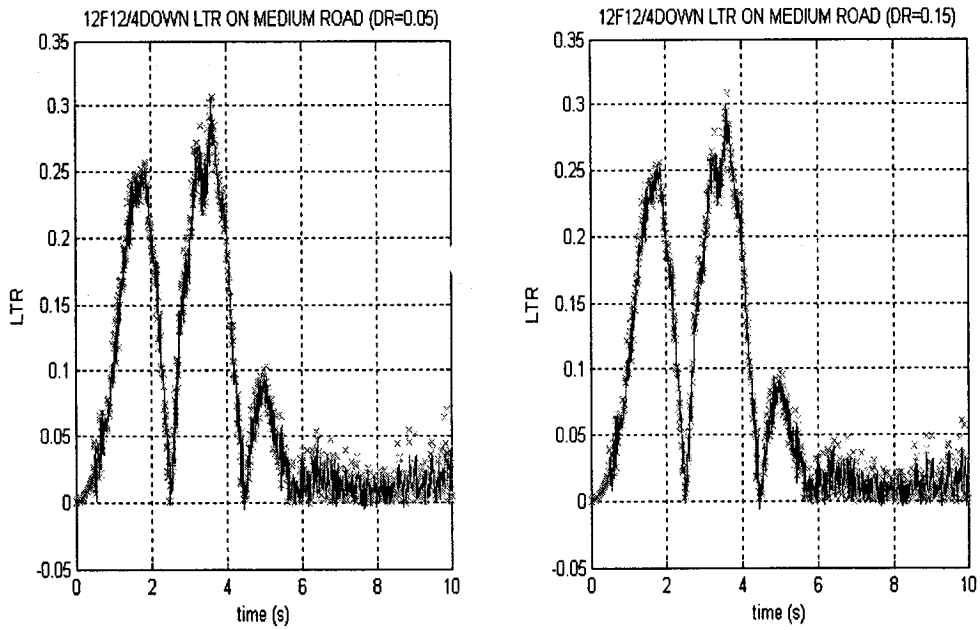

Figure 5-1: Comparisons of filtered and unfiltered LTR responses of configuration 12F12 (××× unfiltered; ——— filtered).

5.2.1 CONFIGURATION 12F12

Table 5-1 summarizes the SRT performance of the tractor-semitrailer configuration 12F12 as functions of the road roughness and suspension damping (DR). The results are presented for perfectly smooth (no roughness), smooth, medium-rough and rough roads, as described in section 3.4.1. The lead axle of the semitrailer, also referred to as the belly-axle, is replaced by the liftable or self-steering axle for the

analyses. The results are attained for the lift-axle up, while those for the lift-axle down are identical to those attained for the conventional axle. The table also illustrates the relative SRT performance of the vehicle semitrailer with a self-steering axle. The analyses are performed for 3 different values of the uncoupled damping ratios for all axles suspensions: 0.05, 0.10, 0.15.

Table 5-1: Summary of SRT responses of configuration 12F12

Trailer axle configurations	Road roughness			
	Perfectly smooth	Smooth	Medium rough	Rough
	Damping ratio = 0.05			
Conventional	0.435	0.428	0.424	0.371
Axle 4 up	0.394	0.407	0.405	0.370
Axle 4 self-steering	0.442	0.437	0.429	0.383
	Damping ratio = 0.10			
Conventional	0.432	0.428	0.424	0.376
Axle 4 up	0.394	0.407	0.409	0.374
Axle 4 self-steering	0.442	0.437	0.435	0.383
	Damping ratio = 0.15			
Conventional	0.429	0.428	0.425	0.377
Axle 4 up	0.394	0.407	0.413	0.376
Axle 4 self-steering	0.442	0.437	0.436	0.383

The results show that the conventional axle (lift axle down) vehicle yields SRT value in the order of 0.43 g , when operating on a perfectly smooth road. The influence of suspension damping is nearly negligible. This value of SRT is comparable with those reported in a number of published studies [64,68] for the smooth road operation. The operation on medium-rough and rough roads, however, yields relatively higher SRT values with additional damping, which is attributed to less variations in vertical tire forces due to interactions with the rough roads under higher damping.

The SRT value tends to be considerably lower, when the liftable belly axle is retracted, as shown in Table 5-1. This is mostly attributed to the higher axle loads, and

higher sprung weights and mass moment of inertia. The influence of road roughness on the resulting SRT values appear to be very small, while the operation on rough roads yields reduction in SRT to nearly 0.37 g , indicating a decreasing of 15%. The combination with liftable axle retracted yields a lower SRT value of 0.39 g than those of the conventional axle, which would not meet the safety dynamics requirement of SRT of 0.4 g , as proposed by El-Gindy [65]. It can thus be concluded that the static roll stability limit of the 12F12 vehicle could decrease by nearly 10%, when the lift axle is retracted while turning. Replacing the conventional axle by a self-steering axle, on the other hand, yields slightly higher SRT values of 0.44 g than those of the conventional vehicle of 0.43 g , while operating on a perfectly smooth road. The influence of road roughness on the SRT response of the combination with self-steering belly axle is similar to that observed for the conventional vehicle.

5.2.2 CONFIGURATION 12F13

Table 5-2 summarizes the SRT performance of the candidate vehicle configuration 12F13 under various road roughness and suspension damping ratios (DR). Similar to the configuration 12F12, the lead axle of the semitrailer, referred to as the belly axle, is replaced by the liftable or the self-steering axle for the analyses. The vehicle configuration 12F13 with conventional belly axle (liftable axle down) yields SRT values in the order of 0.44 g , when operating on a perfectly smooth road, which is slightly higher than that of the configuration 12F12. A comparison of the results with those derived for the previous vehicle configuration 12F12 suggests that the combination with tridem axle trailer yields higher static roll stability limit than the tandem-axle trailer combination (12F12). This observation conforms with the conclusions draw in reported

studies [64,68]. The increase in the road roughness tends to lower the SRT value, as observed in Table 5-1. An increase in suspension damping, however, tends to improve the static roll stability by suppressing the variations in the tire loads, while the vehicle is operating on the rough road. On the smooth and medium-rough roads, the additional suspension damping yields slightly lower SRT value, as observed in Table 5-1. The operation on a rough road with high suspension damping (DR=0.15) yields SRT value comparable to that attained for the perfectly smooth road. As observed for the configuration 12F12, the configuration 12F13 with liftable axle retracted yields slightly lower SRT values than those attained for the conventional axle vehicle. The use of a self-steering axle, instead of the fixed or liftable belly axle, also yields slightly higher values of SRT, as shown in the Table 5-2.

Table 5-2: Summary of SRT responses of configuration 12F13

Trailer axle configurations	Road roughness			
	Perfectly smooth	Smooth	Medium rough	Rough
	Damping ratio = 0.05			
Conventional	0.452	0.446	0.444	0.380
Axle 4 up	0.446	0.443	0.440	0.357
Axle 4 self-steering	0.456	0.459	0.461	0.385
	Damping ratio = 0.10			
Conventional	0.449	0.446	0.442	0.432
Axle 4 up	0.447	0.442	0.440	0.421
Axle 4 self-steering	0.453	0.454	0.455	0.437
	Damping ratio = 0.15			
Conventional	0.446	0.445	0.441	0.434
Axle 4 up	0.444	0.443	0.440	0.429
Axle 4 self-steering	0.451	0.453	0.453	0.444

5.2.3 CONFIGURATION 12F113

Table 5-3 presents the SRT values of the tractor-semitrailer configuration 12F113 as functions of the road roughness and suspension damping. Unlike the previous vehicle

configurations, the semitrailer of this candidate configuration has two single belly-axles, which can be replaced by either liftable or the self-steering axles. The table also illustrates the relative SRT performance of the vehicle trailer with conventional, liftable and self-steering axle.

The results indicate that the conventional axle (liftable axles down) tractor-semitrailer vehicle yields SRT value in the order of 0.44 g , when the vehicle is traveling on a perfectly smooth road, which is comparable with that of the configuration 12F13. The table clearly shows that replacing one of the conventional belly-axles of the semitrailer by the retracted liftable axle can increase the SRT value from 0.44 g to 0.46 g by around 5%, especially when the lead belly axle (axle 4) is retracted. This is attributed to relatively smaller changes in the fixed axle loads and nearly negligible change in the front axle load and thus the resulting restoring moment. The ratio of the sprung to unsprung mass also varies only slightly, when a single axle is retracted. Furthermore, it should be noted that the axle loads of the liftable axles are considerably smaller than those of the fixed axles. However, replacing the conventional belly axles by the self-steering (ss) axles will offset this improvement on the SRT performance of the liftable axles and the SRT values of the vehicle with self-steering axles are comparable with those of the vehicle with conventional axles. The table also shows that although the lead liftable axle retracted can increase the SRT value, the vehicle with leading self-steering axle (axle 4) and trailing retracted axle (axle 5) yields the lowest SRT values. The road roughness has a negligible influence on the SRT values, however, the vehicle operating on a rough road tends to lower its static roll stability limit.

Table 5-3: Summary of SRT responses of configuration 12F113

Trailer axle configurations	Road roughness			
	Perfectly smooth	Smooth	Medium rough	Rough
	Damping ratio = 0.05			
Conventional	0.445	0.443	0.440	0.346
Axle 4 up	0.459	0.455	0.450	0.418
Axles 4 and 5 up	0.457	0.450	0.447	0.455
Axle 4 - ss (self-steering)	0.440	0.439	0.437	0.356
Axle 4 and 5 - ss	0.441	0.441	0.441	0.424
Axle 5 up and 4 - ss	0.439	0.423	0.420	0.388
	Damping ratio = 0.10			
Conventional	0.444	0.442	0.440	0.429
Axle 4 up	0.459	0.453	0.450	0.425
Axles 4 and 5 up	0.454	0.450	0.445	0.451
Axle 4 - ss	0.439	0.439	0.437	0.440
Axle 4 and 5 - ss	0.442	0.446	0.442	0.450
Axle 5 up and 4 - ss	0.438	0.422	0.420	0.389
	Damping ratio = 0.15			
Conventional	0.437	0.441	0.438	0.430
Axle 4 up	0.458	0.453	0.449	0.419
Axles 4 and 5 up	0.453	0.452	0.443	0.448
Axle 4 - ss	0.440	0.441	0.436	0.438
Axle 4 and 5 - ss	0.443	0.446	0.442	0.453
Axle 5 up and 4 - ss	0.438	0.420	0.420	0.398

5.2.4 CONFIGURATION 12F1113

Table 5-4 presents the SRT performance of the tractor-semitrailer configuration 12F1113 under the 4 different road conditions: perfectly smooth, smooth, medium-rough and rough; and 3 levels of suspension damping ratio: 0.05, 0.10, and 0.15. The semitrailer of the configuration comprises a fixed axle tridem and three single axles, which could be fixed, liftable or self-steering (ss). The results show that the configuration 12F1113 with conventional fixed axles yields an SRT value of 0.45 g, when operating on a perfectly smooth road, which is slightly higher than those of previously discussed configurations with conventional axles. Employing liftable axles to replace the fixed single axles can yield higher SRT value when one or more axles are retracted, as observed for 12F113

configuration. Lifting the two leading axles (axles 4 and 5) yields highest value of SRT, which is attributed to the increased restoring moment due to higher loads on the fixed axles.

Table 5-4: Summary of SRT responses of configuration 12F1113

Trailer axle configurations	Road roughness			
	Perfectly smooth	Smooth	Medium rough	Rough
	Damping ratio = 0.05			
Conventional	0.450	0.445	0.445	0.343
Axle 4 up	0.453	0.450	0.448	0.322
Axles 4 and 5 up	0.479	0.478	0.476	0.395
Axles 4, 5 and 6 up	0.457	0.452	0.452	0.415
Axle 4 - ss	0.448	0.444	0.436	0.365
Axles 4 and 5 - ss	0.449	0.444	0.437	0.388
Axles 4, 5 and 6 - ss	0.449	0.445	0.435	0.393
Axle 5 up and 4 - ss	0.442	0.435	0.429	0.362
Axles 5 and 6 up, 4 - ss	0.437	0.429	0.421	0.386
Axle 6 up and 4 - ss	0.435	0.433	0.430	0.365
Axle 6 up, 4 and 5 - ss	0.437	0.436	0.433	0.375
	Damping ratio = 0.10			
Conventional	0.443	0.443	0.440	0.386
Axle 4 up	0.446	0.445	0.443	0.396
Axles 4 and 5 up	0.472	0.472	0.472	0.398
Axles 4, 5 and 6 up	0.456	0.454	0.451	0.380
Axle 4 - ss	0.448	0.442	0.437	0.388
Axles 4 and 5 - ss	0.449	0.443	0.439	0.389
Axles 4, 5 and 6 - ss	0.447	0.442	0.433	0.378
Axle 5 up and 4 - ss	0.442	0.437	0.427	0.355
Axles 5 and 6 up, 4 - ss	0.437	0.431	0.421	0.389
Axle 6 up and 4 - ss	0.429	0.429	0.427	0.369
Axle 6 up, 4 and 5 - ss	0.429	0.430	0.430	0.378
	Damping ratio = 0.15			
Conventional	0.441	0.441	0.440	0.393
Axle 4 up	0.446	0.445	0.442	0.398
Axles 4 and 5 up	0.469	0.468	0.463	0.400
Axles 4, 5 and 6 up	0.454	0.453	0.453	0.410
Axle 4 - ss	0.448	0.442	0.440	0.375
Axles 4 and 5 - ss	0.447	0.446	0.445	0.380
Axles 4, 5 and 6 - ss	0.447	0.447	0.443	0.375
Axle 5 up and 4 - ss	0.437	0.438	0.427	0.365
Axles 5 and 6 up, 4 - ss	0.436	0.430	0.423	0.391
Axle 6 up and 4 - ss	0.426	0.425	0.424	0.372
Axle 6 up, 4 and 5 - ss	0.427	0.430	0.428	0.379

Replacing the conventional axles by self-steering axles, however, tends to reduce the SRT values of the combinations, especially when the suspension damping is relative lower and the road roughness is high. Furthermore, replacing the leading one or two axles by self-steering axles, and the trailing two or one axles by the lifted axles, yields the lowest vehicle static roll stability limit, irrespective of the road roughness and the suspension damping ratio. As observed in Tables 5-1, 5-2 and 5-3, the higher road roughness yields lower SRT values of 12F1113 configuration, irrespective of the suspension damping and axle configurations. For the rough road, higher damping ratio causes slightly higher SRT values. A low suspension damping (DR=0.05) coupled high road roughness yields considerably lower value of SRT (0.34 g), as apposed to 0.45 g for the conventional vehicle operating on a perfectly smooth road. This represents a reduction of 23%, while the combination would not satisfy the recommended requirement of 0.35 g or 0.40 g in two different studies [28,65].

5.3 LOAD TRANSFER RATIO (LTR)

The LTR of an articulated vehicle combination is defined as the ratio of the sum of absolute values of the difference between the right wheel loads and the left wheel loads, to the sum of all the wheel loads, as described in equation (3-1). The magnitude of the LTR has been suggested to provide an indication of the dynamic rollover stability of the vehicle [34]. The LTR values of the combinations considered in this study are computed from the directional response data attained for the vehicle operating at a constant forward speed of 100 km/h and subject to a path-change maneuver, as described in chapter 3. It is recommended that the LTR of a vehicle must not exceed 0.6 [65].

5.3.1 CONFIGURATION 12F12

Table 5-5 summarizes the directional performance of the combination 12F12 in terms of the lateral load transfer ratio (LTR) as functions of the road roughness and suspension damping. The analyses are performed for the fixed, liftable and self-steering belly axle of the semitrailer, 4 different road roughness and 3 levels of suspension damping ratio, as described for the SRT measure. The results suggest that the LTR values of the vehicle configuration are considerably lower than the recommended LTR value of 0.6, irrespective of the trailer axle configurations, road roughness and suspension damping. The conventional fixed axle vehicle yields LTR in the order of 0.27, while operating on a perfectly smooth road, where the influence of damping is negligible. Replacing the conventional belly-axle of the semitrailer by a lifted axle tends to increase the LTR value when the vehicle is operating on the smooth and medium-rough roads. The operation on the rough road with retracted belly axle, however, yields slightly lower LTR value. It should be noted that the LTR, by its definition, is sensitive to the normal loads on the tires. Retracting the liftable axle would impose higher loads on the remaining fixed axles, specifically the drive axle tires and the trailer tandem axle tires. Despite the higher normal loads, the configuration with a single axle lifted yields relatively higher value of LTR, suggesting higher lateral load transfer and dynamic roll motion of the vehicle.

Employing the self-steering axle to replace trailer belly axle tends to offset the degradation of the roll response caused by the lifted axle, when operating on perfectly smooth, smooth and medium-rough roads. The LTR performance of the combination with a self-steering axle traveling on a rough road, however, tends to further deteriorate,

as shown in the table. This is attributed to large variations in the magnitudes of tire forces due to higher tire-road interactions and thus the variations in the effective cornering force of the self-steering axle. The LTR performance of the combination, in general, deteriorates with increasing road roughness, although the influence is relatively small. The influence of road roughness is most significant for the configuration with a self-steering axle, and least significant for that with a lifted axle. The effect of suspension damping on LTR performance of the configurations is almost negligible when the vehicle is operating on smooth roads. The operation on the rough roads, however, yields slightly lower LTR with additional suspension damping by suppressing the variations in the tire forces.

Table 5-5: Summary of LTR responses of configuration 12F12

Trailer axle configurations	Road roughness			
	Perfectly smooth	Smooth	Medium rough	Rough
	Damping ratio = 0.05			
Conventional	0.270	0.291	0.306	0.339
Axle 4 up	0.283	0.299	0.311	0.333
Axle 4 self-steering	0.265	0.274	0.288	0.351
	Damping ratio = 0.10			
Conventional	0.270	0.288	0.302	0.332
Axle 4 up	0.282	0.296	0.307	0.326
Axle 4 self-steering	0.264	0.273	0.286	0.343
	Damping ratio = 0.15			
Conventional	0.270	0.287	0.300	0.332
Axle 4 up	0.281	0.294	0.305	0.326
Axle 4 self-steering	0.264	0.272	0.285	0.334

5.3.2 CONFIGURATION 12F13

The LTR performance of the tractor-semitrailer configuration 12F13 as functions of the road roughness and suspension damping is presented in Table 5-6. The results show that the LTR performance of the configuration 12F13 with conventional axle and

operating on a perfectly smooth road is nearly 0.25, which is slightly lower than the configuration 12F12. The LTR performance, in general, deteriorates only slightly with increasing road roughness, irrespective of the suspension damping, as observed in table 5-5. The phenomenon is more obvious with the self-steering axle, which may be attributed to increased variations in the tire normal loads and thus the cornering forces, due to tire interactions with the road roughness. The effect of suspension damping on the LTR performance is considerably small; the table shows that the increasing suspension damping ratio yields slightly lower LTR value, irrespective of the trailer axle configuration and road roughness, which is mostly attributed to the high suspension damping suppressing the variations in the tire forces.

Table 5-6: Summary of LTR responses of configuration 12F13

Trailer axle configurations	Road roughness			
	Perfectly smooth	Smooth	Medium rough	Rough
	Damping ratio = 0.05			
Conventional	0.245	0.263	0.287	0.322
Axle 4 up	0.284	0.300	0.304	0.347
Axle 4 self-steering	0.247	0.261	0.267	0.331
	Damping ratio = 0.10			
Conventional	0.245	0.259	0.280	0.308
Axle 4 up	0.286	0.299	0.304	0.342
Axle 4 self-steering	0.246	0.257	0.261	0.316
	Damping ratio = 0.15			
Conventional	0.245	0.257	0.275	0.301
Axle 4 up	0.286	0.297	0.303	0.336
Axle 4 self-steering	0.246	0.254	0.257	0.309

For the present configuration, replacing the fixed belly axle by a lifted axle yields considerably higher load transfer and thus deteriorates the LTR performance from 0.25 to 0.29 (16%), while operating on a perfectly smooth road. The use of a self-steering axle to replace the lift axle could not only counteract the degradation of the LTR performance,

but also yield the lowest LTR values, when the vehicle is operating on the smooth or medium-rough road. The LTR performance of the configuration with a self-steering axle on the rough road, however, is slightly inferior to that with the fixed axle.

5.3.3 CONFIGURATION 12F113

Table 5-7 presents the LTR performance of the vehicle configuration 12F113 comprising a tridem trailer with two single axles, which may be either fixed or liftable or self-steering. The results are presented for different road roughness roads and suspension damping ratios, considered in the analysis. The results show that the LTR of configuration 12F113 with conventional axles operating on a perfectly smooth road is 0.22, which is slightly lower than those of the 12F12 and 12F13 configurations. The relative LTR performance of different configurations conforms with the trends observed for the SRT values. The influence of suspension damping on the LTR is almost insignificant as observed for other configurations. The additional suspension damping ratio, however, yields slightly lower LTR values when the vehicle is operating on the rough road. For example, for the vehicle with conventional axles operating on the rough road, an increase in suspension damping ratio from 0.05 to 0.15, causes a decrease in the LTR response from 0.33 to 0.30 (nearly 9%). The LTR values increase with increasing road roughness, irrespective of the suspension damping and axle configurations, which is mostly attributed to the tire-road interactions and the roll content of the road surface.

The vehicle configuration with lead axle (axle 4) raised yields only slightly higher values of LTR, irrespective of the road roughness and damping ratio. Raising a single axle causes relatively smaller change in the normal loads on the remaining axles and thus the LTR. The LTR performance deteriorates most significantly, when both the liftable

Table 5-7: Summary of LTR responses of configuration 12F113

Trailer axle configurations	Road roughness			
	Perfectly smooth	Smooth	Medium rough	Rough
	Damping ratio = 0.05			
Conventional	0.224	0.233	0.242	0.328
Axle 4 up	0.228	0.244	0.263	0.330
Axles 4 and 5 up	0.274	0.292	0.314	0.338
Axle 4 - ss	0.230	0.239	0.246	0.333
Axle 4 and 5 - ss	0.239	0.246	0.252	0.339
Axle 5 up and 4 - ss	0.253	0.267	0.282	0.329
	Damping ratio = 0.10			
Conventional	0.224	0.232	0.241	0.313
Axle 4 up	0.228	0.244	0.262	0.314
Axles 4 and 5 up	0.273	0.287	0.304	0.330
Axle 4 - ss	0.230	0.239	0.245	0.318
Axle 4 and 5 - ss	0.239	0.246	0.249	0.331
Axle 5 up and 4 - ss	0.252	0.263	0.281	0.323
	Damping ratio = 0.15			
Conventional	0.224	0.232	0.241	0.304
Axle 4 up	0.228	0.243	0.261	0.302
Axles 4 and 5 up	0.273	0.285	0.299	0.325
Axle 4 - ss	0.229	0.238	0.245	0.313
Axle 4 and 5 - ss	0.239	0.245	0.249	0.318
Axle 5 up and 4 - ss	0.252	0.260	0.278	0.320

axles are raised, as seen in the table. This configuration yields an LTR of 0.27, when operating on a perfectly smooth surface, indicating an increase of 23%. The LTR value of this configuration approaches as high as 0.34, indicating an increase of 55%, when operating on a rough road. The use of a single self-steering axle tends to yield LTR values that are comparable with those attained for the fixed axle configuration. The LTR performance is slightly deteriorated when two self-steering axles are used, however, the LTR responses of this axle configuration are still lower than those with two retracted belly axles. The combination with a self-steering and a raised axle causes further higher value of LTR on all roads, which are comparable with those attained with two raised axles

5.3.4 CONFIGURATION 12F1113

Table 5-8 summarizes the LTR performance of the vehicle configuration 12F1113 comprising a tridem-axle trailer with three single fixed, liftable or self-steering axles. The results are presented to illustrate the influence of road roughness and suspension damping ratio on the LTR performance. The combination with fixed axles and operating on a perfectly smooth surface yields an LTR value of 0.21, which is lower than those attained for all other configurations. As observed for all previous configurations, the influence of suspension damping on LTR is almost negligible when the combination operates on smooth or medium-rough roads. The effect of damping, however, is evident for operation on rough roads. The LTR response decreases from 0.44 to 0.36, indicating a decreasing of 18%, when the suspension damping ratio increases from 0.05 to 0.15. The LTR performance tends to deteriorate with increasing road roughness, for example, the LTR response increases from 0.21 to 0.35, indicating an increasing of 67%, when the combination with conventional axles with 0.05 suspension damping ratio and operating on the road roughness from perfectly smooth to rough.

The LTR performance of the configuration is strongly dependent upon the trailer axle configurations. The LTR performance deteriorates slightly by using retracted axle to replace a single fixed axle of the semitrailer. The deterioration is most significant when raised liftable axles replace all three single fixed axles. The combination with this axle configuration yields LTR value of 0.26, when operating on a perfectly smooth road, representing an increase of nearly 24% and approaches as high as 0.43, indicating an increasing of 105%, when operating on a rough road. Raising either one or two axles, however, yields considerably smaller increase in the LTR values, as observed in the table.

Table 5-8: Summary of LTR responses of configuration 12F1113

Trailer axle configurations	Road roughness			
	Perfectly smooth	Smooth	Medium rough	Rough
	Damping ratio = 0.05			
Conventional	0.210	0.238	0.267	0.353
Axle 4 up	0.218	0.241	0.274	0.357
Axles 4 and 5 up	0.232	0.253	0.288	0.395
Axles 4, 5 and 6 up	0.262	0.275	0.288	0.436
Axle 4 - ss	0.216	0.240	0.279	0.424
Axles 4 and 5 - ss	0.221	0.243	0.277	0.408
Axles 4, 5 and 6 - ss	0.223	0.243	0.276	0.410
Axle 5 up and 4 - ss	0.228	0.248	0.267	0.432
Axles 5 and 6 up, 4 - ss	0.267	0.270	0.284	0.373
Axle 6 up and 4 - ss	0.231	0.239	0.256	0.418
Axle 6 up, 4 and 5 - ss	0.235	0.243	0.252	0.412
	Damping ratio = 0.10			
Conventional	0.210	0.236	0.260	0.323
Axle 4 up	0.218	0.238	0.267	0.344
Axles 4 and 5 up	0.231	0.251	0.272	0.344
Axles 4, 5 and 6 up	0.262	0.274	0.283	0.379
Axle 4 - ss	0.216	0.239	0.273	0.384
Axles 4 and 5 - ss	0.221	0.243	0.273	0.388
Axles 4, 5 and 6 - ss	0.223	0.242	0.270	0.379
Axle 5 up and 4 - ss	0.228	0.244	0.262	0.378
Axles 5 and 6 up, 4 - ss	0.266	0.267	0.284	0.344
Axle 6 up and 4 - ss	0.231	0.238	0.253	0.380
Axle 6 up, 4 and 5 - ss	0.235	0.240	0.248	0.373
	Damping ratio = 0.15			
Conventional	0.210	0.234	0.256	0.321
Axle 4 up	0.217	0.236	0.263	0.325
Axles 4 and 5 up	0.230	0.249	0.267	0.339
Axles 4, 5 and 6 up	0.262	0.273	0.280	0.363
Axle 4 - ss	0.216	0.237	0.270	0.357
Axles 4 and 5 - ss	0.221	0.242	0.270	0.353
Axles 4, 5 and 6 - ss	0.222	0.241	0.267	0.364
Axle 5 up and 4 - ss	0.227	0.241	0.260	0.342
Axles 5 and 6 up, 4 - ss	0.265	0.267	0.285	0.333
Axle 6 up and 4 - ss	0.231	0.238	0.254	0.349
Axle 6 up, 4 and 5 - ss	0.235	0.238	0.247	0.357

Replacing the fixed axles by the self-steering axles yields comparable results with those attained from the vehicle with conventional axles and offsets the deterioration caused by the retracted single axles of semitrailer. The combination with a leading self-steering axle

(axle 4) and two raised axles (axles 5 and 6), however, yields significantly higher lateral load transfer, which are comparable with those attained with all three raised axles for all roads considered in the analyses.

5.3.5 REARWARD AMPLIFICATION (RA)

The rearward amplification (RA) ratio is a frequency dependent measure, defined as the ratio of peak (positive or negative) lateral acceleration at the center of gravity of the rearmost trailer to that of the lead unit (tractor). The lateral acceleration responses of the two units are evaluated under a standardized path-change maneuver at a constant forward speed of $100\,km/h$, as described in section 3.2.2 [34,65]. The analyses are performed for different combinations equipped with fixed, liftable and self-steering axles, while the vehicle operates on different roads with varying roughness properties.

5.3.6 CONFIGURATION 12F12

Table 5-9 summarizes the RA performance of the tractor-semitrailer configuration 12F12 as functions of the road roughness, suspension damping ratio, and different trailer axle configurations. The configuration with conventional axles yields an RA value of 1.19, while operating on a perfectly smooth road. This value of RA is considerably lower than the recommended limiting value of 2.2 [65], and comparable with those reported in many studies [34]. The effect of suspension damping on the RA response of the combination is negligible, irrespective of the road roughness and axle configurations. The influence of road roughness on RA response is relatively significant. The higher road roughness yields considerably lower value of RA. The RA response of the conventional axle vehicle operating on a rough road reduces to 0.48, a decrease of nearly 60%. It should be noted that RA is the ratio of peak lateral acceleration of the semitrailer to that

of the tractor. Higher or lower peak acceleration of a unit may occur in response to local variations in the road elevation, which could yield either lower or higher RA value depending on the relative magnitudes of tractor and trailer lateral acceleration. The results, in general, thus do not show a definite trend with respect to the road roughness.

Replacing the fixed trailer axle with a raised liftable axle generally causes a slightly higher RA response on perfectly smooth, smooth and medium rough roads, for all damping values considered. The RA values of this axle configuration are observed to be lower than those attained from the conventional semitrailer when the combination operating on rough road, which is mostly attributed to relatively lower trailer lateral acceleration. The use of a self-steering axle tends to yield comparable RA values with those of the vehicle with conventional axles, irrespective of the road roughness and suspension damping considered.

Table 5-9: Summary of RA responses of configuration 12F12

Trailer axle configurations	Road roughness			
	Perfectly smooth	Smooth	Medium rough	Rough
	Damping ratio = 0.05			
Conventional	1.194	1.021	0.873	0.475
Axle 4 up	1.205	1.106	1.005	0.432
Axle 4 self-steering	1.120	0.988	0.872	0.487
	Damping ratio = 0.10			
Conventional	1.194	1.029	0.915	0.495
Axle 4 up	1.203	1.094	0.998	0.470
Axle 4 self-steering	1.115	0.979	0.871	0.486
	Damping ratio = 0.15			
Conventional	1.191	1.032	0.909	0.526
Axle 4 up	1.202	1.085	0.984	0.514
Axle 4 self-steering	1.112	0.971	0.866	0.497

5.3.7 CONFIGURATION 12F13

Table 5-10 summarizes the performance in terms of RA values of the vehicle configuration 12F13 comprising a tridem axle trailer with a single axle, which may be the

conventional, liftable or self-steering axle, as functions of the road roughness and suspension damping. The results show that the RA value of the vehicle configuration with conventional axles is 1.17, while operating on a perfectly smooth surface, which is slightly lower that that of the configuration 12F12. The effect of suspension damping ratio on the RA value of the configuration is negligible when the suspension damping ratio is relatively low (DR = 0.05, 0.10). With the high suspension damping (DR = 0.15), however, the additional suspension damping tends to increase the RA response of the combination. Irrespective of the trailer axle configurations and suspension damping, the rougher road generally tends to decrease the RA performance. When the road roughness is increased from perfectly smooth to rough, the RA response of the configuration 12F13 with conventional axles tends to decrease from 1.17 to 0.53, representing a decreasing of 55%.

Table 5-10: Summary of RA responses of configuration 12F13

Trailer axle configurations	Road roughness			
	Perfectly smooth	Smooth	Medium rough	Rough
	Damping ratio = 0.05			
Conventional	1.175	0.974	0.863	0.512
Axle 4 up	1.194	1.045	0.882	0.529
Axle 4 self-steering	1.163	0.968	0.820	0.511
	Damping ratio = 0.10			
Conventional	1.180	0.978	0.861	0.498
Axle 4 up	1.193	1.036	0.886	0.519
Axle 4 self-steering	1.167	0.966	0.812	0.491
	Damping ratio = 0.15			
Conventional	1.192	1.181	1.048	0.519
Axle 4 up	1.209	1.200	1.182	0.538
Axle 4 self-steering	1.169	1.151	1.034	0.480

Replacing the fixed trailer axle with a raised liftable axle causes a slightly higher RA response, irrespective of the road roughness and the suspension damping. The use of

a self-steering axle instead of the retracted axle tends to yield the lowest values of RA, irrespective of the road roughness and suspension damping, as observed for configuration 12F12.

5.3.8 CONFIGURATION 12F113

Table 5-11 summarizes the directional performance measure in terms of RA of the configuration 12F113 as functions of the road roughness and suspension damping. The RA value of the configuration 12F113 with conventional axles operating on a perfectly smooth road is 1.09, which is lower than those of both the previous configurations 12F12 and 12F13. The effects of suspension damping and road roughness on the RA are also similar to those observed for the 12F12 and 12F13 configurations.

The vehicle configuration with one (axle 4) or two (axles 4 and 5) retracted axles yields slightly higher values of RA response, while operating on perfectly smooth, smooth and medium-rough roads, irrespective of the suspension damping. When the vehicle is operated on the rough road, the lifted axle(s) causes slightly lower RA values. Replacing both the fixed trailer single axles by self-steering axles, instead of the lifted axles, however, yields comparable magnitudes of RA for operation on the perfectly smooth, smooth and medium-rough roads, but slightly higher magnitudes for rough road operation. The influence of the configuration with leading self-steering axle (axle 4) and trailing retracted axle (axle 5) is similar to that of the lifted axles. This particular configuration yields highest RA value of 1.2, when the vehicle is operating on perfectly smooth, smooth and medium-rough roads.

Table 5-11: Summary of RA responses of configuration 12F113

Trailer axle configurations	Road roughness			
	Perfectly smooth	Smooth	Medium rough	Rough
	Damping ratio = 0.05			
Conventional	1.087	0.940	0.818	0.507
Axle 4 up	1.120	0.975	0.834	0.530
Axles 4 and 5 up	1.138	1.003	0.865	0.511
Axle 4 - ss	1.103	0.959	0.815	0.512
Axle 4 and 5 - ss	1.098	0.951	0.823	0.534
Axle 5 up and 4 - ss	1.198	1.001	0.869	0.503
	Damping ratio = 0.10			
Conventional	1.088	0.941	0.828	0.535
Axle 4 up	1.122	0.973	0.863	0.517
Axles 4 and 5 up	1.136	0.989	0.870	0.511
Axle 4 - ss	1.105	0.961	0.806	0.547
Axle 4 and 5 - ss	1.098	0.947	0.806	0.539
Axle 5 up and 4 - ss	1.200	1.000	0.865	0.514
	Damping ratio = 0.15			
Conventional	1.089	0.942	0.827	0.552
Axle 4 up	1.125	0.973	0.860	0.506
Axles 4 and 5 up	1.133	0.985	0.867	0.526
Axle 4 - ss	1.106	0.962	0.825	0.551
Axle 4 and 5 - ss	1.097	0.943	0.805	0.529
Axle 5 up and 4 - ss	1.201	1.002	0.864	0.528

5.3.9 CONFIGURATION 12F1113

Table 5-12 summarizes the RA performance of the vehicle configuration 12F1113 comprising a tridem-axle trailer with three fixed, liftable or self-steering single axles. The results show similar influence of the trailer axle configurations, road roughness and suspension damping ratio, as observed for the six-, seven- and eight-axle combinations in the previous subsections. The RA value of the configuration with conventional fixed axles is 1.07, which is slightly lower than those attained for all other configurations. As observed for all other configurations, the magnitude of RA of the configuration 12F1113 decreases considerably with increasing road roughness. The combination operating on a rough road yields a considerably lower value of 0.49, indicating a decrease of 54%.

Table 5-12: Summary of RA responses of configuration 12F1113

Trailer axle configurations	Road roughness			
	Perfectly smooth	Smooth	Medium rough	Rough
	Damping ratio = 0.05			
Conventional	1.065	0.937	0.841	0.490
Axle 4 up	1.086	0.968	0.872	0.560
Axles 4 and 5 up	1.118	0.960	0.875	0.563
Axles 4, 5 and 6 up	1.113	0.994	0.876	0.567
Axle 4 - ss	1.066	0.965	0.865	0.465
Axles 4 and 5 - ss	1.064	0.927	0.833	0.469
Axles 4, 5 and 6 - ss	1.020	0.880	0.802	0.450
Axle 5 up and 4 - ss	1.124	0.954	0.813	0.483
Axles 5 and 6 up, 4 - ss	1.194	0.977	0.843	0.452
Axle 6 up and 4 - ss	1.142	0.943	0.785	0.450
Axle 6 up, 4 and 5 - ss	1.149	0.962	0.762	0.473
	Damping ratio = 0.10			
Conventional	1.065	0.935	0.846	0.501
Axle 4 up	1.088	0.958	0.850	0.572
Axles 4 and 5 up	1.120	0.954	0.861	0.575
Axles 4, 5 and 6 up	1.112	0.961	0.867	0.583
Axle 4 - ss	1.067	0.956	0.851	0.497
Axles 4 and 5 - ss	1.062	0.934	0.843	0.489
Axles 4, 5 and 6 - ss	1.019	0.885	0.808	0.490
Axle 5 up and 4 - ss	1.127	0.952	0.832	0.541
Axles 5 and 6 up, 4 - ss	1.190	0.981	0.836	0.503
Axle 6 up and 4 - ss	1.144	0.958	0.802	0.501
Axle 6 up, 4 and 5 - ss	1.150	0.973	0.781	0.524
	Damping ratio = 0.15			
Conventional	1.064	0.930	0.837	0.504
Axle 4 up	1.091	0.954	0.840	0.574
Axles 4 and 5 up	1.121	0.948	0.842	0.581
Axles 4, 5 and 6 up	1.111	0.950	0.858	0.594
Axle 4 - ss	1.067	0.943	0.849	0.504
Axles 4 and 5 - ss	1.061	0.932	0.835	0.486
Axles 4, 5 and 6 - ss	1.019	0.878	0.803	0.483
Axle 5 up and 4 - ss	1.129	0.956	0.845	0.579
Axles 5 and 6 up, 4 - ss	1.186	0.981	0.839	0.567
Axle 6 up and 4 - ss	1.147	0.969	0.763	0.546
Axle 6 up, 4 and 5 - ss	1.152	0.973	0.800	0.572

The results suggest that replacing one, two or three (all) single trailer axles by retracted axles could slightly increase the RA value, irrespective of the road roughness and suspension damping. The use of one or more self-steering axles to replace the

semitrailer single axles can decrease the RA values and offset the deterioration caused by one or more lifted axles. Replacing all three single axles by the self-steering axles yields the lowest RA value. A combination of a retracted axle and either one or two self-steering axles causes the RA values to increase. The combination with leading self-steering axle (axle 4) and two trailing lifted axles (axle 5 and 6) yields the highest RA value.

5.4 HIGH-SPEED FRICTION DEMAND (HSFD)

High-speed friction demand characterizes the surface friction level required by the drive axle group of a tractor during a high-speed (100 km/h) path-change maneuver without reaching the full skid condition at the drive axles [65]. The definition of the HSFD measure together with method of its computation has been described in chapter 3. A lower value of HSFD is desirable for the vehicle to retain directional stability on low friction surfaces. The recommended upper limit of HSFD for a tractor-semitrailer is 0.3 [65].

5.4.1 CONFIGURATION 12F12

Table 5-13 summarizes the relative HSFD performance of the 6-axle combination (configuration 12F12) with fixed, liftable and self-steering belly axle. The results are presented for four different road roughness and suspension damping ratios considered in the study. The fixed belly axle configuration yields HSFD value slightly less than 0.12, while operating on a smooth road. The influence of suspension damping on the HSFD measure appears to be negligible for the perfectly smooth surface operation. The friction demand, however, tends to increase with increasing road roughness, which is attributed to variations in the dynamic tire normal loads and cornering forces due to variations in the road elevation. The HSFD value of the fixed axle configuration

approaches nearly 0.17 under rough road and low damping ratio (0.05), indicating an increasing of 42%.

Table 5-13: Summary of HSFD responses of configuration 12F12

Trailer axle configurations	Road roughness			
	Perfectly smooth	Smooth	Medium rough	Rough
	Damping ratio = 0.05			
Conventional	0.118	0.121	0.127	0.166
Axle 4 up	0.112	0.115	0.117	0.153
Axle 4 self-steering	0.114	0.118	0.125	0.166
	Damping ratio = 0.10			
Conventional	0.118	0.121	0.126	0.166
Axle 4 up	0.112	0.113	0.117	0.151
Axle 4 self-steering	0.114	0.118	0.123	0.166
	Damping ratio = 0.15			
Conventional	0.118	0.121	0.126	0.165
Axle 4 up	0.112	0.113	0.117	0.151
Axle 4 self-steering	0.114	0.118	0.122	0.165

Replacing the fixed belly axle with a raised liftable axle imposes higher loads on the drive axle, and thus reduces the friction demand, irrespective of the road roughness and the damping ratio. The use of a self-steering axle instead of the lift axle yields slightly higher value of HSFD than those attained from the vehicle using lifted axle. This axle configuration, however, yield the highest HSFD values under rough road excitation, which is most likely attributed to reduced cornering force ability of the steerable axle. The results suggest that the vehicle configurations with fixed, liftable and self-steering axles would easily satisfy the HSFD requirements. The configuration with raised liftable axle would yield slightly lower value of HSFD.

5.4.2 CONFIGURATION 12F13

Table 5-14 summarizes the HSFD performance of the 7-axle vehicle configuration 12F13 comprising a tridem trailer with a single axle, which may be the

fixed, liftable or self-steering axle. The vehicle configuration with fixed axles yields HSFD value nearly 0.13, while operating on a perfectly smooth surface. This value is slightly higher than that of the 6-axle (12F12) configuration. As observed for 12F12 configuration, the influence of suspension damping ratio on the HSFD measure may be neglected. The friction demand, in general, approaches considerably higher values with increasing road roughness. The HSFD value of the configuration with conventional axles approaches nearly 0.16 under rough road and low damping ratio (DR = 0.05), indicating an increasing of 23%. As observed for 12F12 configuration, the use of a lifted axle yields slightly lower high-speed friction demand, irrespective of the road roughness and suspension damping. Replacing the raised axle with a self-steering axle imposes a higher friction demand.

Table 5-14: Summary of HSFD responses of configuration 12F13

Trailer axle configurations	Road roughness			
	Perfectly smooth	Smooth	Medium rough	Rough
	Damping ratio = 0.05			
Conventional	0.124	0.129	0.134	0.164
Axle 4 up	0.120	0.125	0.132	0.156
Axle 4 self-steering	0.122	0.127	0.132	0.162
	Damping ratio = 0.10			
Conventional	0.124	0.129	0.134	0.164
Axle 4 up	0.120	0.123	0.129	0.154
Axle 4 self-steering	0.122	0.126	0.131	0.161
	Damping ratio = 0.15			
Conventional	0.124	0.128	0.133	0.162
Axle 4 up	0.119	0.122	0.128	0.153
Axle 4 self-steering	0.122	0.126	0.130	0.159

5.4.3 CONFIGURATION 12F113

The 8-axle vehicle combination with trailer with 2 single and a tridem-axle (configuration 12F113) yields HSFD of 0.14 (Table 5-15), while operating on a perfectly

smooth road, which is slightly higher than the 6- and 7-axle combinations (12F12 and 12F13). The influence of suspension damping on the HSFD performance is negligible. Higher suspension damping, however, yields slightly lower HSFD values for operation on medium-rough and rough roads. Increasing road roughness causes high HSFD, as observed for other configurations. The use of raised liftable axles causes higher normal loads on the driver axle tires and thus lower HSFD value, as observed for other configurations. The use of either one or two retracted semitrailer belly axles reduces the HSFD value from 0.14 to 0.12 (14%). However, replacing the single belly axles by one or two self-steering axles, or a combination of leading self-steering axle with trailing retracted axle, would yield considerably higher HSFD.

Table 5-15: Summary of HSFD responses of configuration 12F113

Trailer axle configurations	Road roughness			
	Perfectly smooth	Smooth	Medium rough	Rough
	Damping ratio = 0.05			
Conventional	0.135	0.136	0.139	0.182
Axle 4 up	0.116	0.120	0.124	0.152
Axles 4 and 5 up	0.118	0.121	0.127	0.153
Axle 4 - ss	0.140	0.141	0.144	0.180
Axle 4 and 5 - ss	0.136	0.138	0.141	0.185
Axle 5 up and 4 - ss	0.139	0.144	0.150	0.180
	Damping ratio = 0.10			
Conventional	0.135	0.136	0.139	0.177
Axle 4 up	0.116	0.120	0.123	0.153
Axles 4 and 5 up	0.118	0.120	0.126	0.153
Axle 4 - ss	0.140	0.141	0.143	0.187
Axle 4 and 5 - ss	0.136	0.138	0.140	0.185
Axle 5 up and 4 - ss	0.139	0.144	0.149	0.181
	Damping ratio = 0.15			
Conventional	0.135	0.136	0.138	0.177
Axle 4 up	0.116	0.119	0.123	0.151
Axles 4 and 5 up	0.118	0.120	0.125	0.151
Axle 4 - ss	0.140	0.141	0.143	0.184
Axle 4 and 5 - ss	0.136	0.138	0.140	0.177
Axle 5 up and 4 - ss	0.139	0.143	0.148	0.178

5.4.4 CONFIGURATION 12F1113

Table 5-16 summarizes the relative HSFD performance of the 9-axle tractor-semitrailer configuration 12F1113, employing three fixed, liftable or self-steering axles.

Table 5-16: Summary of HSFD responses of configuration 12F1113

Trailer axle configurations	Road roughness			
	Perfectly smooth	Smooth	Medium rough	Rough
	Damping ratio = 0.05			
Conventional	0.132	0.136	0.140	0.186
Axle 4 up	0.117	0.119	0.121	0.161
Axles 4 and 5 up	0.111	0.116	0.123	0.163
Axles 4, 5 and 6 up	0.114	0.116	0.120	0.154
Axle 4 - ss	0.142	0.147	0.151	0.202
Axles 4 and 5 - ss	0.143	0.147	0.151	0.210
Axles 4, 5 and 6 - ss	0.141	0.146	0.150	0.215
Axle 5 up and 4 - ss	0.135	0.136	0.140	0.187
Axles 5 and 6 up, 4 - ss	0.147	0.155	0.162	0.203
Axle 6 up and 4 - ss	0.142	0.143	0.149	0.186
Axle 6 up, 4 and 5 - ss	0.142	0.144	0.150	0.187
	Damping ratio = 0.10			
Conventional	0.132	0.136	0.139	0.183
Axle 4 up	0.117	0.119	0.121	0.152
Axles 4 and 5 up	0.111	0.115	0.122	0.157
Axles 4, 5 and 6 up	0.114	0.116	0.120	0.152
Axle 4 - ss	0.142	0.147	0.149	0.192
Axles 4 and 5 - ss	0.143	0.147	0.150	0.203
Axles 4, 5 and 6 - ss	0.141	0.146	0.149	0.204
Axle 5 up and 4 - ss	0.135	0.135	0.138	0.177
Axles 5 and 6 up, 4 - ss	0.147	0.154	0.161	0.197
Axle 6 up and 4 - ss	0.142	0.143	0.149	0.183
Axle 6 up, 4 and 5 - ss	0.142	0.144	0.149	0.181
	Damping ratio = 0.15			
Conventional	0.132	0.136	0.138	0.180
Axle 4 up	0.117	0.119	0.120	0.152
Axles 4 and 5 up	0.111	0.115	0.121	0.154
Axles 4, 5 and 6 up	0.114	0.116	0.121	0.150
Axle 4 - ss	0.142	0.147	0.149	0.190
Axles 4 and 5 - ss	0.143	0.147	0.149	0.194
Axles 4, 5 and 6 - ss	0.141	0.146	0.148	0.195
Axle 5 up and 4 - ss	0.135	0.135	0.138	0.169
Axles 5 and 6 up, 4 - ss	0.146	0.153	0.160	0.195
Axle 6 up and 4 - ss	0.142	0.143	0.148	0.179
Axle 6 up, 4 and 5 - ss	0.142	0.144	0.149	0.182

The HSFD value of the multiple axle configuration with fixed axles is comparable with the 8-axle configuration and slightly higher than that those of the 6- and 7-axle configurations (12F12 and 12F13). The influence of the suspension damping is nearly negligible when the vehicle combination is operated on perfectly smooth to medium-rough roads, as observed for other configurations. The HSFD decreases under tire interactions with rough road, which could be suppressed to an extent by increasing the suspension damping. Higher road roughness tends to increase HSFD value, irrespective of the trailer axle configurations and suspension damping.

Raising either one or two or all three single axles (axles 4, 5 and 6) lowers the HSFD, as observed for other configurations, suggesting improved vehicle stability on low friction roads. The HSFD of 0.13 for conventional fixed axles reduces to around 0.11, indicating a decreasing of 15%, when either two or three axles are raised. The use of self-steering axles (axle 4, 5 and 6) causes the HSFD to increase. The highest friction demand is attained when the leading axle (axle 4) is replaced by a self-steering axle and the two trailing axles (axles 5 and 6) are raised.

5.5 LOW-SPEED FRICTION DEMAND (LSFD)

The low-speed friction demand characterizes the tire/road friction level required by the drive axle group of a combination during tight turns, such as a 90 degree turn at constant forward speed of 8.8 km / h [67]. The measure relates to low-speed jackknife potential of the vehicle, when its friction demand exceeds the available pavement friction. The definition of the measure and method of its computation have been described in chapter 3. A lower value of LSFD is desirable to ensure effective and stable tight turn

performance on low friction roads, such as icy roads. The recommended limiting value of LSFD value is 0.1 [67].

5.5.1 CONFIGURATION 12F12

Table 5-17 summarizes the relative LSFD performance of the 6-axle vehicle configuration 12F12 with fixed, liftable and self-steering belly axle. The results also show variations in LSFD under varying road roughness and suspension damping ratio. The results show that the fixed belly axle combination yields LSFD of nearly 0.13, while operating on a perfectly smooth road. The resulting value exceeds the recommended upper limit of 0.1, which suggests that the selected configuration could experience low speed jackknife while making tight turns on a low friction surface, such as an icy road. The increase in suspension damping ratio or road roughness does not affect the LSFD of this combination. This trend is attributed to extremely low speed operation of the vehicle, which yields only minimal variations in the dynamic tire forces.

Table 5-17: Summary of LSFD responses of configuration 12F12

Trailer axle configurations	Road roughness			
	Perfectly smooth	Smooth	Medium rough	Rough
	Damping ratio = 0.05			
Conventional	0.131	0.134	0.138	0.136
Axle 4 up	0.039	0.039	0.039	0.039
Axle 4 self-steering	0.186	0.187	0.189	0.189
	Damping ratio = 0.10			
Conventional	0.131	0.134	0.137	0.135
Axle 4 up	0.038	0.038	0.038	0.038
Axle 4 self-steering	0.186	0.186	0.188	0.189
	Damping ratio = 0.15			
Conventional	0.131	0.134	0.137	0.135
Axle 4 up	0.037	0.037	0.037	0.037
Axle 4 self-steering	0.186	0.186	0.188	0.189

The LSFD performance of the vehicle can be most significantly enhanced by replacing the fixed axle with a raised liftable axle, as evident from the results. Raising the liftable belly axle yields significantly lower off-tracking performance of the vehicle, in the order of 0.04. This lower value satisfies the recommended LSFD requirement and thus offers lower low-speed jackknife potential. The reduction in the LSFD is attributed to relatively higher loads on the drive axle tires resulting in higher cornering forces due to drive axle tires. The use of self-steering axle instead of the raised liftable axle causes the highest LSFD value and exceeds those of the fixed axle combination, which is most likely attributed to relative changes in the articulation angle and the effective cornering force.

5.5.2 CONFIGURATION 12F13

Table 5-18 summarizes the relative LSFD performance of the 7-axle vehicle configuration 12F13 comprising a tridem-axle semitrailer with a fixed, liftable or self-steering belly axle. Owing to the low speed, the effect of suspension damping and road roughness is negligible, and thus not discussed. The addition of an axle to the semitrailer causes higher off-tracking and lower articulation angle, and thus considerably higher LSFD than the 6-axle configuration. The LSFD of the 7-axle combination with fixed belly axle trailer is around 0.29, considerably higher than the recommended upper limit of 0.1. These results suggest that this configuration with a fixed belly axle could experience low-speed jackknife while making tight turns on a low friction surface.

The LSFD performance of the vehicle can be most significantly enhanced by replacing the fixed axle with a raised liftable axle, as evident from the results. Raising the liftable axle yields significantly lower off-tracking performance of the vehicle, relatively

higher loads on the drive axle tires, and thus lower magnitude of LSFD (in the order of 0.08). The use of self-steering axle instead of the raised liftable axle causes the LSFD value to exceed those of the fixed axle combination.

Table 5-18: Summary of LSFD responses of configuration 12F13

Trailer axle configurations	Road roughness			
	Perfectly smooth	Smooth	Medium rough	Rough
	Damping ratio = 0.05			
Conventional	0.290	0.291	0.295	0.286
Axle 4 up	0.083	0.084	0.088	0.090
Axle 4 self-steering	0.408	0.410	0.413	0.403
	Damping ratio = 0.10			
Conventional	0.290	0.291	0.295	0.285
Axle 4 up	0.083	0.084	0.087	0.088
Axle 4 self-steering	0.408	0.410	0.412	0.403
	Damping ratio = 0.15			
Conventional	0.290	0.291	0.295	0.285
Axle 4 up	0.083	0.084	0.086	0.087
Axle 4 self-steering	0.408	0.409	0.412	0.403

5.5.3 CONFIGURATION 12F113

The relative LSFD performance characteristics of the 8-axle vehicle configuration 12F113 with two fixed, liftable or self-steering belly axles are summarized in Table 5-19. The addition of another fixed belly axle to the semitrailer causes the LSFD to increase further to nearly 0.54, irrespective of the suspension damping and road roughness. This configuration is thus considered to be high-risk combination in view of low-speed jackknife on icy or slippery roads. The LSFD performance of the vehicle improves most significantly when the two single belly axles are replaced by liftable axles and raised during the tight turn maneuver, this axle configuration yields LSFD value approaching close to 0.07. The use of self-steering axles further deteriorates the LSFD performance, as observed for other vehicle configurations. While the use of a single raised axle (axle 4)

yields significant reduction in the LSFD, the combination of a lead self-steering axle and raised trailing axle causes significantly higher value of LSFD, in the order of 0.66.

Table 5-19: Summary of LSFD responses of configuration 12F113

Trailer axle configurations	Road roughness			
	Perfectly smooth	Smooth	Medium rough	Rough
	Damping ratio = 0.05			
Conventional	0.538	0.538	0.538	0.538
Axle 4 up	0.223	0.226	0.230	0.251
Axles 4 and 5 up	0.070	0.071	0.072	0.072
Axle 4 - ss	0.672	0.672	0.672	0.672
Axle 4 and 5 - ss	0.698	0.698	0.698	0.698
Axle 5 up and 4 - ss	0.659	0.659	0.659	0.659
	Damping ratio = 0.10			
Conventional	0.538	0.538	0.538	0.538
Axle 4 up	0.223	0.226	0.229	0.251
Axles 4 and 5 up	0.070	0.071	0.072	0.074
Axle 4 - ss	0.672	0.672	0.672	0.672
Axle 4 and 5 - ss	0.698	0.698	0.698	0.698
Axle 5 up and 4 - ss	0.662	0.662	0.662	0.662
	Damping ratio = 0.15			
Conventional	0.538	0.538	0.538	0.538
Axle 4 up	0.223	0.226	0.229	0.251
Axles 4 and 5 up	0.070	0.071	0.072	0.074
Axle 4 - ss	0.672	0.672	0.672	0.672
Axle 4 and 5 - ss	0.698	0.698	0.698	0.698
Axle 5 up and 4 - ss	0.662	0.662	0.662	0.662

5.5.4 CONFIGURATION 12F1113

The relative LSFD performance characteristics of the 9-axle vehicle configuration 12F1113 with different axles are summarized in Table 5-20. The results demonstrate most significant influences of liftable and self-steering axles, as observed for the 6-, 7- and 8-axle combinations. The LSFD of the fixed axle combination increases to nearly 0.68 due to addition of one more axle and the associated increase in low-speed off-tracking. Replacing one or more fixed belly axles of the semitrailer by retracted axles yields significantly lower LSFD values. The LSFD decreases from 0.68 to 0.07,

Table 5-20: Summary of LSFD responses of configuration 12F1113

Trailer axle configurations	Road roughness			
	Perfectly smooth	Smooth	Medium rough	Rough
	Damping ratio = 0.05			
Conventional	0.678	0.678	0.678	0.678
Axle 4 up	0.329	0.330	0.330	0.351
Axles 4 and 5 up	0.160	0.164	0.168	0.192
Axles 4, 5 and 6 up	0.064	0.064	0.068	0.081
Axle 4 - ss	0.549	0.549	0.549	0.549
Axles 4 and 5 - ss	0.511	0.511	0.511	0.511
Axles 4, 5 and 6 - ss	0.532	0.532	0.532	0.532
Axle 5 up and 4 - ss	0.883	0.883	0.883	0.883
Axles 5 and 6 up, 4 - ss	/	/	/	/
Axle 6 up and 4 - ss	0.566	0.566	0.566	0.566
Axle 6 up, 4 and 5 - ss	0.641	0.641	0.641	0.641
	Damping ratio = 0.10			
Conventional	0.669	0.669	0.669	0.669
Axle 4 up	0.330	0.330	0.337	0.346
Axles 4 and 5 up	0.160	0.163	0.167	0.186
Axles 4, 5 and 6 up	0.064	0.064	0.064	0.079
Axle 4 - ss	/	/	/	/
Axles 4 and 5 - ss	/	/	/	/
Axles 4, 5 and 6 - ss	/	/	/	/
Axle 5 up and 4 - ss	0.887	0.887	0.887	0.887
Axles 5 and 6 up, 4 - ss	/	/	/	/
Axle 6 up and 4 - ss	/	/	/	/
Axle 6 up, 4 and 5 - ss	/	/	/	/
	Damping ratio = 0.15			
Conventional	0.669	0.669	0.669	0.669
Axle 4 up	0.330	0.330	0.330	0.340
Axles 4 and 5 up	0.160	0.162	0.166	0.180
Axles 4, 5 and 6 up	0.063	0.065	0.067	0.079
Axle 4 - ss	/	/	/	/
Axles 4 and 5 - ss	/	/	/	/
Axles 4, 5 and 6 - ss	/	/	/	/
Axle 5 up and 4 - ss	0.888	0.888	0.888	0.888
Axles 5 and 6 up, 4 - ss	/	/	/	/
Axle 6 up and 4 - ss	/	/	/	/
Axle 6 up, 4 and 5 - ss	/	/	/	/

' / ' – LSFD > 1.0

representing a decreasing of 85%, when all the three fixed axles are replaced by liftable axles and retracted. This particular axle configuration could lead to the lowest LSFD

value and the off-tracking performance. The use of self-steering axles instead of the fixed axles also yields higher values of LSFD, as observed for the 6-, 7- and 8-axle configurations.

5.6 SUMMARY

The influence of conventional, liftable and self-steering trailer axles, together with the road roughness and suspension damping ratio on the directional dynamics of the multiple axles articulated heavy vehicles are investigated through assessment of relative performance measures. The results suggest that the steady turning rollover threshold (SRT) of the combination with a raised liftable axle would deteriorate, when the increase in the loads supported by the remaining axles is considerably large. The SRT responses of combinations with fixed and self-steering axle are quite comparable. The LTR, considered as a measure of dynamic rollover, generally increases as one or more liftable axles are retracted, suggesting reduced dynamic roll stability limit. The vehicle operation on relatively rough roads could further deteriorate the static as well as dynamic roll stability limits due to variations in the dynamic tire forces and the cornering forces. The addition of suspension damping, however, tends to suppress the tire forces variations and thus enhance the SRT and LTR. The combinations with multiple single axles, replaced by raised lift axles, could yield higher SRT due to relatively small change in the loads on tires of the remaining axles and increase in the net restoring moment. The rearward amplification of the vehicle combination tends to increase with higher damping and lower road roughness, and when the liftable axles are retracted. The vehicle combinations with raised liftable axles yield most significant performance benefits in terms of high speed

and low speed friction demand. The results thus suggest that liftable axle, when raised, would provide better stability on slippery roads, but yield lower roll stability limits.

CHAPTER 6 : ROAD DAMAGE POTENTIAL ANALYSIS

6.1 GENERAL

Owing to the high magnitudes of dynamic tire loads of heavy vehicles transmitted to the pavements, a range of methods have evolved to assess the road damaging potential of heavy vehicles. Heavy vehicle design parameters affecting the degree of damage sustained by a road can be classified according to: axle configuration (weight and spacing), tire configuration (number of tires per axle, type and inflation pressure), static load sharing ability of the suspension, and dynamic tire forces. A number of studies have reviewed the significance of these factors in details [5,40,41]. These studies have invariably emphasized the importance of the dynamic component of the heavy vehicle tire forces as a major factor contributing to the road damage. The dynamic components of the tire forces are not only quite significant compared to the mean tire force, but also exhibit high "spatial repeatability" for different vehicles operating on the roads [52-55]

Dynamic tire forces applied to the road surfaces by heavy vehicles are believed to be an important cause of premature road failure, although the failure mechanisms are not well understood. Dynamic tire forces are caused by vibration of a moving vehicle excited by the road surface roughness. They are influenced by the vehicle speed, axle configuration and load, road roughness, gross vehicle weight and the design of the vehicle, particularly its suspension system [8,45,46]. A comprehensive review of the factors that influence the road damage potential of dynamic tire forces has been presented by Cebon [67]. The vehicle load supported by a tire directly affects the magnitude of dynamic tire forces transmitted to the pavement and thus the pavement damage potential

of the heavy vehicle. Heavy vehicle combinations with one or more liftable axle trailers are currently being used to enhance the load carrying capacity of the vehicle. The primary purpose of these axles is to enhance the mobility of the vehicle during turns by retracting these axles, and thereby reduce the magnitude of off-tracking and tire wear. Retracting the liftable axles however imposes considerably higher load damaging potential of the vehicle, as the remaining conventional axle tires share the loads supported by the liftable axles. The resulting higher tire loads not only impose high magnitudes of dynamic forces to the pavement, but could also degrade the directional performance, as illustrated in the previous chapter. In this chapter, the relative damage potentials of tractor-semitrailer combinations with conventional and liftable axles are investigated, when one or more liftable axles are retracted, using the performance measures described in chapter 3. The analyses for the vehicle with self-steering axles are not performed as the results would be identical to that with the conventional axles during straight line driving.

6.2 ASSESSMENT OF ROAD DAMAGE POTENTIAL

Vehicle generated road damage is greatly related to the magnitudes of tire forces transmitted to the road, which comprise static and dynamic components. The static loads depend on the geometry and mass distribution of the vehicle, and the load sharing characteristics of the axle suspension. The dynamic components of the tire forces are the result of the vehicle vibration caused by the road roughness and tire-road interactions. The intensity of such vibration and consequent dynamic tire forces primarily depend upon the suspension design as well as the vehicle and axle configuration. In order to gain an understanding of factors influencing the dynamic tire forces and consequently the road damage potential of different vehicle configurations, this study focuses on three major

contributory factors: (1) road surface profile, (2) vehicle characteristics, and (3) the mode of vehicle operation.

The roughness profiles of three different roads, classified as smooth, medium-rough and rough, as described in the section 3.4.2, are considered to study influence of road roughness. The vehicle characteristics considered in the study include the gross weight of the vehicle, axle configuration, weight distribution, and the suspension properties. The role of axle suspension damping ratio, is investigated by selecting three levels of suspension damping ratio: 0.05, 0.10, and 0.15. For the analysis, the vehicle is assumed to operate at a constant forward speed of $100\,km/h$ with no steering input. For the selected mode of operation, fixed and the self-steering axles are considered to possess same characteristics in generating the dynamic tire forces. The dynamic tire forces and thus the road damaging potential of the candidate vehicle with one or more lift axle retracted are specifically investigated by considering the resulting load distribution, as described in section 4.2. The analyses are performed by using the modified yaw/roll model of the heavy articulated vehicle under the defined inputs of road roughness. The static and dynamic tire load responses are analyzed to derive the performance measures described in section 3.3. These include the Equivalent Single Axle Load (ESAL) of each single axle and total vehicle to assess the static loading properties of different vehicle configurations, Dynamic Load Coefficient (DLC), Road Stress Factor (RSF), Dynamic Aggregate Force Criterion (DAFC) and Dynamic Aggregate Stress Criterion (DASC).

6.3 EQUIVALENT SINGLE AXLE LOAD (ESAL)

The American Association of State Highway Officials (AASHO) performed large scale road tests in Canada and USA to study the pavement damage potentials of heavy

vehicles [4]. The study built six test tracks including flexible and rigid pavements and employed over 200 vehicles, and acquired data for nearly 17 million vehicle-miles in two years. A regression analysis of the test data evolved into a 'fourth power law', which has served as the key design rule for the design of pavements and the operating practices. The study proposed that the decrease in pavement serviceability caused by a heavy vehicle axle could be related to the fourth power of the axle static load [3]. The loads applied by the multiple axle vehicles or by the mixed traffic on a road could be converted into a number of Equivalent Standard Axle Loads (ESALs) by applying the fourth power law to each axle, such that

$$\text{ESAL} = \left(\frac{F_{szl}}{P_0} \right)^4 \tag{6-1}$$

where F_{szl} is the static load of axle l and P_0 is the standard axle load, taken as $80\,kN$.

The ESAL is used to convert wheel loads of various magnitudes to an equivalent number of "standard" or "equivalent" loads, which yields the amount of damage an axle could do to the pavement. The method could be conveniently applied to define the equivalent number of axles for any configuration of vehicle employing axle loads other than $80\,kN$. The combination with lift axle would yield considerably large number of equivalent axles, when the axle is retracted, and thus pose more pavement damage risk. The ESAL for different configurations of the candidate vehicles are computed using the static axle loads, and the "load equivalent factor" (LEF) for each configuration is computed by summing the ESALs.

6.3.1 CONFIGURATION 12F12

Table 6-1 summarizes the ESAL for each axle with lift axle (axle 4) down and up. The table also presents the LEF for the entire 6-axle vehicle configuration 12F12, when the semi-trailer single axle of the vehicle is lifted up or on the ground. The table shows that when the single axle of the semi-trailer is lifted up, the static load of this axle is distributed among the other axles, which leads higher LEF of the vehicle. The LEF of the combination increases by 104%, when the liftable axle is retracted, suggesting far greater road damaging potential of the vehicle. This increase in LEF is mostly attributed to the corresponding increase in the ESAL of semi-trailer tandem axle (235%). While the ESAL of the tractor front axle increases only slightly (19%), the ESAL of the tractor drive axle increases considerably (71%).

Table 6-1: ESAL and LEF of Configuration 12F12

Configuration 12F12	Axle 4 down		Axle 4 up		
	Static load *kN*	ESAL	Static load *kN*	ESAL	Percent increase
Axle 1	49.0	0.14	51.2	0.17	19%
Axle 2	88.2	1.48	100.9	2.53	71%
Axle 3	88.2	1.48	100.9	2.53	71%
Axle 4	93.6	1.87	/	/	/
Axle 5	93.6	1.87	126.6	6.26	235%
Axle 6	93.6	1.87	126.6	6.26	235%
LEF	506.2	8.71	506.2	17.75	104%

6.3.2 CONFIGURATION 12F13

Table 6-2 summarizes the ESAL and LEF of the 7-axle vehicle configuration 12F13 with the single liftable axle (axle 4) of the semitrailer on the ground and retracted. Since the liftable axle load is distributed among three semitrailer axles rather than two axles in the case of configuration 12F12, the LEF of this configuration increases by 68%

as compared to 104% for the configuration 12F12, when the axle 4 is lifted up. This is also evident from relatively smaller increase (109%) in the ESAL of the trailer axles, when compared to that observed for configuration 12F12 (235%). The corresponding increasing in the drive axle ESAL, however, is relatively larger due to higher load transfer to the drive axle, as evident in Table 6-2.

Figure 6-1 illustrates a comparison of total vehicle ESAL or LEF for the 6- and 7-axle configurations 12F12 and 12F13 with axle 4 on the ground and retracted. The results suggest that the configuration 12F13 yields lower LEF than the configuration 12F12, when the liftable axle (axle 4) is retracted or on the ground, even through the GVW of configuration 12F13 (555.7 kN) is larger than that of the configuration 12F12 (506.2 kN). From the static load point of view, a tractor-semitrailer employing a tridem axle in semitrailer yields considerably lower road damage potential than the vehicle using a tandem axle semitrailer, especially when the liftable axle is raised.

Table 6-2: ESAL and LEF of Configuration 12F13

Configuration 12F13	Axle 4 down		Axle 4 up		
	Static load kN	ESAL	Static load kN	ESAL	Percent increase
Axle 1	49.0	0.14	51.6	0.17	23%
Axle 2	88.2	1.48	103.1	2.76	87%
Axle 3	88.2	1.48	103.1	2.76	87%
Axle 4	82.6	1.13	/	/	/
Axle 5	82.6	1.13	99.3	2.37	109%
Axle 6	82.6	1.13	99.3	2.37	109%
Axle 7	82.6	1.13	99.3	2.37	109%
LEF	555.7	7.63	555.7	12.80	68%

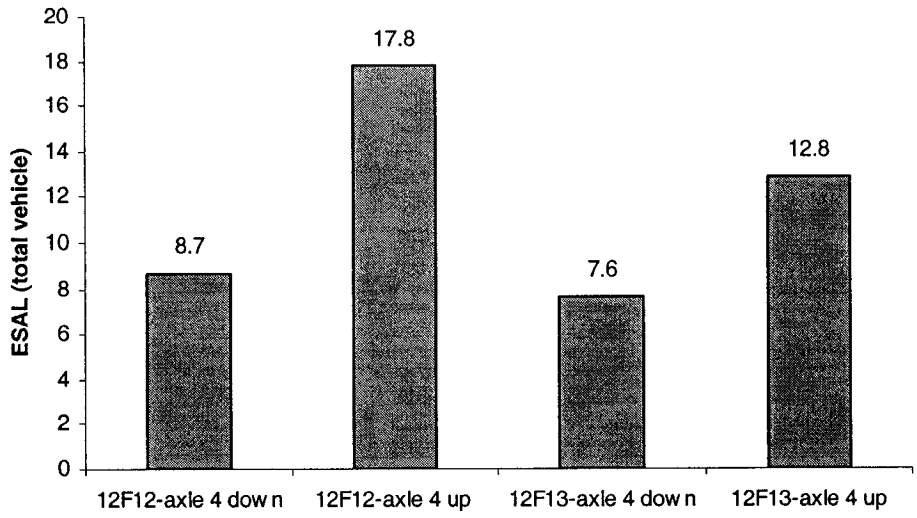

Figure 6-1: Comparison of LEF of configurations 12F12 and 12F13.

6.3.3 CONFIGURATION 12F113

The ESALs and LEF for the 8-axle combination (12F113) are investigated for four different operating conditions: ① all axles on the ground; ② semitrailer lead single axle (axle 4) lifted up; ③ semitrailer trailing single axle (axle 5) lifted up; and ④ both of the single axles of the semitrailer (axles 4 and 5) lifted up. The results attained for these conditions are discussed using the corresponding notations: ①, ②, ③ and ④.

Table 6-3 summarizes the axle loads, the ESAL and LEF for the configuration 12F113 under different operating conditions. The vehicle ESALs or the LEF corresponding to the operating conditions are further compared in Figure 6-2. The results show that the conditions ② and ③ involving retraction of either one of the liftable axles yield similar LEF values (8.29 and 8.00), which is attributed to somewhat comparable load distribution caused by raising axle 4 or axle 5. The raising of axle 4 or axle 5, however, yield 35% or 30% higher ESALs of the vehicle, which are considerably lower than those attained for tandem and tridem axle semitrailer configurations (12F12 and

12F13). Lifting either of the two liftable axles, however, tends to load the other axle, in the immediate vicinity, most significantly. The ESAL due to trailing lift axle (axle 5) increases by 377%, when the leading (axle 4) is raised. The corresponding increase in the lead axle ESAL is 392%, when the trailing axle (axle 5) is raised. The lifting of axle 4 also imposes considerably larger load on the tractor drive axles (49%), when compared to those caused by lifting axle 5 (11%). The total ESAL of the vehicle increases most significantly, when both (axles 4 and 5) are raised corresponding to condition ④. The total ESAL or LEF increases to 13.46, which is 119% higher than the value attained under condition ①, all axles on the ground.

A comparison of Figure 6-1 and 6-2 suggests that a combination with larger number of semitrailer axles yields relatively lower LEF and thus lower pavement damage potential, when all axles are on the ground. A tandem axle semitrailer combination (12F12) with single liftable axle raised imposes greatest pavement damage potential. The LEF of the configuration 12F113 with two axles raised approaches 13.46, which is nearly 24% lower than that of 12F12 configuration with single axle raised, even through the GVW of configuration 12F113 is higher.

6.3.4 CONFIGURATION 12F1113

The ESALs for individual axles and the total 9-axle combination are evaluated under different operating conditions: ① all axles of the vehicle on the ground; ② semitrailer leading single axle (axle 4) lifted up; ③ semitrailer middle single axle (axle 5) lifted up; ④ semitrailer trailing single axle (axle 6) lifted up; ⑤ two of the semitrailer single axles (axles 4 and 5) lifted up; ⑥ two of the semitrailer single axles (axles 5 and 6) lifted up; and ⑦ all of the semitrailer liftable axles (axles 4, 5 and 6) lifted up.

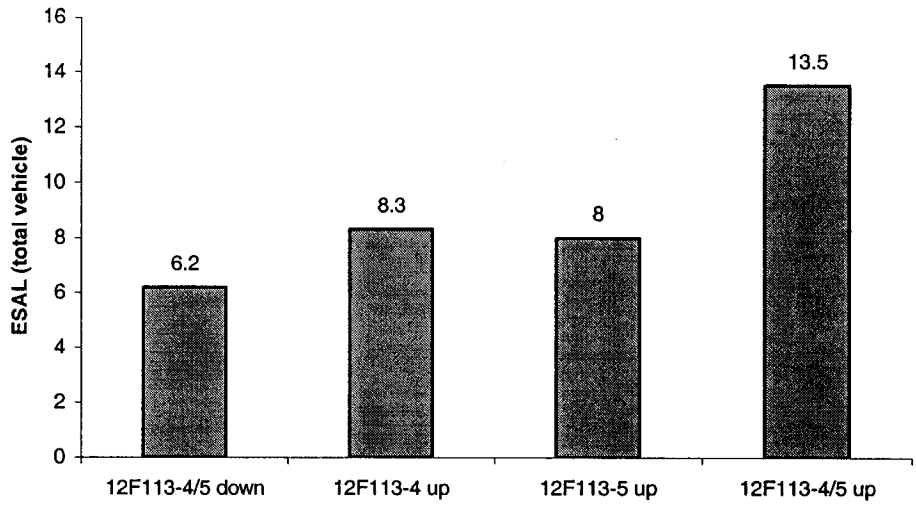

Figure 6-2: Comparison of LEF of configuration 12F113. corresponding to different operating conditions.

Table 6-3: ESAL and LEF of Configuration 12F113

Configuration 12F113	① Axles 4 and 5 down		② Axle 4 up		
	Static load *kN*	ESAL	Static load *kN*	ESAL	Percent increase
Axle 1	49.0	0.14	50.6	0.16	14%
Axle 2	88.2	1.48	97.4	2.20	49%
Axle 3	88.2	1.48	97.4	2.20	49%
Axle 4	49.0	0.14	/	/	/
Axle 5	50.0	0.15	73.8	0.73	377%
Axle 6	78.4	0.92	80.1	1.00	9%
Axle 7	78.4	0.92	80.1	1.00	9%
Axle 8	78.4	0.92	80.1	1.00	9%
Total	559.6	6.15	559.6	8.29	35%
	③ Axle 5 up			④ Axles 4 and 5 up		
Axle 1	49.4	0.15	3%	52.8	0.19	35%
Axle 2	90.4	1.63	11%	110.2	3.60	144%
Axle 3	90.4	1.63	11%	110.2	3.60	144%
Axle 4	73.0	0.69	392%	/	/	/
Axle 5	/	/	/	/	/	/
Axle 6	85.4	1.30	41%	95.5	2.03	120%
Axle 7	85.4	1.30	41%	95.5	2.03	120%
Axle 8	85.4	1.30	41%	95.5	2.03	120%
Total	559.6	8.00	30%	559.6	13.46	119%

Table 6-4 summarizes the axle loads, ESAL of individual axles and LEF of the vehicle combination corresponding to the seven operating conditions. Figure 6-3 presents a comparison of the LEF value corresponding to different operating conditions. The results show that the LEF of this configuration (condition ①) is considerably lower than all of the other configurations discussed previously, which is attributed to its larger number of axles and lower axle loads, when compared to those of the other combinations. Lifting either one of the liftable axles from the ground yields similar increase in the LEF of the combination. The LEF increases from 5.97 to 6.97, 6.74 and 6.97, when axle 4, 5 or 6 is raised, corresponding to operating conditions ②, ③ and ④, respectively. The raising of a single lift axle, however, tends to impose higher load on the remaining lift axles on the ground, specifically the axle located close to the lifted axles. The increase in the ESAL of the lift axles on the ground ranges from 153% to 497%, when one of the axles is raised. The least variation is observed for the front axle ESAL, which varies from 1% to 8%. The lifting of the lead axle (axle 4, condition ②) imposes nearly 28% higher ESAL of the drive axles, while that of the trailing axle (axle 6, condition ④) causes the ESAL of the tridem axles to increase by 30%.

The operating conditions involving two of the liftable axles raised from the ground (conditions ⑤ and ⑥) also yield comparable LEF values, which are higher than those attained for conditions ②, ③ and ④. The ESALs of the total vehicle increase by 53% and 45%, when axles 4 and 5 (condition ⑤), and axles 5 and 6 (condition ⑥) are raised. The conditions ⑤ and ⑥ cause most significant increases in the ESALs of the drive axles and the tridem axles, respectively, in excess of 70%. The LEF of the vehicle

increases most significantly from 5.97 (all axles on ground) to 13.9, when all three lift axles are retracted, as illustrated in Table 6-4 and Figure 6-3.

A comparison of the results attained for the configuration 12F1113 with those of the previous three configurations suggests that with all axles on the ground, the heaviest configuration 12F1113 yields the lowest LEF value. The LEF of the configuration 12F1113 with all three axles retracted (13.9062) is similar to those of the configurations 12F113 (13.4639) and 12F13 (12.8002), with two and single axles raised. The LEF value of the configuration 12F1113 is considerably lower than those of configurations 12F12 and 12F13, when only one axle is raised..

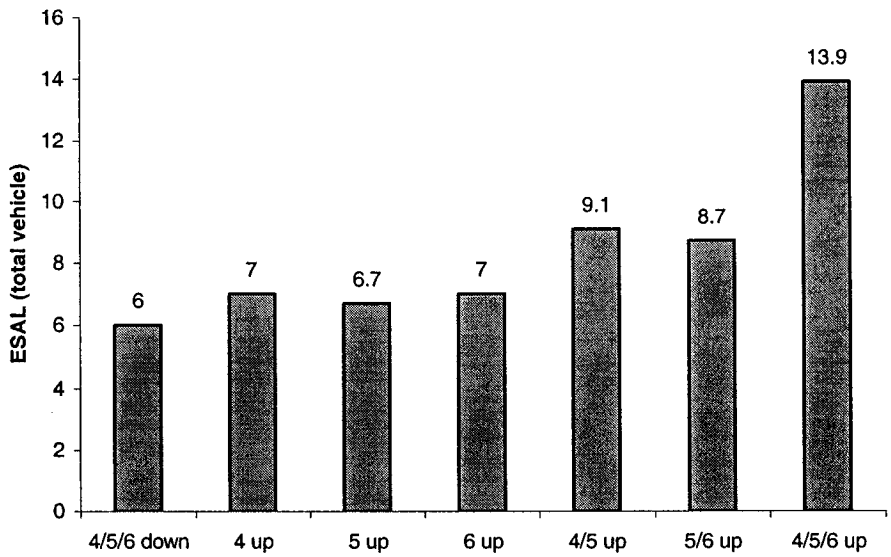

Figure 6-3: Comparison of LEF of configuration 12F1113 corresponding to different operating conditions.

Table 6-4: ESAL and LEF of Configuration 12F1113.

Configuration 12F1113	① Axles 4, 5 and 6 down		② Axle 4 up		
	Static load *kN*	ESAL	Static load *kN*	ESAL	Percent increase
Axle 1	49.0	0.14	50.0	0.15	8%
Axle 2	88.2	1.48	93.8	1.88	28%
Axle 3	88.2	1.48	93.8	1.88	28%
Axle 4	32.3	0.03	/	/	/
Axle 5	32.3	0.03	49.0	0.14	427%
Axle 6	39.2	0.06	41.4	0.07	25%
Axle 7	78.4	0.92	78.8	0.94	2%
Axle 8	78.4	0.92	78.8	0.94	2%
Axle 9	78.4	0.92	78.8	0.94	2%
Total	564.5	5.97	564.5	6.96	17%

	③ Axle 5 up			④ Axle 6 up		
Axle 1	49.4	0.14	4%	49.1	0.14	1%
Axle 2	90.7	1.65	12%	88.7	1.51	3%
Axle 3	90.7	1.65	12%	88.7	1.51	3%
Axle 4	42.9	0.08	210%	35.9	0.04	52%
Axle 5	/	/	/	50.6	0.15	497%
Axle 6	49.4	0.14	153%	/	/	/
Axle 7	80.4	1.02	11%	83.8	1.20	30%
Axle 8	80.4	1.02	11%	83.8	1.20	30%
Axle 9	80.4	1.02	11%	83.8	1.20	30%
Total	564.5	6.73	13%	564.5	6.97	17%

	⑤ Axles 4 and 5 up			⑥ Axles 5 and 6 up		
Axle 1	51.3	0.16	20%	49.6	0.14	5%
Axle 2	101.6	2.59	76%	91.7	1.72	17%
Axle 3	101.6	2.59	76%	91.7	1.72	17%
Axle 4	/	/	/	61.1	0.34	1175%
Axle 6	60.4	0.36	527%	/	/	/
Axle 7	82.7	1.13	24%	89.6	1.57	71%
Axle 8	82.7	1.13	24%	89.6	1.57	71%
Axle 9	82.7	1.13	24%	89.6	1.57	71%
Total	564.5	9.14	53%	89.6	8.66	45%

	⑦ Axles 4, 5 and 6 up		
Axle 1	52.8	0.19	35%
Axle 2	110.4	3.62	146%
Axle 3	110.4	3.62	146%
Axle 7	96.9	2.15	134%
Axle 8	96.9	2.15	134%
Axle 9	96.9	2.15	134%
Total	564.5	13.90	133%

6.4 DYNAMIC LOAD COEFFICIENT (DLC)

Dynamic Load Coefficient (DLC) is a convenient measure of characterizing variation in the tire force over a period of time. It is a statistical measure reflecting tire force deviations from its mean value, which is close to the static tire load. The DLC has been suggested as an effective measure to perform relative road friendliness assessments of different vehicles and suspensions, in view of the pavement damage potential [34,69,70]. The DLC has been found to be strongly dependent on speed, suspension design, axle loads, vehicle configuration and road roughness [8,49,57-59]. The DLC due to different axle tires under varying operating conditions, discussed in section 6.3, are computed for each candidate vehicle configuration. The influences of road roughness and suspension damping on the DLC are also investigated, and the results are discussed in the following subsections.

6.4.1 CONFIGURATION 12F12

Table 6-5 illustrates comparisons of the DLC due to selected axle tire forces of the 6-axle configuration 12F12 corresponding to different operating conditions (axle 4 raised or down), road roughness and suspension damping ratio. Since drive axles (axle 2 and 3) and rear axles of semitrailer (axle 5 and 6) are tandem-axle groups, the table presents the results for only one of the axles (axles 3 and 6). The results show that the DLC due to tire forces are strongly influenced by the road roughness and the suspension damping ratio. An increase in suspension damping, in general, yields lower values of DLC, irrespective of the road roughness, since the damping helps to suppress the variations in dynamic tire forces to an extent. Such trends have also been reported in a number of published studies [62,70]. The effect of suspension damping is more evident

under rough roads excitations. As an example, the DLC due to rearmost axle tires, while operating on a rough road, reduces from 0.149 to 0.118 (21%), when damping ratio is increased from 0.05 to 0.15, with axle 4 down. The DLC of the same tires increases from 0.0149 corresponding to a smooth road operation to 0.118 under a rough road excitation, when the suspension damping ratio is held constant at 0.15. These trends, suggesting strong dependence on the road roughness and damping ratio, conform to those reported in the published studies [34,70].

Table 6-5: DLC due to tire forces of configuration 12F12

Road	Damping ratio	Axle 4 on the ground			
		Axle 1	Axle 3	Axle 4	Axle 6
Smooth	0.05	0.020	0.034	0.012	0.021
	0.10	0.018	0.025	0.009	0.016
	0.15	0.017	0.021	0.008	0.015
Medium-rough	0.05	0.040	0.067	0.024	0.048
	0.10	0.036	0.051	0.017	0.040
	0.15	0.035	0.044	0.016	0.038
Rough	0.05	0.201	0.183	0.150	0.149
	0.10	0.167	0.154	0.123	0.128
	0.15	0.152	0.139	0.113	0.118
		Axle 4 raised			
		Axle 1	Axle 3	Axle 6	
Smooth	0.05	0.023	0.028	0.020	
	0.10	0.019	0.021	0.018	
	0.15	0.017	0.018	0.017	
Medium-rough	0.05	0.044	0.057	0.040	
	0.10	0.036	0.042	0.036	
	0.15	0.034	0.037	0.036	
Rough	0.05	0.191	0.179	0.110	
	0.10	0.158	0.137	0.093	
	0.15	0.144	0.119	0.086	

The table shows the influence of the lift axle operating condition on the DLC due to individual axle tire forces. Raising the liftable axle from the ground, in general, yields lower values of DLC for most of the axle tires, irrespective of the suspension damping and road roughness. The resulting lower values of DLC, however, do not imply enhanced

road friendliness of the vehicle with a raised axle. The lower value of DLC of a tire force is attributed to its definition, which involves normalization with respect to the mean or static tire force. Raising of an axle imposes higher loads in most of the axle tires, as evident from Tables 6-1, which causes the DLC values to decrease. This is also evident from relatively higher DLC values for the front axle tire loads due to their smaller loads, and relatively lower DLC values of the semitrailer tandem axle tires (axle 6) due to their higher loads. From the results, it may be concluded that a measure based upon the DLC cannot be applied to study the relative road damaging potential of vehicle combinations with liftable axles.

6.4.2 CONFIGURATION 12F13

Table 6-6 illustrates comparisons of the DLC due to each axle tire forces of the 7-axle configuration 12F13 as a function of the axle operating condition (axle 4 raised or down), road roughness and suspension damping ratio. Since the drive axles (axle 2 and 3) and rear axles of semitrailer (axles 5, 6 and 7) represent the tandem- and tridem-axle groups, respectively, the table summarizes the results for one of the axles within the group (axles 3 and 7). The results show that the road roughness and suspension damping have a strong influence on the DLC due to tire forces of each axle. An increase in the suspension damping yields lower values of DLC under all road roughness conditions considered. The effect of suspension damping is more evident under the rough road excitations, the DLC due to rearmost axle tires, while operating on a rough road, reduces from 0.166 to 0.144, indicating a decreasing of 13%, when damping ratio is increased from 0.05 to 0.15, with axle 4 down. The DLC of the same tires increases from 0.0475

corresponding to a smooth road operation to 0.144 under a rough road excitation, when the damping ratio is held constant at 0.15.

The table also shows the influence of the lift axle operating condition on the DLC due to individual axle tire forces. Although raising the liftable axle 4 from the ground causes higher static load for each axle, which is illustrated in table 6-2, lower values of DLC are obtained for most of the axle tires, irrespective of the suspension damping and road roughness.

Table 6-6: DLC due to tire forces of configuration 12F13

Road	Damping ratio	Axle 4 on the ground			
		Axle 1	Axle 3	Axle 4	Axle 7
Smooth	0.05	0.021	0.043	0.040	0.058
	0.10	0.018	0.033	0.035	0.052
	0.15	0.018	0.028	0.033	0.048
Medium-rough	0.05	0.041	0.073	0.066	0.082
	0.10	0.037	0.062	0.061	0.072
	0.15	0.035	0.053	0.057	0.069
Rough	0.05	0.201	0.185	0.142	0.166
	0.10	0.167	0.147	0.121	0.151
	0.15	0.154	0.134	0.114	0.144
		Axle 4 raised			
		Axle 1	Axle 3	Axle 7	
Smooth	0.05	0.020	0.031	0.020	
	0.10	0.017	0.022	0.016	
	0.15	0.016	0.019	0.015	
Medium-rough	0.05	0.039	0.063	0.047	
	0.10	0.035	0.046	0.041	
	0.15	0.033	0.039	0.039	
Rough	0.05	0.187	0.137	0.154	
	0.10	0.155	0.117	0.125	
	0.15	0.141	0.107	0.114	

6.4.3 CONFIGURATION 12F113

Table 6-7 presents the DLC due to each axle of the 8-axle configuration 12F113 as functions of the road roughness and suspension damping ratio. The configuration comprises a tridem-axle trailer with two single belly axles, which may be either fixed or

Table 6-7: DLC due to tire forces of configuration 12F113

Road	Damping ratio	① Axle 4 and 5 on the ground				
		Axle 1	Axle 3	Axle 4	Axle 5	Axle 8
Smooth	0.05	0.019	0.029	0.042	0.062	0.082
	0.10	0.017	0.025	0.039	0.057	0.074
	0.15	0.017	0.023	0.037	0.053	0.068
Medium-rough	0.05	0.038	0.053	0.069	0.099	0.106
	0.10	0.035	0.047	0.064	0.095	0.105
	0.15	0.034	0.044	0.062	0.092	0.103
Rough	0.05	0.204	0.206	0.314	0.245	0.194
	0.10	0.169	0.166	0.258	0.218	0.194
	0.15	0.152	0.143	0.235	0.205	0.185
		② Axle 4 raised				
		Axle 1	Axle 3	Axle 5	Axle 8	
Smooth	0.05	0.019	0.037	0.043	0.066	
	0.10	0.017	0.030	0.039	0.059	
	0.15	0.017	0.026	0.037	0.054	
Medium-rough	0.05	0.039	0.071	0.081	0.100	
	0.10	0.035	0.055	0.075	0.089	
	0.15	0.034	0.048	0.070	0.085	
Rough	0.05	0.195	0.160	0.143	0.171	
	0.10	0.161	0.137	0.131	0.168	
	0.15	0.146	0.125	0.127	0.165	
		③ Axle 5 raised				
		Axle 1	Axle 3	Axle 4	Axle 8	
Smooth	0.05	0.019	0.038	0.039	0.038	
	0.10	0.017	0.029	0.033	0.036	
	0.15	0.017	0.024	0.030	0.034	
Medium-rough	0.05	0.037	0.048	0.068	0.071	
	0.10	0.034	0.047	0.063	0.062	
	0.15	0.033	0.045	0.060	0.058	
Rough	0.05	0.199	0.165	0.149	0.160	
	0.10	0.168	0.139	0.133	0.144	
	0.15	0.152	0.126	0.128	0.138	
		④ Axle 4 and 5 raised				
		Axle 1	Axle 3	Axle 8		
Smooth	0.05	0.019	0.027	0.021		
	0.10	0.016	0.020	0.016		
	0.15	0.016	0.017	0.015		
Medium-rough	0.05	0.038	0.056	0.048		
	0.10	0.033	0.041	0.042		
	0.15	0.032	0.035	0.040		
Rough	0.05	0.185	0.126	0.157		
	0.10	0.155	0.105	0.130		
	0.15	0.141	0.098	0.118		

liftable axles. The table shows the DLC due to the tire forces of one of the axles (axles 3 and 8) within the tandem (axles 2 and 3) and the tridem (axles 6, 7 and 8) axle groups.

The results show that the road roughness and suspension damping ratio have similar influence on the DLC due to each axle of configuration 12F113 as those of 12F12 and 12F13 configurations. An additional suspension damping yields lower values of DLC, irrespective of the road roughness and axle configuration. The effect of suspension damping is more evident under rough roads, for example, the DLC due to rearmost axle tires (axle 8), while operating on a rough road, reduces from 0.194 to 0.185, when damping ratio (DR) is increased from 0.05 to 0.15, with axle 4 down. The increasing road roughness causes higher DLC value, irrespective of suspension damping ratio. For instance, the DLC of the same tires increases from 0.0686 corresponding to a smooth road operation to 0.185 under a rough road, when the DR is held constant at 0.15.

The table also shows the influence of the lift axle operating conditions, described in section 4.2, on the DLC due to individual axle tire forces. Although raising the liftable axles 4 and 5 from the ground causes higher static loads for each axle (Table 6-2), this condition yields lowest value of DLC of the tires on each axle, irrespective of the suspension damping and road roughness. The vehicles with fixed axles, however, yields higher DLC value in spite of the lower static loads of the tires on the most of axles.

6.4.4 CONFIGURATION 12F1113

Table 6-8 presents the DLC due to each axle of the 9-axle configuration 12F1113 as functions of the road roughness and suspension damping ratio. The configuration comprises a tridem-axle trailer with three single belly axles, which may be either fixed or lifted axles. The results are presented for only one of the axles (axles 3 and 9) for the

tandem and tridem group of axles. The results show similar influences of the road roughness and suspension damping ratio on DLC. The table also shows the influence of the lift axle operating conditions, described in section 4.2, on the DLC due to individual axle tire forces. The higher static axle loads caused by raising retracted axles yields lower values of DLC. This trend is more obvious when the vehicle operation on medium-rough or rough roads and the suspension damping is relatively high (DR = 0.10, 0.15), as observed for other configurations.

6.5 ROAD STRESS FACTOR (RSF)

The measure of road stress factor (RSF) as a performance index for road damage potential of heavy vehicle has been discussed in chapter 3. The measure of RSF is based on the fourth power law applied to static load, which is extended to include the dynamic component of the tire load. The relative road damage potential of selected configurations with conventional and raised liftable axles are evaluated in terms of RSF, using equation (3-8). Considering that the RSF is a direct function of fourth power of the static axle load, and the DLC due to dynamic tire force, the RSF tends to increase significantly with the increasing axle load. Higher axle loads caused by operation with one or more raised axles thus cause significantly higher RSF due to tire forces. The effects of suspension damping and road roughness are mostly characterized by the DLC. The influences of road roughness and damping ratio on the RSF are thus relatively small and identical to those observed for DLC due to tire forces in the previous section. The results attained under different road roughness and suspension damping ratios are further addressed in the following subsections.

Table 6-8: DLC due to tire forces of configuration 12F1113

Road	Damping ratio	① Axles 4, 5 and 6 down						② Axles 4 raised					③ Axles 5 raised				
		Axle 1	Axle 3	Axle 4	Axle 5	Axle 6	Axle 9	Axle 1	Axle 3	Axle 5	Axle 6	Axle 9	Axle 1	Axle 3	Axle 4	Axle 6	Axle 9
Smooth	0.05	0.020	0.031	0.066	0.074	0.077	0.082	0.020	0.036	0.048	0.073	0.079	0.019	0.032	0.052	0.044	0.061
	0.10	0.018	0.027	0.060	0.068	0.069	0.074	0.018	0.029	0.043	0.065	0.071	0.017	0.027	0.047	0.041	0.055
	0.15	0.017	0.025	0.057	0.063	0.063	0.068	0.017	0.026	0.041	0.060	0.064	0.017	0.025	0.044	0.039	0.052
Medium-rough	0.05	0.039	0.050	0.125	0.135	0.118	0.126	0.040	0.064	0.083	0.124	0.117	0.039	0.083	0.110	0.084	0.132
	0.10	0.035	0.043	0.116	0.122	0.108	0.113	0.036	0.050	0.072	0.108	0.104	0.035	0.057	0.091	0.074	0.113
	0.15	0.034	0.041	0.109	0.116	0.102	0.106	0.034	0.045	0.069	0.103	0.099	0.034	0.048	0.085	0.070	0.101
Rough	0.05	0.203	0.256	0.484	0.492	0.433	0.233	0.200	0.214	0.310	0.390	0.242	0.201	0.215	0.417	0.342	0.201
	0.10	0.171	0.186	0.386	0.382	0.335	0.217	0.169	0.160	0.257	0.312	0.205	0.171	0.173	0.294	0.284	0.174
	0.15	0.154	0.150	0.327	0.326	0.305	0.201	0.151	0.143	0.234	0.281	0.194	0.151	0.153	0.261	0.255	0.166
Road	DR	④ Axles 6 raised				⑤ Axles 4 and 5 raised				⑥ Axles 5 and 6 raised				⑦ Axles 4, 5 and 6 raised			
		Axle 1	Axle 3	Axle 4	Axle 5	Axle 9	Axle 1	Axle 3	Axle 6	Axle 9	Axle 1	Axle 3	Axle 4	Axle 9	Axle 1	Axle 3	Axle 9
Smooth	0.05	0.020	0.047	0.068	0.036	0.067	0.024	0.055	0.028	0.072	0.023	0.029	0.029	0.035	0.019	0.031	0.028
	0.10	0.018	0.039	0.059	0.031	0.058	0.020	0.041	0.020	0.062	0.018	0.022	0.021	0.027	0.017	0.020	0.022
	0.15	0.017	0.033	0.054	0.030	0.051	0.018	0.033	0.017	0.053	0.017	0.020	0.018	0.024	0.016	0.017	0.020
Medium-rough	0.05	0.039	0.071	0.135	0.072	0.093	0.044	0.078	0.054	0.103	0.046	0.058	0.058	0.078	0.038	0.063	0.064
	0.10	0.035	0.058	0.111	0.057	0.085	0.038	0.065	0.039	0.091	0.037	0.046	0.042	0.066	0.034	0.041	0.055
	0.15	0.034	0.054	0.102	0.053	0.082	0.036	0.059	0.033	0.088	0.034	0.041	0.035	0.062	0.032	0.034	0.053
Rough	0.05	0.203	0.214	0.393	0.360	0.192	0.189	0.188	0.298	0.190	0.205	0.188	0.288	0.167	0.186	0.140	0.159
	0.10	0.170	0.161	0.337	0.279	0.163	0.162	0.156	0.235	0.171	0.170	0.153	0.226	0.146	0.156	0.114	0.134
	0.15	0.153	0.143	0.299	0.244	0.155	0.146	0.134	0.207	0.159	0.152	0.135	0.201	0.136	0.141	0.101	0.125

6.5.1 CONFIGURATIONS 12F12 AND 12F13

Tables 6-9 and 6-10 summarize the RSF values of different axle tires of the 6- and 7-axle configurations 12F12 and 12F13 with fixed and a single raised trailer belly axle, respectively, as functions of the road roughness and suspension damping. The influences of suspension damping and the road roughness on the RSF due to tire forces are negligible, since the RSF is predominantly related to fourth power of the static tire load. Higher axle loads thus cause high RSF and thus high pavement damage potential, as evident for the trailer axles (axles 4 and 6) for the conventional vehicles, and axles 3 and 6, when the belly axle is raised. Although the effects of road roughness and suspension

Table 6-9: The RSF due to tire forces of configuration 12F12

Unit: $\times 10^{16}\ N^4$

Road	Damping ratio	① Axle 4 on the ground			
		Axle 1	Axle 3	Axle 4	Axle 6
Smooth	0.05	36	381	480	481
	0.10	36	380	480	480
	0.15	36	379	480	480
Medium-rough	0.05	36	388	481	486
	0.10	36	384	480	484
	0.15	36	382	480	484
Rough	0.05	45	456	577	593
	0.10	42	433	523	527
	0.15	41	422	516	520
		② Axle 4 raised			
		Axle 1	Axle 3	Axle 6	
Smooth	0.05	43	651	1610	
	0.10	43	650	1610	
	0.15	43	649	1610	
Medium-rough	0.05	43	661	1620	
	0.10	43	655	1620	
	0.15	43	653	1620	
Rough	0.05	53	774	1720	
	0.10	49	722	1690	
	0.15	48	704	1680	

damping are relatively small, the tire-road interactions cause higher values of RSF on higher roughness roads and lower suspension damping ratio, which is attributed to higher DLC value.

For the 12F12 configuration, the RSF value of the rearmost axle (axle 6), while operating on the rough road with suspension damping is 0.15, increases from 520×10^{16} N^4 to 1680×10^{16} N^4 when axle 4 is raised, suggesting an increase of 223%, which is comparable to the increase in the ESAL value for the axle 6. The corresponding increase in the RSF of the rearmost axle (axle 7) tires of the 12F13 configuration is 100%. The relatively smaller increase in the RSF is attributed to relatively lower increase in the normal load of tires of the tridem axle group.

Table 6-10: The RSF due to tire forces of configuration 12F13

Unit: $\times10^{16}$ N^4

Road	Damping ratio	① Axle 4 on the ground			
		Axle 1	Axle 3	Axle 4	Axle 7
Smooth	0.05	36	382	293	296
	0.10	36	381	293	295
	0.15	36	380	292	294
Medium-rough	0.05	36	390	298	302
	0.10	36	387	297	299
	0.15	36	384	296	299
Rough	0.05	45	457	326	339
	0.10	42	428	316	331
	0.15	41	419	313	327
		② Axle 4 raised			
		Axle 1	Axle 3		Axle 7
Smooth	0.05	44	711		608
	0.10	44	709		608
	0.15	44	708		608
Medium-rough	0.05	45	724		615
	0.10	45	716		613
	0.15	45	713		612
Rough	0.05	54	787		694
	0.10	51	765		665
	0.15	50	756		655

6.5.2 CONFIGURATION 12F113 AND 12F1113

Tables 6-11 and 6-12 summarize the RSF due to selected axle tires of 8- and 9-axle configurations, 12F113 and 12F1113, respectively, with two- and three-single liftable axles. The tables summarize the results corresponding to different operation conditions, described in section 4.2. The effects of suspension damping and road roughness are relatively small, as observed for the 6- and 7-axle configurations. The results clearly show that the RSF due to drive axle tires (axle 3) increase most significantly when all the liftable axles are raised. The lifting of the lead axle (axle4) alone imposes significantly higher loads on the derive axles and thus the corresponding RSF. The lifting of trailing liftable axle (axle 5 for 12F113 and axle 6 for 12F1113 configurations) causes most significant increase in the RSF of tridem axle tires.

6.6 DYNAMIC AGGREGATE FORCE COEFFICIENT (DAFC)

The dynamic aggregate force coefficient (DAFC) provides a measure of the road damaging effects of all the axles of a vehicle to be assessed at a particular point on the road. This measure involves summation of the dynamic tire forces due to each axle, raised to a power 4. The DAFC due to different vehicle configurations considered in this study are evaluated to study the influence of operating conditions, road roughness and suspension damping ratio. The definition of measure and method of analysis are discussed in section 3.3.4. The magnitudes of DAFC due to different vehicle configurations are discussed in view of the road damage potential and spatial repeatability.

Figures 6-4 and 6-5 illustrate the spatial variations in the DAFC magnitudes of 6- and 7-axle configurations, 12F12 and 12F13, as a function of the road roughness and

Table 6-11: The RSF due to tire forces of configuration 12F113

Unit: $\times 10^{16}\ N^4$

Road	Damping ratio	① Axle 4 and 5 on the ground				
		Axle 1	Axle 3	Axle 4	Axle 5	Axle 8
Smooth	0.05	36	380	36	40	246
	0.10	36	379	36	40	244
	0.15	36	379	36	40	243
Medium-rough	0.05	36	384	37	41	252
	0.10	36	383	37	41	252
	0.15	36	382	37	41	251
Rough	0.05	45	477	58	53	290
	0.10	42	441	51	50	290
	0.15	41	425	48	49	285
		② Axle 4 raised				
		Axle 1	Axle 3	Axle 5	Axle 8	
Smooth	0.05	41	568	188	264	
	0.10	41	566	188	263	
	0.15	41	565	187	262	
Medium-rough	0.05	41	580	193	273	
	0.10	41	574	192	269	
	0.15	41	571	191	268	
Rough	0.05	51	651	209	303	
	0.10	47	627	205	301	
	0.15	46	616	204	300	
		③ Axle 5 raised				
		Axle 1	Axle 3	Axle 4	Axle 8	
Smooth	0.05	37	422	179	336	
	0.10	37	420	178	336	
	0.15	37	419	178	335	
Medium-rough	0.05	38	424	182	343	
	0.10	38	424	181	341	
	0.15	38	423	181	340	
Rough	0.05	46	487	201	385	
	0.10	44	467	196	375	
	0.15	43	458	195	371	
		④ Axle 4 and 5 raised				
		Axle 1	Axle 3	Axle 8		
Smooth	0.05	48	926	520		
	0.10	48	924	520		
	0.15	48	923	520		
Medium-rough	0.05	49	939	526		
	0.10	49	931	524		
	0.15	49	929	524		
Rough	0.05	59	1010	596		
	0.10	56	983	572		
	0.15	54	975	563		

Table 6-12: The RSF due to tire forces of configuration 12F1113 (Unit: $\times 10^{16}\ N^4$)

Road	Damping ratio	① Axles 4, 5 and 6 down						② Axles 4 raised					③ Axles 5 raised				
		Axle 1	Axle 3	Axle 4	Axle 5	Axle 6	Axle 9	Axle 1	Axle 3	Axle 5	Axle 6	Axle 9	Axle 1	Axle 3	Axle 4	Axle 6	Axle 9
Smooth	0.05	36	380	7.02	7.06	15.3	246	39	488	37	19	250	37	425	22	38	267
	0.10	36	380	6.98	7.02	15.2	244	39	486	36	19	248	37	424	22	38	266
	0.15	36	380	6.97	7.00	15	243	39	486	36	19	247	37	424	21	38	266
Medium-rough	0.05	36	384	7.48	7.59	16	259	39	496	38	20	261	38	440	23	39	289
	0.10	36	382	7.39	7.45	15.8	254	39	491	37	20	257	38	431	22	39	282
	0.15	36	382	7.32	7.39	16	252	39	490	37	20	255	38	429	22	38	278
Rough	0.05	45	532	17.6	18.0	33	315	49	620	58	36	328	47	543	45	65	327
	0.10	42	458	13.4	13.3	25.2	304	46	559	51	30	303	44	500	33	56	310
	0.15	41	430	11.5	11.4	23.4	294	44	544	48	28	297	43	483	30	52	305
Road	DR	④ Axles 6 raised				⑤ Axles 4 and 5 raised				⑥ Axles 5 and 6 raised			⑦ Axles 4, 5 and 6 raised				
		Axle 1	Axle 3	Axle 4	Axle 5	Axle 9	Axle 1	Axle 3	Axle 6	Axle 9	Axle 1	Axle 3	Axle 4	Axle 9	Axle 1	Axle 3	Axle 9
Smooth	0.05	36	393	11	41	316	44	677	93	301	38	445	88	406	49	934	555
	0.10	36	391	11	41	314	43	672	93	299	38	444	87	405	49	931	554
	0.15	36	390	11	41	313	43	670	93	297	38	443	87	405	49	930	553
Medium-rough	0.05	37	399	12	42	324	44	690	94	310	38	451	89	418	49	951	565
	0.10	37	396	11	42	321	44	682	93	306	38	448	88	414	49	938	562
	0.15	37	395	11	42	320	44	679	93	305	38	447	88	412	49	935	561
Rough	0.05	46	496	21	75	377	53	809	144	356	48	538	132	471	59	1040	637
	0.10	43	449	18	61	358	50	764	124	344	45	506	114	455	56	1000	612
	0.15	42	436	16	56	353	49	737	117	337	43	492	109	449	55	986	604

damping ratio. The figures present a comparison of the DAFC magnitudes of the vehicle configurations with liftable axle (axle 4) on the ground and raised. The results show nearly negligible effect of suspension damping, when the vehicle is operating on the smooth and medium-rough roads. For the operation on the rough road, however, a higher damping ratio yields lower DAFC magnitude by suppressing the variations in the tire forces. The influence of road roughness is also notable, as observed from the figures; higher road roughness causes higher DAFC magnitudes. The magnitudes of DAFC increase up to two fold, when the liftable axle is raised for both the vehicle configurations, suggesting considerably high road damage potential. The 6-axle configuration, 12F12, exhibits a spatial repeatability pattern in the DAFC, while operating on the medium-rough road. Peak magnitudes of DAFC occur along the road surface near $x = 130\text{m}$ and 150 m. The operation on the rough road, these peak magnitudes occur near $x = 110\text{m}$, 150m and 190m. This pattern tends to become most emphasized when the liftable axle is raised. The peak magnitudes of DAFC corresponding to $x = 130\text{m}$ and 150m for medium-rough road, and $x = 110\text{m}$, 150m and 190m for the rough road, can be reduced by increasing the suspension damping. Such peak magnitudes are also evident for the 7-axle configuration near $x = 130\text{m}$ and 150m for the medium-rough road, and near $x = 110\text{m}$, 140m and 190m for the rough road. The peak magnitudes of DAFC are attributed to localized high elevations of the road, while the difference in the locations of the peak responses of the two configurations are due to differences in the axle groups used and the nature of load distributions.

Figures 6-6 illustrate the variations in the magnitudes of DAFC attained corresponding to 11 different locations of road surface of the 8-axle vehicle configuration

12F113. The results show the influences of the operating conditions, road roughness and suspension damping ratio on the DAFC magnitudes. The results show similar effects of suspension damping and road roughness, as observed for the 6- and 7-axle configurations (12F12 and 12F13). The magnitudes of DAFC increase considerably when either one of two liftable axles is raised, irrespective of the road roughness. The DAFC magnitudes increase most significantly, when both the liftable axles are raised. The DAFC of the combination with both axles raised is nearly twice of that of the conventional 8-axle vehicle with all axles on the ground. Moreover, the results show peak magnitudes of DAFC near $x = 130\text{m}$ and 150 m for the medium-rough road, and near $x = 110\text{m}$, 140 m and 190m for the rough road, suggesting spatial repeatability of the loading due to high-localized elevations of the road surface. It should be noted that the locations of the peak DAFC magnitudes of configuration 12F113 are similar to those of the both previous configurations 12F12 and 12F13.

Figure 6-7 shows the variations in DAFC magnitudes of the 9-axle vehicle configuration 12F1113 corresponding to 11 different locations on the road surface. The results show the influences of 7 different operating conditions, and different road roughness and suspension damping ratio. The results show trends similar to those observed for the other vehicle configurations. The peak magnitudes of the DAFC also occur near $x = 130\text{m}$ and 150m for the medium-rough road, and near $x = 110\text{m}$, 140m and 190m for the rough road.

6.7 DYNAMIC AGGREGATE STRESS COEFFICIENT (DASC)

The dynamic aggregate stress coefficient (DASC) is derived upon summing the contact stress (ratio of dynamic tire force to the idealized tire-road contact area) of each

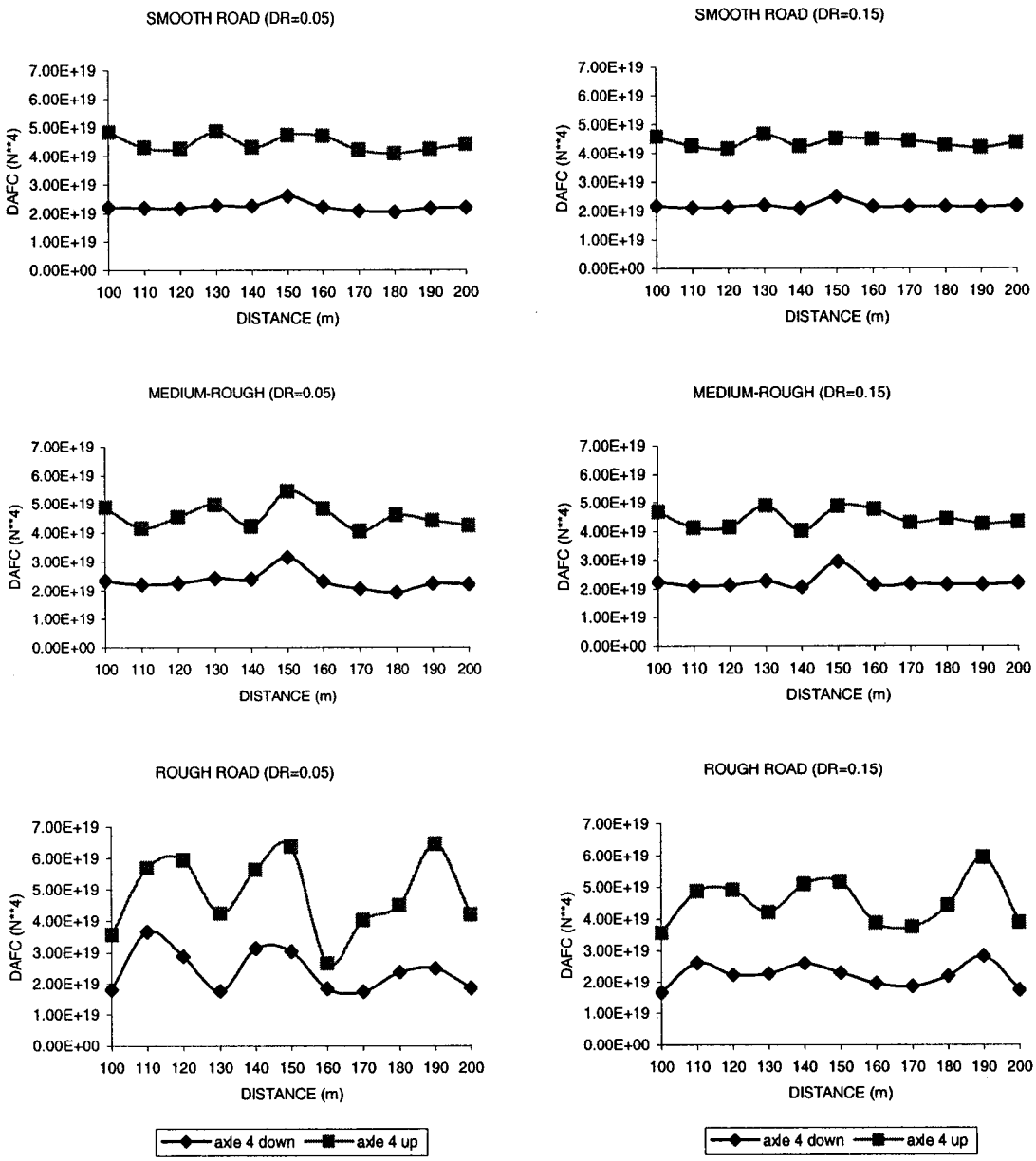

Figure 6-4: Influence of suspension damping, road roughness and the liftable axle operating condition on the magnitude of DAFC of 6-axle configuration 12F12.

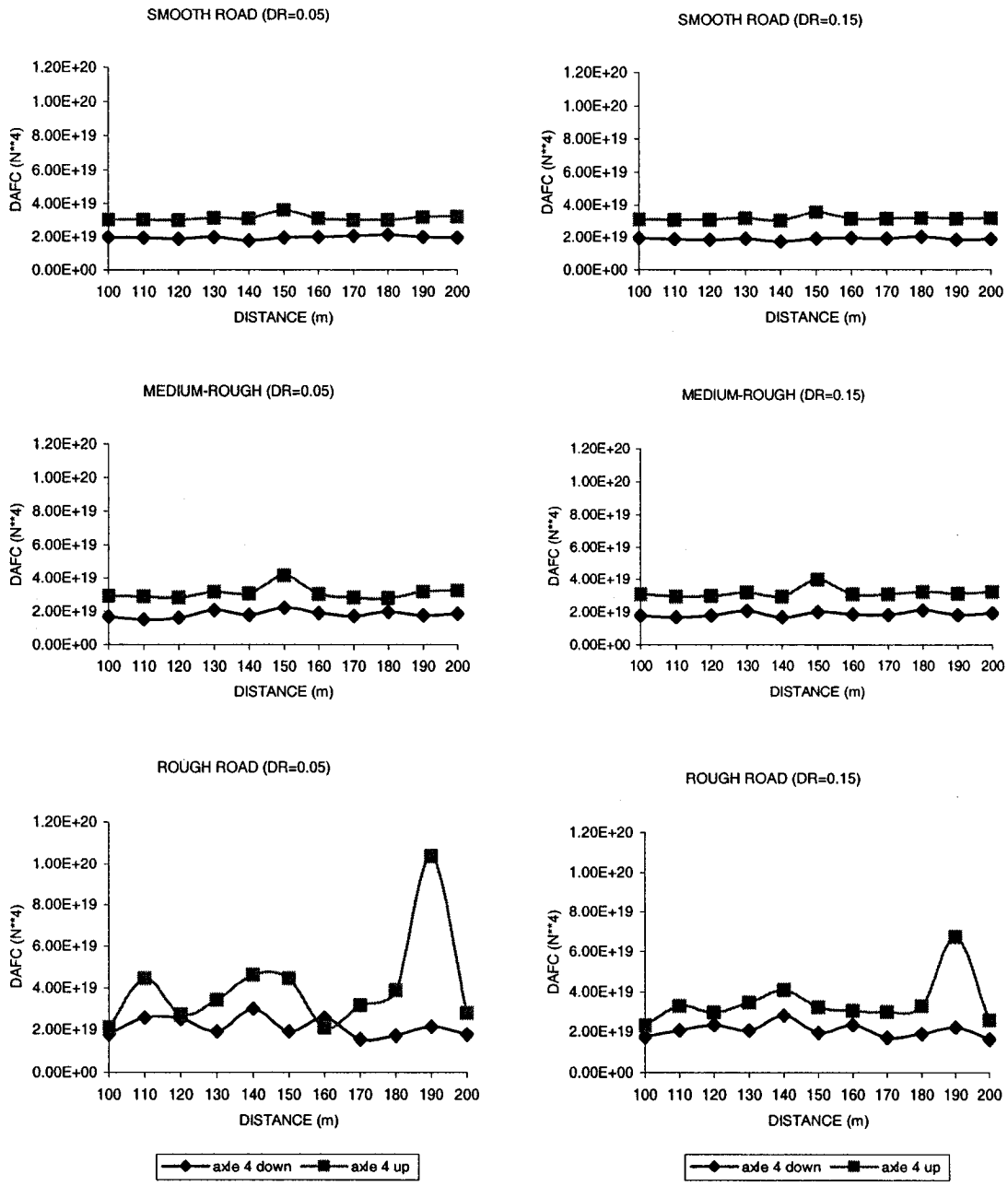

Figure 6-5: Influence of suspension damping, road roughness and the liftable axle operating condition on the magnitude of DAFC of 7-axle configuration 12F13.

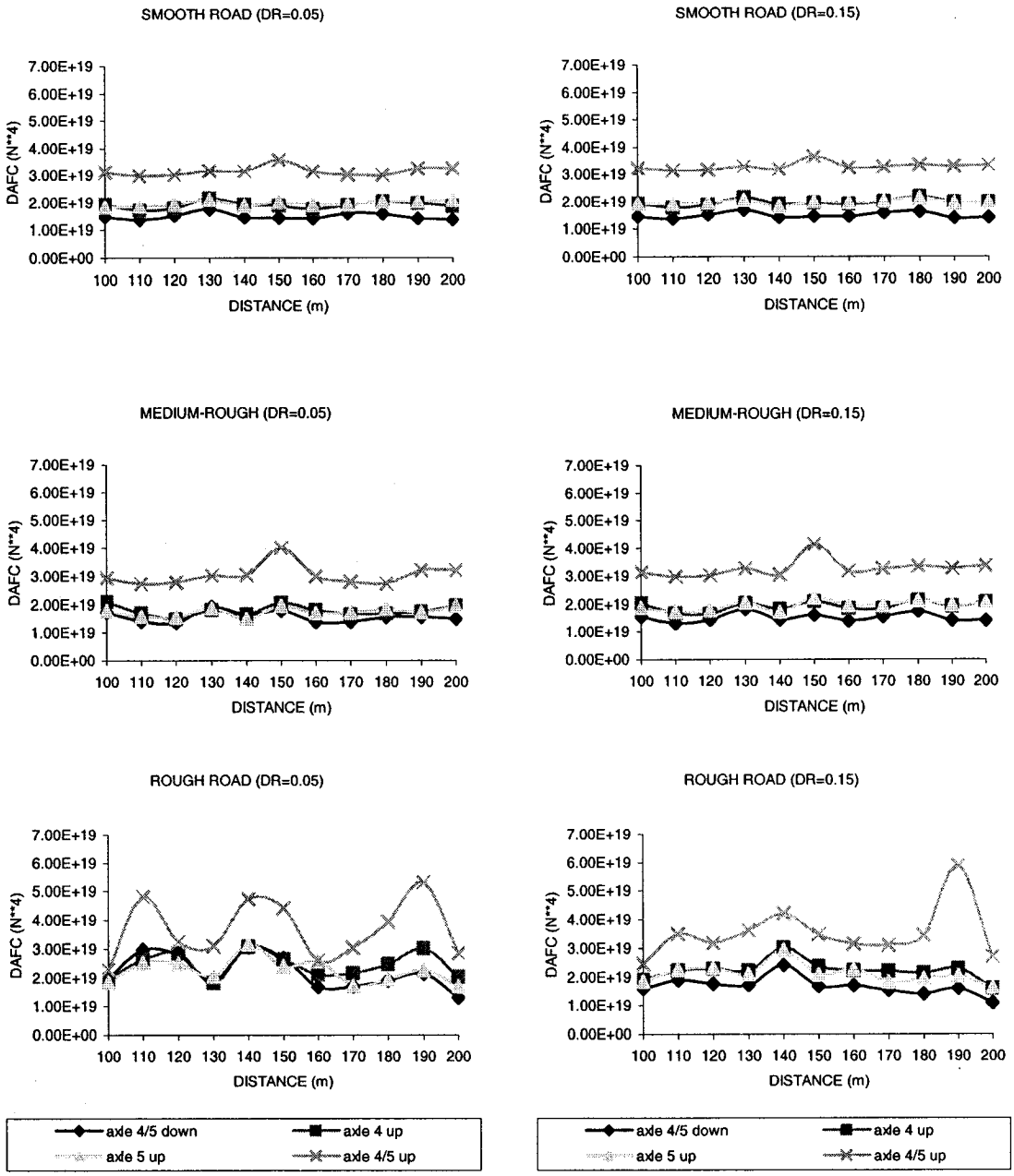

Figure 6-6: Influence of suspension damping, road roughness and the liftable axle operating condition on the magnitude of DAFC of 8-axle configuration 12F113.

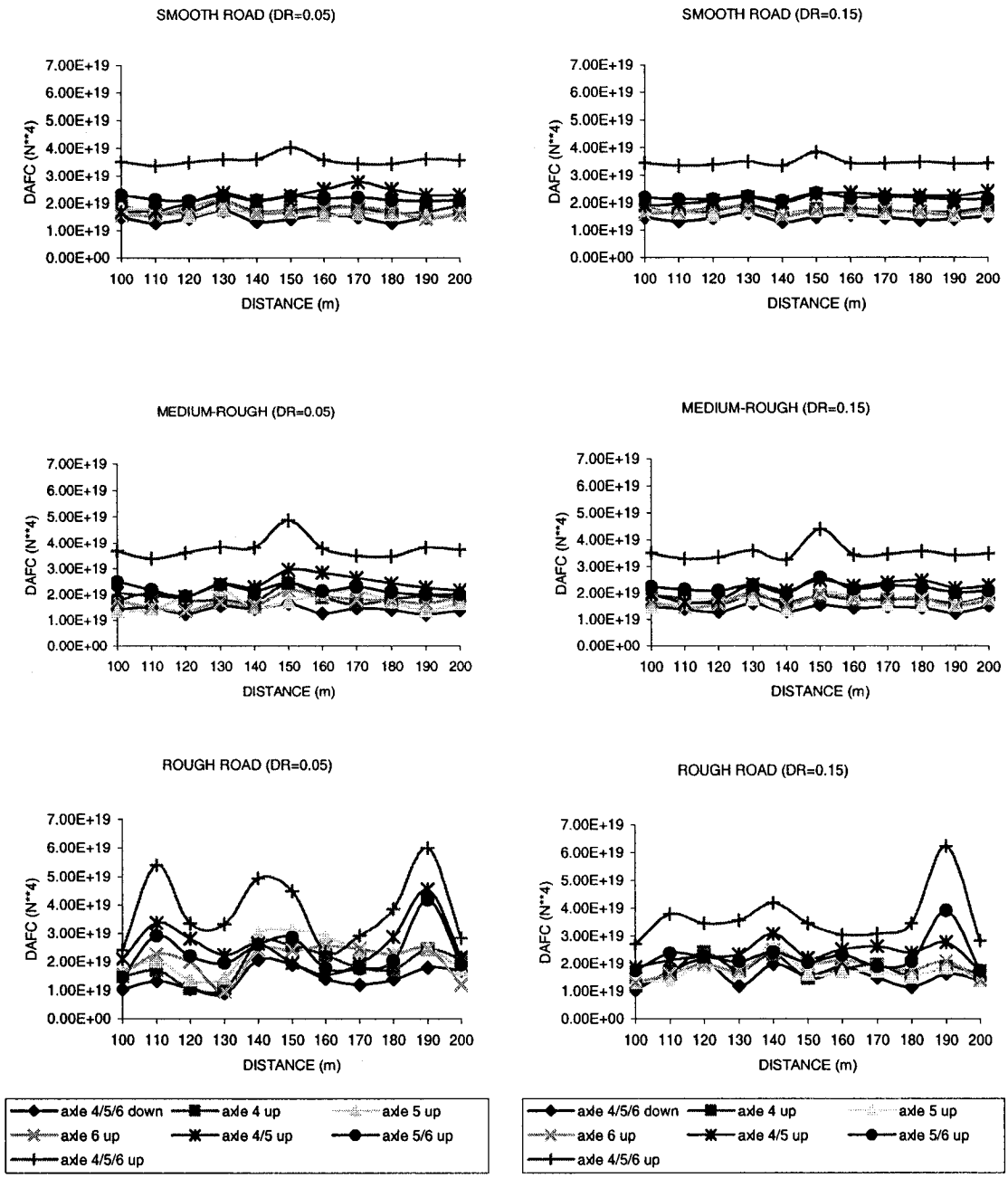

Figure 6-7: Influence of suspension damping, road roughness and the liftable axle operating condition on the magnitude of DAFC of 9-axle configuration 12F1113.

axle at a particular point along the road surface [70]. This measure is thus similar to the DAFC, as evident from the Figures 6-8 to 6-11. The figures show the variations in DASC magnitudes corresponding to 11 different locations along the road surface ($100\text{m} \leq x \leq 200\text{m}$) for the four candidate vehicle configurations under various operating conditions, road roughness and suspension damping ratio. The results, in-general, are similar to those attained for DAFC. The results also show the peak responses corresponding to certain locations along the road, suggesting the spatial repeatability of the dynamic loads.

6.8 SUMMARY

The influences of liftable axles, operating conditions, road roughness and suspension damping ratio on the dynamic tire forces, and consequently the road damage potential of selected vehicle configurations are investigated in terms of various performance measures. These include the static tire force measures: Equivalent Single Axle Load (ESAL) and Load Equivalent Factor (LEF), and the dynamic tire force measures: Dynamics Load Coefficient (DLC), Road Stress Factor (RSF), Dynamic Aggregate Force Coefficient (DAFC) and Dynamic Aggregate Stress Coefficient (DASC). The simulation results suggest that the combinations with multiple axle semitrailer yield higher ESAL for each axle and LEF for the combination, when one or more liftable axles are raised. The increase in ESAL and LEF, however, is relatively small, when more axles are employed for the semitrailer. Higher axle loads caused by the raised axles yield lower values of the dynamic load coefficient (DLC), which is attributed to its definition. The results thus suggest enhanced road friendliness of the combination despite higher axle loads. The measure of DLC is thus not considered to be suitable for

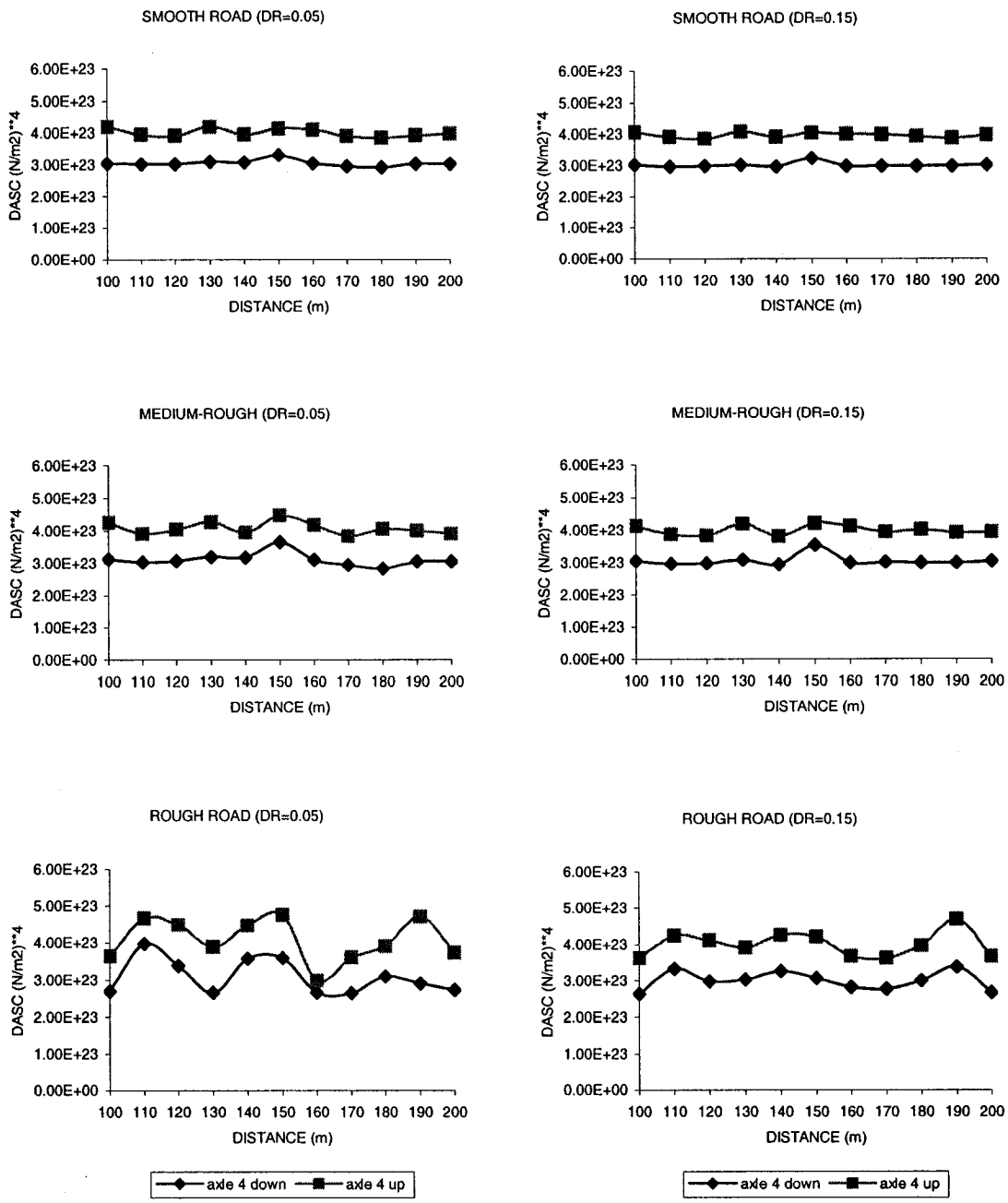

Figure 6-8: Influence of suspension damping, road roughness and the liftable axle operating condition on the magnitude of DASC of 6-axle configuration 12F12.

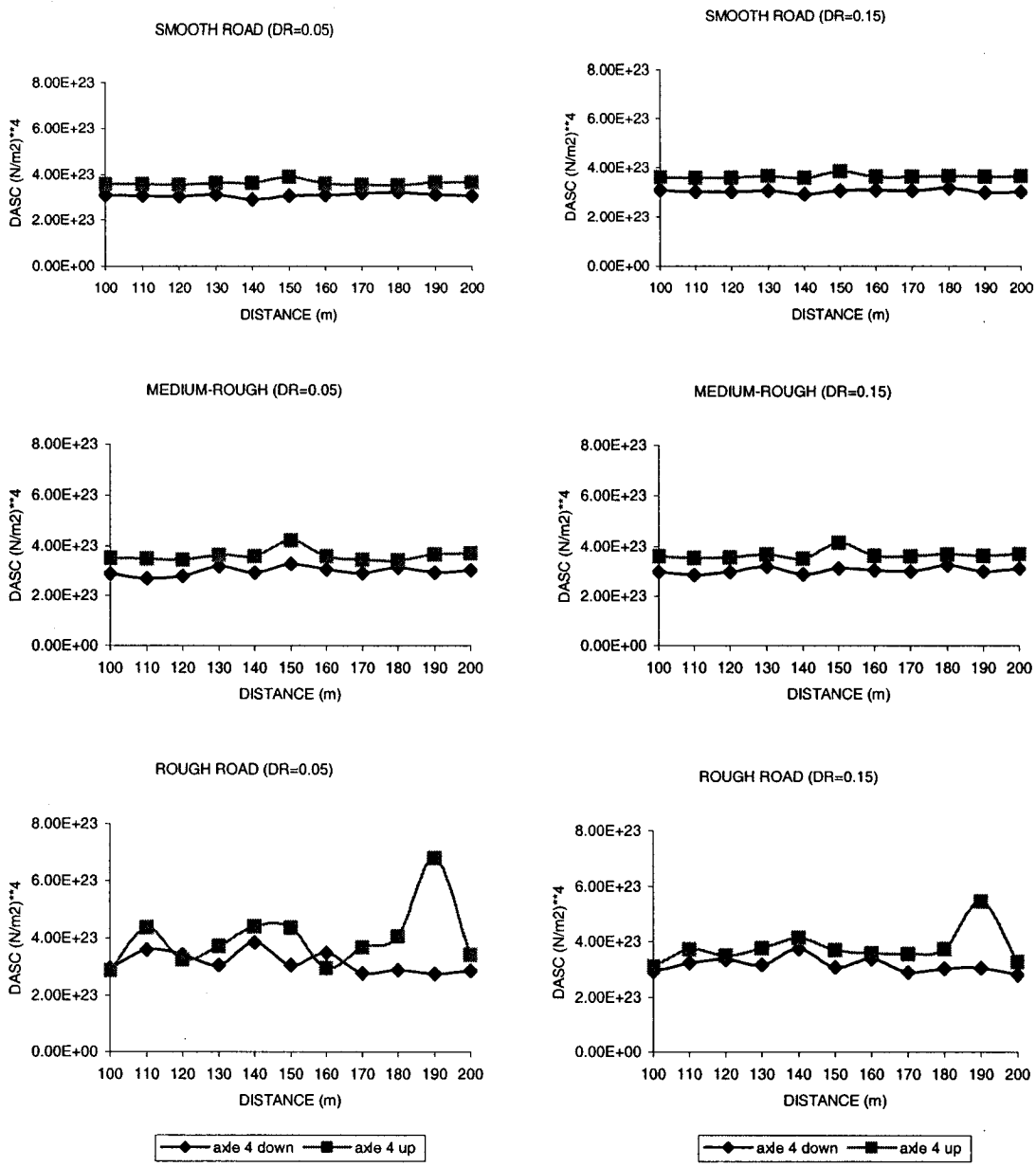

Figure 6-9: Influence of suspension damping, road roughness and the liftable axle operating condition on the magnitude of DASC of 7-axle configuration 12F13.

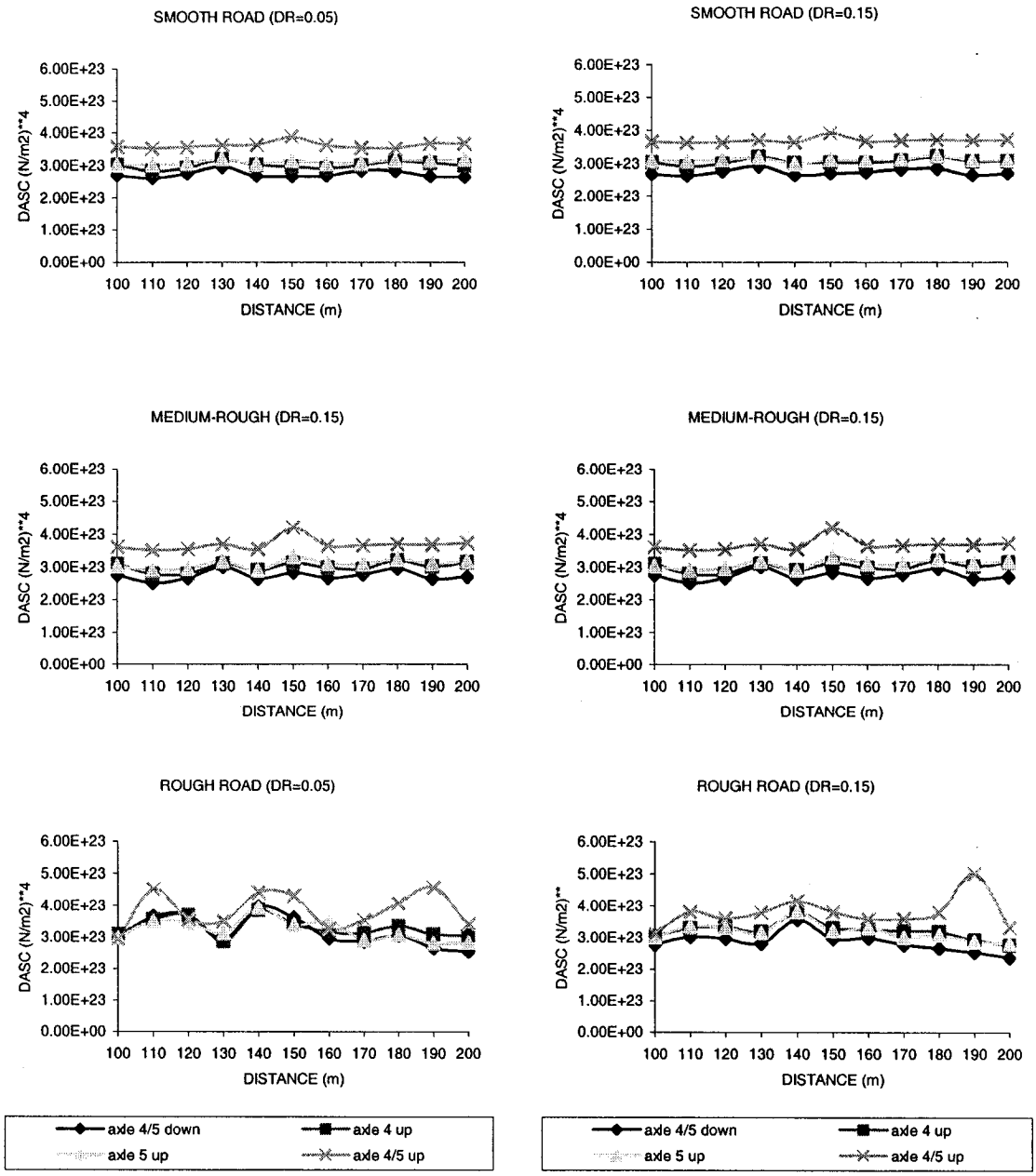

Figure 6-10: Influence of suspension damping, road roughness and the liftable axle operating condition on the magnitude of DASC of 8-axle configuration 12F113.

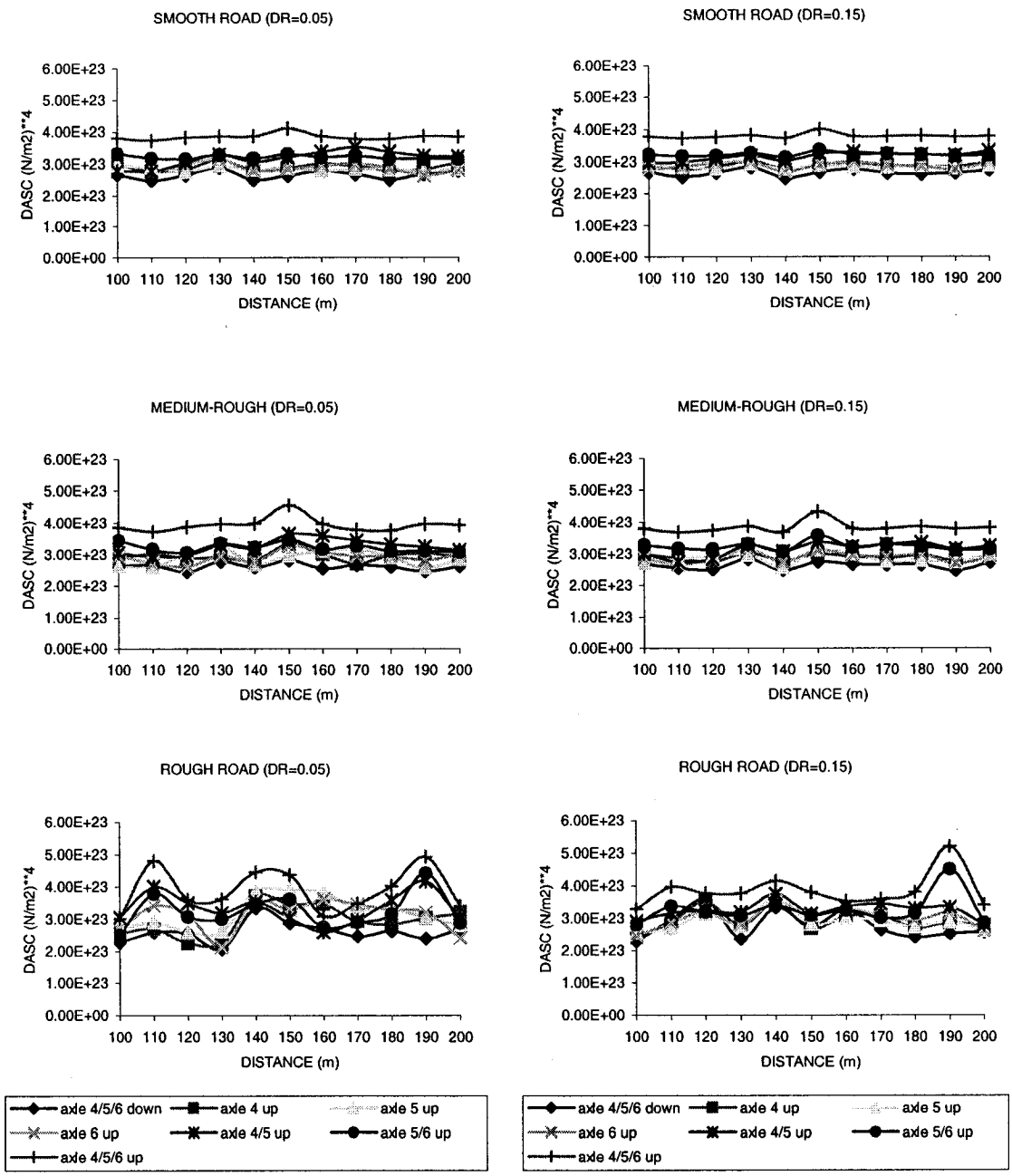

Figure 6-11: Influence of suspension damping, road roughness and the liftable axle operating condition on the magnitude of DASC of 9-axle configuration 12F1113.

assessing road damaging potential of the combinations with liftable axles. The road damaging properties of different vehicle combinations with liftable axle down and raised are thus investigated in terms of the DAFC and DASC measures. These measures increase most significantly as one or more axles are raised, suggesting higher road damaging risk. The dynamic variations in tire forces increase further with increasing road roughness but decrease slightly with increase in suspension damping. The DAFC and DASC measures, as a function of the coordinates of the road profile, reveal higher magnitudes of DAFC and DASC due to localized elevations of the road profile, suggesting spatial repeatability of the dynamic tire forces.

CHAPTER 7 : CONCLUSIONS AND SUGGESTIONS FOR FUTURE RESEARCH

7.1 MAJOR CONTRIBUTIONS

The directional dynamics and stability performance, dynamic tire forces and consequently road damaging potential of the vehicle combinations, are strongly influenced by their configurations, weights and dimensions. Multiple axle semitrailers with liftable axles are frequently used to enhance the maneuverability of the combination during turns. The liftable axles, when retracted, impose larger loads on the remaining axle tires and alter the inertial properties of the vehicle. The handling and directional dynamic performance of such vehicles may thus be affected in an adverse manner. Furthermore, the retracted liftable axle vehicles impose significantly larger dynamic forces on the pavement that may cause premature pavement failure. Alternatively, self-steering axles are employed to limit the magnification of the pavement loads and achieve acceptable maneuverability during turns. The reduced cornering forces due to self-steering axle tires, however, could yield degraded directional performance of the vehicle combination. Although, the directional dynamics and pavement loading performances of heavy vehicles have been analyzed in many studies, the analyses have been limited to conventional fixed axles alone.

In this dissertation, the directional performance and pavement loading characteristics of different multiple axle articulated vehicles with fixed, liftable and self-steering axles, are investigated through computer simulations. This forms the major contribution of the dissertation research. The dissertation research involved the development of a general-purpose analytical model of a multiple axle articulated vehicle

with 6 to 9 axles, including conventional, liftable and self-steering axles, and dynamic interactions of the tires with random road surface profiles. The specific contributions of this dissertation research are summarized below:

- Development of an analytical model of a self-steering axle incorporating the restoring mechanism and centering spring.
- Development of a general-purpose three dimensional model of a multiple axle articulated vehicle incorporating liftable and self-steering axles, and tire interactions with randomly rough road surfaces.
- Formulation of performance measures for assessment of relative directional dynamics and pavement loading characteristics of conventional, liftable and self-steering axles.
- The influences of road roughness and suspension damping ratio on the handling, directional dynamics and pavement loading characteristics of different vehicle configurations
- The influences of one or more raised liftable axles on the equivalent single axle loads, dynamic road stresses and handing performances of the vehicle combination.
- The role and potential benefits of self-steering axle in limiting the dynamic pavement loads.

7.2 CONCLUSIONS

Following conclusions may be drawn from the simulation results attained in this study:

- The directional dynamics and pavement loading characteristics of multiple axle articulated vehicles operating on random road profiles with conventional, liftable or self-steering axles can be effectively investigated using the modified constant velocity yaw/roll program developed in this study.
- The static and dynamic roll stability limits of multiple axle articulated vehicles can be assessed in terms of static rollover threshold (SRT), load transfer ratio (LTR) and rearward amplification factor (RA).

- The low- and high-speed jackknife potential on low friction surfaces could be assessed in terms of the friction demands at low and high speeds (LSFD and HSFD).

- The pavement damage potential of heavy vehicles are mostly represented by the equivalent single axle load (ESAL), road stress factor (RSF), dynamic aggregate force and stress (DAFC and DASC) factors, while the commonly used dynamic load coefficient (DLC) due to tire forces is not suited for assessing the combinations with liftable axles.

- The majority of the performance measures related to pavement loading and directional dynamics are strongly influenced by the road roughness and suspension damping ratio.

- The vehicle operation with one or more liftable axles raised generally yields lower roll stability limit, but enhance maneuverability during turns and significantly lower jackknife potential on low friction surfaces. Such operation, however, poses significantly higher static and dynamic tire forces to the pavement that would cause premature pavement failure.

- The results clearly show that vehicles with raised liftable axle cause pavement stresses of magnitudes that could be 50% higher than those caused by conventional axle vehicles. This is also evident from the higher magnitudes of the road stress factor and dynamic aggregate force criterion, evaluated from the static and dynamic components of the tire forces.

- The higher road roughness and lower suspension damping cause considerably higher magnitudes of DAFC and DASC due to tire forces, especially their peak values.

- The results show comparable locations of peak magnitudes of DAFC and DASC along the road surface for all the four candidate vehicle configurations considered in this study, which is attributed to localized extreme elevations of the road profile and demonstrates the phenomenon of 'spatial repeatability' of the dynamic tire forces on particular locations along a road.

- Higher road roughness, lower suspension damping ratio, and operation with one or more raised liftable axles causes considerably larger peak values of DAFC and DASC, and more evident 'spatial repeatability' of the tire forces

- The axles with higher static axle load caused by a raised liftable axle yield lower magnitudes of dynamic load coefficient (DLC) of tire forces, while the magnitudes of RSF, DAFC and DASC increase. The rate of increase in the RSF is comparable to that of ESAL value for the vehicles. The DLC measure is thus considered to be inadequate for assessing the road damaging potential of vehicles with raised liftable axle, which is attributed to its definition.

- Higher road roughness yields higher magnitudes of dynamic load coefficient (DLC) due to tire forces. Higher suspension damping, however, causes slightly lower values of DLC and thus the RSF performance.

- The retracted liftable axles increase the static tire forces of the remaining axles and thus the ESAL of the axles and LEF of the entire vehicle combination, suggesting higher road damaging potential. The LEF of the vehicle combination could increase by more than 100%, when the liftable axle is raised.

- The significant increases in ESAL, LEF, RSF, DAFC and DASC, caused by raised liftable axle, could be suppressed through the use of self-steering axles that would provide adequate maneuverability during turns.

- The static roll stability limits (SRT) of articulated vehicles can be slightly enhanced by using multiple axle semitrailers. The SRT limit, in general, decreases, when one or more liftable axles are raised. The use of self-steering axles, however, yields SRT values similar to those of the conventional axle vehicles.

- The dynamic roll stability limits, assessed in terms of load transfer ratio (LTR), also reduce, when one or more liftable axles are raised.

- The vehicle operation on rough roads yields lower static and dynamic roll stability limits, while the influence of damping is nearly negligible. The LTR may increase by as much as 30%, when vehicle operations on rough roads.

- The use of self-steering axles, instead of liftable axles, should be encouraged to retain acceptable roll stability limits and maneuverability during turns.

- The vehicle combinations with large number of semitrailer axles generally yield lower rearward amplification tendencies. Irrespective of the vehicle configurations, higher road roughness tends to lower the RA values by as much as 60%, which is attributed to higher tractor acceleration caused by leaf-spring suspension. The effect of suspension damping on the RA performance is negligible, irrespective of vehicle and trailer axle configurations. Using retracted axles in the semitrailer yields slightly higher RA values, while the use of self-steering axles generally yield RA values comparable to those of the vehicles with conventional axles.

- The liftable axle trailers offer most significant benefit in terms of maneuverability during turns and the jackknife potential of the vehicle combination on low friction surfaces, such as icy roads. The high- and low-speed friction demands of the driver axles of the candidate vehicle configurations reduce most significantly, when one or more liftable axles are raised.

- The LSFD of the drive-axle tires increases most significantly with increase in the number of semitrailer axles, which suggests that multiple axle trailers are more susceptible to jackknife at low speeds on icy roads. The LSFD of a six-axle trailer is 0.68 compared to 0.13 for the three-axle trailer. The vehicle operation with three axles of the six-axle trailer raised reduces the LSFD to nearly 0.06.

- Both the low- and high-speed friction demands of drive-axle tires increase with increasing road roughness. A higher suspension damping is desirable when operating on rough roads.

7.3 SUGGESTIONS FOR FUTURE WORK

This dissertation research presents a preliminary effort to enhance the understanding of the influences of road roughness, suspension damping ratio and trailer axle configurations (conventional, liftable and self-steering axles) on the directional dynamic performance, and dynamic tire forces and thus the road damage potentials of heavy vehicle combinations. The dissertation, however, focuses on the relative performance characteristics based on a few selected measures related to directional stability and control characteristics. The road damaging potentials of vehicles are

assessed assuming the constant speed vehicle operation on a straight road without steering input, while the relative directional performances are assessed in the absence of braking. Furthermore, the self-steering axle is modeled assuming linear cornering characteristics.

Owing to the high practical significance of the impact of liftable axles on the highway infrastructure, further efforts are desirable to contribute to the revision of current regulations on the use of such axles. Some of the essential tasks that should be conducted in the near future are listed below:

- A more comprehensive model of the self-steering axle should be developed to incorporate the kinematics of the linkages, and nonlinear cornering characteristics of the axle, and coulomb friction. The model validation should be undertaken, although it would require comprehensive laboratory facilities.

- The general-purpose model proposed in this study should be further enhanced to include the braking dynamics to permit for relative analyses under simultaneous application of braking and steering maneuvers. The validity of the model should also be examined on the basis of field data.

- The relative performance analyses of conventional, liftable and self-steering axles should be undertaken for braking and yaw dynamic performance measures, such as braking efficiency, stop distance, yaw damping ratio (YDR), off-tracking, lateral friction utilization, etc.

- The directional performance characteristics of heavy vehicles are invariably investigated under perfectly smooth road surfaces, while the results of this study suggest strong effects of road roughness. Further efforts are thus recommended to perform comprehensive analyses under typical road and revise the desired performance measures.

- Further efforts are also needed to determine optimal locations of self-steering axles to enhance the low-speed maneuverability and off-tracking, and high-speed directional performance.

REFERENCE

1. Robert D. Ervin et al., 'Influence of Size and Weights Variables on the Stability and Control Properties of Heavy Trucks', Report UMTRI-83-10-2, University of Michigan Transportation Research Institute, 1983.

2. C. Choi et al., 'Air Lift Axle Study', CVOS-TR-79-06, Commercial Vehicles Operation and Safety Systems Research and Development Branch, 1979.

3. Potter, T. E. C et al., 'Assessing 'Road-Friendliness': A Review', IMech. E., J. Auto Eng, 1997.

4. Anon, 'The AASHO Road Test, Report 5, Pavement Research', Highway Research Board, Special Report 61E, 1962.

5. Rama Krishna Vallurupalli, 'Directional Dynamic Analysis of an Articulated Vehicle with Articulation Dampers and Forced-Steering', M.A.Sc thesis, Department of Mechanical Engineering , Concordia University, Canada, 1993.

6. Leblanc, P. A. et al., 'Self-Steering Axles: Theory and Practices', SAE paper 891633, 1989.

7. Vlk. F, 'Lateral Dynamics of Commercial Vehicle Combinations – a Literature Survey', Vehicle Systems Dynamics, vol. 11, no. 6, pp. 305-324, 1982.

8. David Cebon, 'Interaction Between Heavy Vehicles and Roads', The Thirty-Ninth L. Ray Buckendale Lecture, 1993.

9. Huber, L. and Dietz, O. 'Pendelbewegungen Von Lastkraftwagen – Anhangern und iher Vereidung', VDI-Zeitschrift, vol. 81, no. 16, pp. 459-463, 1937.

10. Dietz, O. 'Pendelbewegungen an Strassen – Anhangerzugen' DKF, Heft 16, 1938.

11. Dietz, O. 'Uber das Spuren und Pendeln von Lastkraftwagen – Anhangern', Atz, vol. 41, no. 15, 1939.

12. Zeigler, H. 'Die Querschwingungen von Kraftwagenanhagern', Ing. – Archiv, vol. 9, no. 2, pp. 96-108, 1938.

13. Zeigler, H. 'Der Einfluss von Bremsung und Steigung auf die Querschwingungen von Kraftwagenanhagern', In. – Archiv, vol. 9, no. 2, pp. 241-243, 1938.

14. Laurien, F. 'Untersuchung der Anhangernseitenschwingungen in Strassinzugen', Dissertation, TH, Hannocer, 1955.

15. Paslay, P. R. and Slibar, A. 'Uber quersvhwingungen von gelenkten Anhangern', Ing. – Archiv, vol.26, no.6, pp. 383-386, 1958.

16. Zakin, J. C. 'Causes of the Origin of Trailer Oscillations' (in Russian), Avtomob.promyshlennost, vol. 26, no. 11, pp. 9-12, 1959.

17. Zakin, J. C. 'Lateral Stability of Trailer Movement' (in Russian), Avtomob.promyshlennost, vol. 26, no. 2, pp. 27-31, 1960.

18. Zakin, J. C. 'Applied Theory of Trailer Movement Stability' (in Russian), Transport, Moscow, 1967.

19. Morozov, B. I. et al., 'Research of the Full Trailer Oscillations' (in Russian). Works NAMI, Moscow, no. 48, pp. 29-39, 1962.

20. Meyer, J. 'Zer Prage der Querschwingungen eine Zweiachsigen I. Kw. Anhangers', Techn. Mitteilungen Krupp, Forsch. –Berichte, vol. 21, no. 1, pp. 34-36, 1963.

21. Schmid, I. 'Das Fahrstabilitatsverhalten zwei – und dreigliedriger Fahrzeugketten', Dissertation TH, Stuttgart, 1964.

22. Jindra, F. 'Off-tracking of Tractor-Trailer Combinations', Automobile Engineer, vol. 53, no. 3, pp. 96-101, 1963.

23. Gerlach, R. 'Utersuchung der Querschwingungen von Lastzugen auf Analogrechnern', 8. Kraftfahrzeugtechnische Tagung, Karl-Marx-Stadt, Vortrag A 9,

Kammerder Technik, Fachverband Fahrzeugbau und verkehr IZV Automobilbau, 1968.

24. Nordstorm, O., Magnusson, G. and Strandberg. L. 'The Dynamic Stability of Heavy Vehicle Combinations' (in Swedish), VTI Rapport no. 9, Statens Vagoch trafikinstitut, Stockholm, 1972.

25. Nordstorm, O., and Strandberg. L. 'The Dynamic Stability of Heavy Vehicle Combinations', International Conference of Vehicle System Dynamics, Blacksberg, Virginia, Report no. 67A, Statens Vag-och trafikinstitut, Linkoping, 1975.

26. Nordstorm, O., and Nordmark, S., 'Test Procedure for the Evaluation of the Lateral Dynamics of Commercial Vehicle Combinations', Automobile – Industries, vol. 23, no. 2, pp. 63-69, 1978.

27. Bakhmutskii, M. M. and Gineburg, I. I., 'Relation of Road Train Steering Response and Handling Performance within System Articulated Vehicle – Driver', (in Russian), Avtomob. Promyshiennost, vol. 39, no. 2, pp. 32-33, 1973.

28. Mallikarjunarao and Fancher. P, 'Analysis of the Directional Response Characteristics of Double Tanker', Society of Automotive Engineers, Paper no. 81064, pp. 4007-4026, 1979.

29. Johnson, D. B. and Huston, J. C, 'Nonlinear Lateral Stability Analysis of Road Vehicles Using Liapunov's Second Method', SAE, Paper no. 841507, 1984.

30. Susemihl, E. A. and Kranter, A. I., 'Automatic Stabilization of Tractor Jackknife in Tractor-Semitrailer Trucks', SAE, Paper no. 740138, 1974.

31. Wong, J. Y. and EI-Gindy, M., 'Computer Simulation of Heavy Vehicle Dynamic Behavior – User Guide to UMTRI Models', no. 3, Road and Transportation Association of Canada, 1985.

32. EI-Gindy, M. and Wong, J. Y., 'A Comparison of Various Computer Simulation Models For Predicting the Directional Responses of Articulated Vehicles', Vehicle System Dynamics, no. 16, pp. 249-268, 1987.

33. Leucht, P. M., 'The Directional Dynamics of the Commercial Tractor-Semitrailer Vehicle during Braking', Society of Automatic Engineers, Paper no. 700371, 1970.

34. Raju Isaac Samuel Raj, ' Influence of Road Roughness and Directional Maneuvers on the Dynamic Performance of Heavy Vehicles', M.A.Sc thesis, Department of Mechanical Engineering, Concordia University, Canada, June 1998.

35. Woodrooffe, J. et al., 'Development of Design and Operational Guidelines for the C-Converter Dolly'.

36. Billing, A. M., 'Tests of Self-Steering Trailer Axles', Ontario Ministry of Transportation and Communications, Report CVOS 79-82.

37. Billing, J. R. et al., 'Performance of Infrastructure – Friendly Vehicles', Ontario Ministry of Transportation, CSTT-HVC-TR-058, 2003.

38. Woodrooffe, J., LeBlanc, P. and El-Gindy, M., 'Self Steering and Commercial Vehicle', The Third International IRTENZ seminar, Christ Church, New Zealand, August 1989.

39. Billing, J. R. et al., 'Development of Regulating Principles for Multi-Axles Semitrailer', Second International Symposium of Heavy Vehicle Weights and Dimensions, Kelowna, British Columbia, June 18-22, 1989.

40. Aurell, J. and Edlund, S., 'The influence of Steered Axles on the Dynamic Stability of Heavy Vehicles', SAE, Paper no. 892498, Journal of Commercial Vehicles, 1989.

41. Sankar, S., Rakheja, S. and Alain Piche, 'Directional Dynamics of a Tractor-Semitrailer with Self- and Force-Steering Axles', SAE, Paper no. 912686, 1991.

42. Von Becker P, 'Commercial Vehicle Design – Road Stress: Effect on the Transport Policy Decisions.' Strasse und Autobahn (Translated by TRRL as WP/V&ED/87/28), 12, pp 493-498, 1985.

43. Anon, 'The Allocation of Road Track Costs 1991/1992', Department of Transport, 1991.

44. Wilding, T., 'The Long and Short of Our Weighty Laws.' Roadway, (March) pp. 25-29, 1990.

45. Morris, J. R., 'Effects of Heavy Vehicle Characteristics on Pavement Response – Phase 1', TRB, Prepared for NCHRP project, pp. 1-25, 1987.

46. Magnusson G, Carlsson, H, E. and Ohlsson, E., 'The Influence of Heacy Vehicles' Springing Characteristics and Tyre Equipment on the Deterioration of the road', VTI (Translated by TRRL as WP/V&ED/86/16, 1986), Report no. 270, 1984.

47. Eisenmann, D., Birman, D. and Hilmer A, 'Effects of Commercial Vehicle Design on Road Stress – Research Results Relating to the Roads', Strasse und Autobahn, (Translated by TRRL as WP/V&ED/87/29, 1986), 37 (6), pp. 238-244, 1987.

48. Monismith, C. L et al., 'Truck Pavement Interactions –Requisite Research', SAE Conference on Vehicle/Pavement Interaction, SP 765, SAE Trans, Indianapolis, SAE, 1998.

49. Sweatman, P. F., 'A Study of Dynamic Wheel Forces in Axle Group Suspensions of Heavy Vehicles', Australian Road Research Board, Special Report SR27, 1983.

50. Mitchell, C., 'An Experimental Assessment of Steel, Rubber and Air Suspensions of Heavy Good Vehicles', IMechE Seminar, London, 1991.

51. Woodrooffe, J. H. F. and LeBlanc, P. A., 'Heavy Vehicle Suspension Variations Affecting Road Life', Proc. ARRB/FORS Symposium on Heavy Vehicle Suspension Characteristics, Canberra, Australia, 1987.

52. Cole, D. J. et al., 'Spatial Repeatability of Measured Dynamic Tyre Forces', J. Auto. Eng, IMech E, 210(D3), PP. 185-197, 1996.

53. Cole, D. J. and Cebon, D., 'Spatial Repeatability of Dynamic Tyre Forces Generated by Heavy Vehicles', J. Automobile Engineering Proc. IMech. E, Part D, 206, pp. 17-27, 1992.

54. Collop, A. Cebon, D. and Cole, D.,'Effects of Spatial Repeatability on Long-term Flexible Pavement Performance', IMech. E. J., 210(C2), PP. 97-110, 1996.

55. Collop, A. et al., 'Investigation of Spatial Repeatability using a Tire Force Measure Mat', Transportation Research Record, 1448, pp. 1-7, 1994.

56. Ervin, R. D. et al., 'Influence of Truck Size and Weight Variables on the Stability and Control Properties of Heavy Vehicles', University of Michigan Transportation Research Institute, UMTRI-83-10/2, 1983.

57. Mitchell, C. and Gyenes, L.,'Dynamic Pavement Loads Measured for a Variety of Truck Suspensions', The Second International Conference on Heavy Vehicle Weights and Dimensions, Kelowna, British Columbia, 1989.

58. Hahn, W. D., 'Effects of Commercial Vehicle Design on Road Stress – Vehicle Research Results', Institut fur Kruftfahrwesen, Universiat Hannover (Translated by TRRL as WP/V&ED/87/38), 1985.

59. Hu, G., 'Use of a Road Simulator for Measuring Dynamic Wheel Loads', SAE Conference on Vehicle/Pavement Interaction, SAE 881194, SP765, Indianapolis, SAE, 1988.

60. Eisenmann, J., 'Dynamic Wheel Load Fluctuations – Road Stress', Strasse und Autobahn, 4, pp. 127-128, 1975.

61. Walloschek, H. J., 'Road Loading as a Function of Vehicle Characteristics', Proc. ARRB/FORS Symposium on Heavy Vehicle Suspension Characteristics, Canberra, Australia, 1987.

62. Cebon, D., 'An Investigation of the Dynamic Interaction Between Wheeled Vehicles and Road Surfaces', PhD Thesis, University of Cambridge, 1985.

63. Gillespie, T. D. and MacAdam, C. C., 'Constant Velocity Yaw/Roll Program User's Manual', the University of Michigan Transportation Research Institute, UMTRI-82-39, 1982.

64. Gillespie, T. D. and Winkler, C. B., 'On the Directional Characteristics of Heavy Vehicles', Vehicle System Dynamics, vol. 6, no. 2-3, pp. 120-123, 1977.

65. El Gindy, M. 'An Overview of Performance Measures for Heavy Commercial Vehicles in North America', Int. J. of Vehicle Design, vol. 16, nos. 4/5, pp. 441-463. 1995.

66. XiaoBo Yang, 'A Closed-Loop Driver/Vehicle Directional Dynamic Predictor', a PhD thesis, Department of Mechanical Engineering, Concordia University, Canada, 1999.

67. J. Christian Gerde,' Safety Performance and Robustness of Heavy Vehicle AVCS', California PATH Program, Year One Report for MOU 390, Stanford University, January 2002.

68. Shekinah Errington and Chris Winkler,' Rollover of Heavy Commercial Vehicles', UMTRI Research Review, ISSN 0739 7100, Vol. 31, No. 4.

69. D J Cole and D Cebon, ' Influence of Tractor-Trailer Interaction on Assessment of Road Damaging Performance', Engineering Department, Cambridge University, England, July 1996.

70. D Cebon, 'Handbook of Vehicle-Road Interaction', Engineering Department, Cambridge University, England, ISBN 90 265 1554 5, Page 311,1991.

71. Kinder, D. F. and Lay, M. G., 'Review of the Fourth Power Law', ARRB, Internal Report, Air000-248, 1988.

72. Damien, T. M. et al., 'Pavement Profiling Various Pavements: Ottawa/Smith Falls', John Emery Geo-technical Engineering Report, 1992.

73. Gordan D. Gronberg, 'Use of Pavement Condition Data in Highway Planning and Road Life Studies', HRB, Highway Research Record 40, pp. 37-50, 1963.

74. 'Vehicle Weight and Dimension Limits in Ontario', Ministry of Transportation in Ontario, 2000.